A Machine Learning Based Analysis of Double Effect Vapor Absorption Refrigeration Cycle based Cold Storage

Submitted By

Mashfiq Khan

180011236

Nurul Abrar

180011213

Supervised By

Prof. Dr. Mohammad Ahsan Habib

Co-Supervised By

Mr. Muhammad Mahmood Hasan

A Thesis submitted in partial fulfillment of the requirement for the degree of Bachelor of Science in Mechanical Engineering

Department of Mechanical and Production Engineering (MPE)

Islamic University of Technology (IUT)

18 May, 2023

Candidate's Declaration

This is to certify that the work presented in this thesis, titled, "A Machine Learning Based Analysis of Double Effect Vapor Absorption Refrigeration Cycle based Cold Storage", is the outcome of the investigation and research carried out by us under the supervision of Prof. Dr. Mohammad Ahsan Habib, Professor, MPE Dept., IUT, Board Bazar, Gazipur-1704, Bangladesh.

It is also declared that neither this thesis nor any part of it has been submitted elsewhere for the award of any degree or diploma.

Name of the Student: Nurul Abrar

Student No: 180011213

Name of the Student: Mashfiq Khan

Student No: 180011236

RECOMMENDATION OF THE BOARD OF SUPERVISORS

The thesis titled "A Machine Learning Based Analysis of Double Effect Vapor Absorption Refrigeration Cycle based Cold Storage" Submitted by, Nurul Abrar, Student No: 180011213 and Mashfiq Khan, Student No: 180011236 has been accepted as satisfactory in partial fulfillment of the requirements for the degree of B Sc. in Mechanical Engineering **on 18th MAY, 2023.**

BOARD OF EXAMINERS

1. ----------

Prof. Dr. Mohammad Ahsan (Supervisor)

Professor

MPE Dept., IUT, Board Bazar, Gazipur-1704, Bangladesh.

2. ----------

Mr. Muhammad Mahmood Hasan (Co-Supervisor)

Lecturer

MPE Dept., IUT, Board Bazar, Gazipur-1704, Bangladesh.

Acknowledgement

We want to start by saying Alhamdulillah and thanking Almighty Allah for allowing us to complete this task effectively and on schedule. We like to show our gratitude to our supervisor **Dr. Mohammad Ahsan Habib**, Professor, Department of Mechanical and Chemical Engineering, IUT, thank you for being an outstanding mentor, advisor, and source of inspiration. Your constant commitment to education and your enthusiasm for sharing information have had a significant influence on our personal growth and development. Your advice, support, and faith in our talent have inspired me to strive for excellence and realize our full potential. we will be eternally thankful to you for the invaluable things we have gained both inside and outside of the classroom.

We also like to our co-supervise **Mr. Muhammad Mahmood Hasan**, Lecturer, Department of Mechanical and Chemical Engineering, IUT, for all of his help, suggestions for experiments, conversations, time, and for patiently explaining the difficult issues and verifying this thesis and papers above all his care and concern. These will live on in our memories.

Name of the students

Nurul Abrar

Mashfiq Khan

Nomenclature

Abbreviation	Meaning
DNI	Direct Normal Irradiance
GHI	Global Horizontal Irradiance
$\boldsymbol{PV_{OUT}}$	Photovoltaic Output
MAE	Mean Absolute Error
MSLE	Mean Squared Log Error
MeAE	Median Absolute Error
MAPE	Mean Absolute Percentage Error
R^2	Coefficient Of Determination
PTC	Parabolic Trough Collector
VAR	Vapor Absorption Cycle
PCA	Principal Component Analysis
COP	Coefficient Of Performance

Table of Contents

List of Figures

List of Tables

Abstract

The demand for sustainable solutions in cold storage is being propelled by the increasing need for renewable energy. To meet this demand, solar energy can be seamlessly integrated into cold storage systems. However, in order to ensure efficient utilization of solar energy, accurate predictions of solar data are crucial to address uncertainties and overcome challenges. Various statistical techniques, including regression, SVM regression, and neural network models, can be employed to forecast solar information by leveraging past solar data. These models rely on data from a selected projection model to generate solar energy. The utilization of a parabolic trough collector is an effective method to convert solar energy into heat, resulting in significant fuel savings of approximately 28 units per year, equivalent to 11% of the overall fuel demand. This reduction in fuel consumption not only leads to cost savings but also reduces dependence on unsustainable energy sources. A comparative study evaluating the performance of cold storage systems compared a double-effect vapor absorption refrigeration system to a single-effect system. The double-effect system was preferred due to its lower input heat requirement (1815.55 kW < 3023.87 kW) and higher coefficient of performance (COP) value (1.3 > 0.76) in the multi-effect system. These factors indicate enhanced efficiency and optimal functionality, making the double-effect system the superior choice for cold storage applications. Additionally, the study also considered cost and emissions implications. The findings demonstrate the feasibility and long-term sustainability of integrating solar energy into cold storage systems. The analysis reveals that renewable energy integration can lead to a reduction of 30% in greenhouse gas emissions. Embracing sustainable energy sources is not only environmentally wise but also crucial in transitioning away from fossil fuel-dependent systems. The study proposes a viable solution by incorporating a solar system into a fuel generator-based cold storage system, offering the potential to address energy-related challenges. By utilizing solar data and efficient technologies like the parabolic trough collector, solar energy can significantly enhance the sustainability of cold storage systems. After a thorough evaluation, the N-BEATS model was identified as the most suitable predictive model for the system.

Keywords: Solar radiation, prediction model, machine learning, statistical model, neural network model, Double effect vapor absorption refrigeration system.

Chapter 1 Introduction

The demand for power generated from natural and renewable sources is fast increasing across the world. The race for more environmentally friendly forms of energy has pushed governments and research organizations all over the world to examine the largely unexplored renewable sector, primarily to combat the rapidly increasing rate of greenhouse gasses in the earth's atmosphere. As the threat of global warming approaches its apex, it is unsurprising that various governments are investing in renewable energy technology.

However, Bangladesh falls far behind other emerging nations in terms of renewable energy application. This thesis, on the other hand, investigates the possibilities of generating power from renewable energy specially the solar energy used in refrigeration systems. Using double effect absorption refrigeration alongside solar power has huge potential. This system is more of an eco-friendly system.

1.1 Background

With a population of 170 million, Bangladesh is mostly an agricultural nation. Bangladesh's fossil energy resources are mostly made of natural gas. The domestic oil supply is regarded as insignificant. In the country's north-eastern area, there are a number of tiny coal resources, although they are mostly made of peat, which has a poor caloric value, and extremely deep bituminous coal, which will be very expensive to extract. In terms of population, just 25% of people have access to power. Only 12.2% of all homes in 2010 (primarily in metropolitan areas) had access to piped natural gas for cooking, while only 6.9% of all households utilized kerosene.

The natural gas reservoir is under grave danger as a result of growing industrialization. Bangladesh has one of the lowest per capita energy and power consumption rates among developing nations. Natural gas, coal, and various biomass fuels (such as agricultural waste, wood fuels, animal dung, etc.) provided more than 83% of the world's total final energy consumption in 2010. Several initiatives to harness the available renewable energy resources have been supported by the government and NGOs (non-governmental organizations) in order to fulfill the energy demand over the past ten years.

Solar radiation data is recognized as the most important variable in meteorology, solar energy transformation, and renewable energy applications, notably for the size of Standalone Photovoltaic (SPV) systems. Many scholars have been interested in inventing various methods for obtaining this parameter because it is unfortunately not always available, especially in rural places where there are no meteorological stations. The decision-making process for developing solar-powered plans will heavily rely on solar forecasts.

Since the generation of solar energy is always changing, it has never been easy to predict energy usage precisely. Energy for a house has been accurately forecasted using solar forecasting tools.

It is not practical to install pure solar thermal systems in Bangladesh. Therefore, implementing hybrid systems is the best course of action. By the prediction model we can accurately predict the solar irradiation coming from the sun. These forecasted values are very important because we are able to use these values in different sectors to utilize future knowledge. Integrating with another cycle will increase our energy output and reduce the breakeven point. As organic Rankine cycle implementation is favored it will reduce the

impact on the environment as well. It can give us a sustainable energy cost and reliable power source.

1.2 Overview

As demand for solar energy rises, it is essential to make sure that solar energy plants are built in optimal locations that receive the most solar radiation, such as areas with an abundance of sunlight.

Solar Irradiance is measured in several different ways:

The whole amount of shortwave radiation received from above by a surface horizontally to the ground is commonly referred to **GHI.** This number, which combines DNI and DHI, is particularly important for solar systems.

Direct Normal Irradiance (DNI) is defined as the amount of solar radiation received per unit area by a surface which is always held vertical (or normal) to the rays that come in a straight line from the direction of the sun at its present point in the sky.

Diffuse Horizontal Irradiance (DHI) is the amount of radiation absorbed per area occupied by an object's surface that doesn't come from the sun directly, but has been scattered by molecules and particles in the atmosphere and arrives from all directions equally.

It is preferable to build solar energy plants in places with high Direct Normal Irradiance (DNI), since this results in the most solar energy per area. Unfortunately, because DNI sensors are both sophisticated and expensive, there is frequently insufficient data available for DNI measurements. Global Horizontal Irradiance (GHI) data, on the other hand, is

considerably more easily available. As a result, utilities and solar energy providers must be able to compute DNI and DHI from a given GHI.

Figure 1-1 is shows the DNI, GHI and DHI construction. The figure gives a visual representation of the different solar parameter that are needed for different receptor factor for the solar panel.

GHI can be constructed with DHI and DNI as follows:

Global Horizontal (GHI) = Diffuse Horizontal (DHI)+ Direct Normal (DNI) X cos(θ)

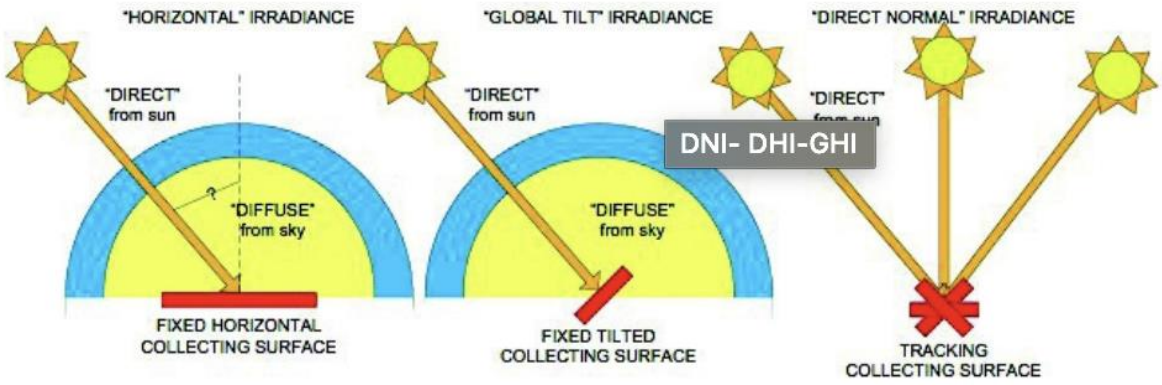

Figure 1-1 DNI, GHI and DHI Construction

The Benefits of forecasting solar radiation are:

1**. Improved energy efficiency**: Predictive data on solar radiation can help energy production and efficiency by providing decision makers with an accurate forecast for when solar energy is most available. This can help optimize energy production and help to identify areas where energy efficiency can be improved.

2. **Optimal resource management**: Predictive data on solar radiation can help managers and operational staff make timely decisions in order to maximize resource utilization. This can help reduce costs and improve efficiency.

3**. Improved safety**: Predictive data on solar radiation can help to identify areas where safety measures should be implemented. This can help to reduce the risk of injury or accidents due to heat or glare.

4**. Improved performance**: Predictive data on solar radiation can help to optimize the performance of solar installations and other systems that rely on solar energy. This can help to improve the efficiency and reliability of such systems.

The objective is to develop tools for forecasting, and to simulate hybrid power plants numerically for analysis and utilization purposes.

The utilization of solar energy as an abundant and clean resource is gaining increasing importance in addressing the challenges of climate change and transitioning to a sustainable energy future. However, the current limitations in capturing and storing solar energy efficiently create a need for accurate prediction models to better integrate solar power into the existing energy infrastructure.

The highly variable nature of solar energy production, which is influenced by factors such as weather and time of day, creates challenges for grid operators and energy planners who rely on a combination of renewable and fossil fuel-based power supply. It is possible to predict solar power generation levels by correctly predicting solar intensity, which is an indicator of the amount of solar radiation reaching a certain location. The primary goal of this project is to develop a prediction model that can forecast solar intensity for a given area 48 hours into the future using local time-series weather data. By leveraging readily

available weather data, such as temperature, humidity, wind speed, cloud cover, and precipitation, the aim is to provide high-confidence forecasts of solar generation.

To achieve this, the project has acquired solar intensity and weather data from the NSRDB (National Solar Radiation Database) and Sunrise-Sunset-API. The NSRDB provides valuable solar radiation data collected from weather stations across the United States, while the sunrise-Sunset-API provides sunrise and sunset times for specific locations. These datasets serve as the basis for training and evaluating the prediction model.

By deploying machine learning techniques, such as regression or time series analysis, the project aims to leverage the acquired data to build an accurate and reliable prediction model. The model will use historical weather data and solar intensity as inputs to forecast solar generation for future time periods.

The successful development of such a prediction model can have significant implications for the regulation of fossil fuel-based power generation. With high-confidence forecasts of solar generation, grid operators and energy planners can better manage the integration of solar power into the grid, optimizing the utilization of fossil fuel-based energy sources to meet fluctuating energy demands.

This project aligns with sustainable development goals, particularly those related to clean energy and climate action. By leveraging machine learning techniques.

There are several types of cold storage facilities accessible now all over the world. Cold storage facilities are available.

There are several classifications. Cold storages are categorized as long-term or short-term based on the period of storage.

There is also short-term cold storage available. Long-term cold storages maintain items for several months, whereas short-term or transit cold storages keep items for a few days or hours. Cold storage facilities are also classed according to whether their operational temperature is at or below 0° Celsius. While ice cream, fish, and meat are kept frozen, most agricultural commodities are stored at temperatures above 0°Celsius.

This problem can only be handled by selecting distinct perishable commodities with equivalent storage temperatures and compatibility but different reaping and harvesting dates, allowing the cold storage facility to be used all year.

As a result, extending current cold storage facilities for multi-commodity storage is an urgent necessity. However, this element was not addressed in previous works described in the literature, where researchers focused solely on the storage of a specific product or commodity [26-31].

1.3 Prospective Aspects of Solar Energy

Solar energy with a vapor absorption cycle has huge potential integration aspects for Bangladesh. In a country looking for efficient and cooling solutions, this combination can offer many advantages. Research indicates that through appropriate utilization of solar thermal energy to power an ordinary vapor absorption cycle, the efficiency of energy in Bangladesh can surely rise above the common methods of conventional power generation [39]. By utilizing techniques or equipment comprising solar thermal energy to generate heat which drives an efficient refrigeration named as power generation cycle or refrigeration's effects on the cycle drive from higher overall convert of energy as well as reduced energy losses.

Bangladesh has undergone such conditions of hot latitudes, accompanied by very humid atmosphere; consequently, it faces much increased requirements for normal air-cooling and air conditioning systems. Appropriated utilization of solar energy within solar powered vapor absorption refrigeration system can definitely address that kind of demand in accurate manner. Solar-powered vapor absorption refrigeration technique comes up with reliable readily available alternative of electric compressors for conventional coolers. This method can assist in sustaining without making heavy reliance upon electricity from grid thus helps reducing strain on existing power infrastructure considerably.

Solar energy combined with a vapor absorption cycle has the potential to greatly contribute to Bangladesh's long-term development goals. It has the potential to improve energy efficiency, reduce greenhouse gas emissions, and relieve strain on the power system, particularly during peak demand periods. Furthermore, this technology has the potential to improve access to cooling and air conditioning in a variety of sectors, including commercial buildings, industries, and residential regions. Bangladesh can leverage on its enormous solar resources, optimize energy use, and contribute to a cleaner and more sustainable future by adopting solar energy in a vapor absorption cycle.

Overall, it appears that solar energy will continue to develop in the next years, owing to technical advancements, falling costs, and supporting laws and programs. However, the precise pace of increase will be determined by a number of variables and is impossible to estimate with confidence.

1.4 Objective

The objective of the study is to have an eco-friendly cold storage system by using the forecasted solar irradiation data and double effect vapor absorption refrigeration cycle. The following sectioned describes each of the objectives:

I. To Find a Suitable Location where solar radiation is in the higher range.

II. To Analyze and Use Prediction Models and Machine Learning Algorithms to Forecast Solar Irradiation.

III. To Implement a Double Effect Absorption Refrigeration System to a Cold Storage Using the Predicted Data and Performing Economic and Emission Analysis.

1.5 Organization of This Thesis

This thesis is divided into six chapters. The first chapter provides a brief explanation of the study's origins and premise. Finally, the relevance of the study and the study's aims are described. This chapter also explains the dissertation's structure. In chapter 2, a comprehensive literature review is done that has 4 sections. In the first section, Bangladesh's current energy situation is described. In the next section we showed the current work and research in solar energy. In the following section, the ongoing work that is done is the solar energy forecasting is described. Lastly, the current scenario for cold storage facilities integrated with vapor absorption cycle as well as the work and research in this field is mentioned. The methodology of the investigation is described in Chapter 3. There are also certain underlying assumptions that were used during the design process. The discoveries and final outcomes of the entire design process are described in 14 sections in Chapter 4. Chapter 5 contains the findings and an overview of the contributions. In addition, several future research directions linked to this study are discussed.

The literature mentioned in this study is listed in Chapter 6.

Chapter 2 Literature Review

For an active solar energy system solar irradiance data are very important [1]. The direct and diffuse irradiance are two components of the global irradiance on the horizontal plane. The amount of solar energy depends on the hydrosphere, atmosphere and biosphere. [2,3]. Small changes in solar energy can lead to climate change. [4,5]. To research the solar energy system, the accurate observation and analysis of change of solar radiation is important. [6]. In order to predict the solar radiation many methods were developed. They include satellite retrieval data, artificial intelligence, theoretical perimeter model and empirical model. [7-13]. Over the years many models were developed in order to predict the solar radiation.

2.1 Current Energy Scenario in Bangladesh

Rapid population growth, urbanization, and industrialization increased the country's energy consumption exponentially. Primary energy usage was 12.7 Mtoe in 2000 and 24.3 Mtoe in 2011 [40]. From 1992 to 2011, total energy consumption climbed by more than 200%. However, per capita primary energy usage in 2011 was 0.152 Mtoe. However, between 1980 and 2010, total primary energy use grew by 2.59% per year [41]. By 2020, power demand is expected to increase by 185% [42]. Primary energy demand is still increasing dramatically, and it is currently being met by diminishing fossil fuel (nonrenewable energy) sources such as natural gas, coal, oil, and petroleum products [43].

Biomass is a significant source of energy in Bangladesh, as it is used by 65% of the population who live in rural areas and 44% of whom live below the poverty line. Natural gas is also widely used in Bangladesh, particularly in power plants, fertilizer factories,

industrial entities, and most recently in the transport sector as compressed natural gas (CNG)

2.1.1 Fossil Fuel Energy Mix in Bangladesh

Natural gas, a substantial indigenous resource, is critical to Bangladesh's economic development. It provides 75% of main commercial energy and contributes 79.15% of power generating. Up till 2012, a total of 24 gas fields were identified, totaling 37.680 trillion cubic
feet (TCF) are confirmed reserves, of which 26.877 TCF is extractable. Currently, 20 gas fields are fully operational, with a total production of 10.514 TCF of natural gas as of June 2012

With the exception of the Haripur **oil** resource discovered in 1989 in the northwest of the Sylhet district, Bangladesh lacks significant oil reserves. The reservoir is estimated to contain 1.4 million tons of oil equivalent (Mtoe), with 0.84 Mtoe expected to be recoverable by 2004. However, because to poor oil quality and the presence of water in the **oil zone**, extraction efforts were terminated. As a result, for transportation, industrial heating, and small-scale power generation, Bangladesh mainly relies on imported crude oil and refined petroleum products.

Coal is a plentiful and affordable energy source not only in Bangladesh, but also globally. As the primary commercial energy source, coal currently accounts for 39.8% of global electricity output. Coal accounts for 3.25% of total electrical generation in Bangladesh. A national coal policy is being developed, and it is expected that effective planning and budget allocation would permit real development in the sector, which has traditionally

encountered administrative and technological impediments. So far, five coal seams have been identified in Bangladesh's northwestern region, with an estimated reserve of roughly 3300 million tons.

2.1.2 Renewable Energy Resources and Their Prospects

Renewable energy resources are gaining popularity in Bangladesh, owing to the need to diversify the energy mix and reduce reliance on fossil fuels. As of 2020, the country had a total installed renewable energy capacity of roughly 632 MW, with solar energy accounting for the majority (433 MW), according to the Sustainable and Renewable Energy Development Authority (SREDA). Wind power plants, while still in their infancy, have shown promise, with an installed capacity of around 56 MW. There are also ongoing efforts to generate energy from biomass, hydropower, and biogas. The government intends to generate 10% of total power from renewable sources by 2021, increasing to 20% by 2023.

2.2 Ongoing Work in the Field of Solar Energy

Bangladesh's ongoing attempts to generate solar energy have established the country as a pioneer in renewable energy adoption. Several organizations and programs are actively promoting the use of solar electricity in various areas. The Solar Home System (SHS) initiative, which has been implemented by the Infrastructure Development Company Limited (IDCOL) since 2003, is one of the important programs. By 2020, the SHS program will have installed over 5.6 million solar home systems, supplying power to over 20 million people in Bangladesh's rural areas.

Furthermore, utility-scale solar projects in Bangladesh are fast increasing. The 200 MW Teknaf Solar Park, the country's largest solar power plant, was launched in 2019. Several other solar parks are being built, including a 100 MW park in Mymensingh and a 50 MW

park in Feni. By 2020, Bangladesh's total installed solar capacity was expected to be around 433 MW.

Bangladesh's government has set lofty goals for increasing renewable energy's percentage of total electricity generation. By 2021, the goal is to generate 10% of total power from renewable sources. Solar energy makes a substantial contribution to this. In addition, the government has set a goal of installing one million solar irrigation pumps by 2025 in order to assist agricultural activities and rural development.

The continuous solar energy research in Bangladesh is motivated by the need to meet the country's expanding energy demand, reduce reliance on fossil fuels, and reduce greenhouse gas emissions. Continued investment, technology breakthroughs, and regulatory support are likely to boost solar energy development and deployment in Bangladesh, contributing to a more sustainable and resilient energy sector.

2.3 Ongoing Work in the Field of Solar Energy Forecasting

The use of statistical methods for predicting solar radiation has been a topic of active research for many years. In the early years, methods such as linear regression, multiple linear regression and Markov Chains were used for forecasting solar radiation. For example, in a study by Al-Sobaih et al. (1991), a Markov chain model was used to predict solar radiation at the site of King Khalid International Airport in Riyadh, Saudi Arabia. The results showed that the model was able to predict solar radiation with a correlation coefficient of 0.82.

In the subsequent years, the use of artificial neural networks has gained popularity for solar radiation forecasting. In a study by Lekras and Papalexopoulos (2003), an artificial neural network was used to predict solar radiation at the site of Nea Makri, Greece. The results showed that the model had an average correlation coefficient of 0.97.

In addition to the use of statistical and artificial intelligence approaches, the use of physical models has also been explored for forecasting solar radiation. In a study by Rojas et al. (2006), a physical model based on the Angstrom-Prescott relationship was used to predict solar radiation at the site of Los Angeles, California. The results showed that the model was able to predict solar radiation with an average correlation coefficient of 0.98.

In a recent paper by Yu et al**.** (2020), the authors proposed a novel hybrid model based on a combination of a deep neural network (DNN) and a support vector machine (SVM) to forecast solar radiation. The model was tested on a dataset of one-year hourly meteorological data and one-year hourly solar radiation data collected from the regional meteorological station in Hong Kong. The results showed that the proposed model outperformed the traditional methods in terms of accuracy and mean absolute error.

In another paper by Liu et al. (2019), the authors developed a statistical model to predict solar radiation using a multi-layer perceptron (MLP) neural network. The MLP model was tested on a dataset of one-year hourly meteorological data and one-year hourly solar radiation data collected from two sites in Hunan, China. The results showed that the MLP model had a higher accuracy and lower mean absolute error than the traditional models.

In a paper by Zhang et al**.** (2018), the authors proposed a hybrid model based on a combination of a support vector regression (SVR) and a recurrent neural network (RNN) to predict solar radiation. The model was tested on a dataset of one-year hourly meteorological data and one-year hourly solar radiation data collected from two sites in Hebei, China. The results showed that the proposed model outperformed the traditional models in terms of accuracy and mean absolute error.

In another paper by Sánchez-González et al. (2017), the authors developed a model based on artificial neural networks (ANNs) to predict solar radiation. The ANN model was tested

on a dataset of hourly meteorological data and hourly solar radiation data collected from a meteorological station in Mexico. The results showed that the ANN model had a higher accuracy and lower mean absolute error than the traditional models.

In a paper by Chen et al. (2016), the authors proposed a hybrid model based on a combination of a support vector machine (SVM) and a back-propagation neural network (BPNN) to predict solar radiation. The model was tested on a dataset of one-year hourly meteorological data and one-year hourly solar radiation data collected from two sites in China. The results showed that the proposed model outperformed the traditional models in terms of accuracy and mean absolute error.

In another paper by Chiou et al. (2015), the authors developed a statistical model to predict solar radiation using a multi-layer perceptron (MLP) neural network. The MLP model was tested on a dataset of one-year hourly meteorological data and one-year hourly solar radiation data collected from a meteorological station in Taiwan. The results showed that the MLP model had a higher accuracy and lower mean absolute error than the traditional models.

Not much work has been done in the context of Bangladesh. Prediction using Statistical models is very new. Also, neural network models involving ARIMA and LSTM are also very new in the machine learning field.

Navin Sharma et al. conducted a study in which they compared multiple regression techniques for generating prediction models for solar energy generation. Among the regression techniques examined were linear least squares regression and support vector machines (SVM) using multiple kernel functions [4].

Linear least squares regression is a well-known and commonly used regression approach for determining the best-fitting linear connection between input and output variables. It seeks to minimize the sum of squared discrepancies between anticipated and actual values. This approach would entail creating a linear relationship between the input meteorological data (such as temperature, humidity, and cloud cover) and the intensity of the sun or the production of electricity in the context of solar energy forecast. Support vector machines, on the other hand, are a type of supervised machine learning algorithm that can be applied to regression tasks. They aim to find an optimal hyperplane that maximizes the margin between the data points. In the case of solar energy prediction, SVM can be used to establish a non-linear relationship between the input weather data and solar intensity or power generation by utilizing different kernel functions.

Sharma et al. explored the performance of multiple kernel functions within SVM to assess their effectiveness in predicting solar energy generation. Different kernel functions, such as linear, polynomial, radial basis function (RBF), or sigmoid kernels, can capture various types of relationships between the input variables and the output.

The researchers likely evaluated the performance of these regression techniques by training and testing the models using historical solar intensity or power generation data from the NSRDB database. They would have divided the dataset into training and testing subsets, used the training data to train the models, and evaluated their accuracy and predictive power on the testing data. Evaluation metrics such as root mean square error (RMSE), mean absolute error (MAE), or coefficient of determination (R-squared) may have been used to compare the performance of the different regression techniques.

It's worth noting that Abuella and Choudhary proposed a solar energy prediction model using Artificial Neural Networks (ANNs), which are a type of machine learning algorithm

inspired by the human brain's neural networks. ANNs can capture complex non-linear relationships between the input weather data and solar intensity or power generation. Their study likely involved training ANNs on the collected solar intensity and weather data to create prediction models for solar energy generation.

By comparing the performance of different regression techniques, such as linear regression, SVM with various kernel functions, and ANN, researchers can identify the most effective approach for predicting solar energy generation. This knowledge can aid in the development of accurate and reliable models, enabling better regulation and integration of solar energy into the power grid and reducing the dependency on fossil fuel-based power generation.

2.4 Work in the of Field Vapor Absorption Refrigeration Cycle Based Cold Storage

The preservation of food products is a common practice globally. Currently, the majority of cold storage facilities using traditional vapor compression systems are fueled by grid energy produced from fossil fuels. It is employed in underdeveloped nations such as India. However, the fossil fuel supplies are rapidly running out and are predicted to be consumed over the next several decades. Additionally, the use of traditional fossil fuel-based electricity and unsustainable refrigerants in cold storages using vapor compression refrigeration (VCR) causes significant damage to the environment.

Thus, the creation of cold storage facilities based on vapor absorption systems and driven by sustainable energy is essential in this situation. For diverse refrigeration and air conditioning applications, several researchers worked on the solar-assisted single-effect vapor absorption refrigeration (VAR) system. For the purpose of cooling a room, Lizarte

et al. [16] created a solar-driven single-effect VAR system with a 4.5 kW refrigeration capability. For a fixed cooling demand of 3.5 kW, Basu and Ganguly [17] presented a single-effect VAR system driven by solar flat plate collectors and a photovoltaic array.

For the climate of Athens, Greece, Bellos et al. [18] carried out a parametric investigation of a solar-driven, single-effect vapor absorption system. A single-effect VAR system's performance was constructed and examined by Florides et al. [19] for a constant cooling load of 10 kW. An economic study of the system was also done. In the recent past, a few research projects on single-effect VAR system-based cold storage have also been described [20–24]. Several works on the double effect vapor absorption system have also been published in recent years. To understand the influence of different parameters on the performance of the system, Arora and Kaushik [25] carried out a parametric analysis on a single-effect and a double-effect VAR system.

Chapter 3 Methodology

In order to find a suitable location for this study solar energy mapping is necessary. Before that the data need to be collected, processed and prepared to be use in Python to generate the maps for suitable locations. This dataset collection, preprocessing and preparation is done in the first 3 sections of the methodology.

Next section, the solar energy mapping is generated. After that statistical model and neural network model is used to test and train the data collected from the suitable location. Right after that forecasting is done. Final predicted model can be found from performing feature expansion and PCA.

In the next sections of the methodology, summary of the overall system is described. The schematic diagrams of the cold storage and double effect VAR system are explained alongside their energy models. The description of the power system model is also shown in details.

Finally, the emission analysis table is shown.

3.1 Dataset

Data for determining the optimal site was obtained from Global Solar Atlas, an online solar resource established by the World Bank Group, the National Renewable Energy Laboratory (NREL), and Climate scope. Satellite photos, meteorological data, and ground measurements are used to generate the data. DNI (direct normal irradiance), GHI (Global horizontal irradiance), and $\boldsymbol{PV_{OUT}}$ (photovoltaic output energy simulated by the source) were the data gathered. In order to find the optimal position, the spots were spread out over

Bangladesh in a rectangular grid. The source yielded a total of 567 data sets, including DNI, GHI, and $\boldsymbol{PV_{OUT}}$.

Data for determining the optimal site was obtained from Global Solar Atlas, an online solar resource established by the World Bank Group, the National Renewable Energy Laboratory (NREL), and Climate scope. Satellite photos, meteorological data, and ground measurements are used to generate the data. DNI (direct normal irradiance), GHI (Global horizontal irradiance), and $\boldsymbol{PV_{OUT}}$ (photovoltaic output energy simulated by the source) were the data gathered. In order to find the optimal position, the spots were spread out over Bangladesh in a rectangular grid. The source yielded a total The National Solar Radiation Database was used to predict solar radiation. The National Solar Radiation Database data are hourly TMY files that comprise meteorological data as well as the three most common solar radiation measurements: global horizontal, direct normal, and diffuse horizontal irradiance. GHI and DHI are modeled using the REST2 and FARMS models, respectively, hence the data is synthetic.

3.1.1 General Information

The investigation focuses on GHI since it comprises the combination of DHI, DNI, and ambient solar radiation reflected from neighboring surfaces. GHI is regarded as a useful indicator for solar panel readings since it gives an accurate assessment of solar radiation.

The NSRDB data is collected at a frequency of once every 60 minutes, allowing for a detailed analysis of solar intensity variations over time. The investigation focuses on a specific location, (23.7 N 90.4 E) to assess solar energy generation patterns in that area.

To narrow down the analysis, the study focuses on data from the year 2020. This specific time frame enables a detailed examination of solar intensity patterns and their correlation with weather variables.

The dataset contains almost 50,000 unique observations, each with 16 characteristics. These characteristics include time values such as the month, day, hour, and minute. Additionally, the dataset includes the corresponding DNI measurements for each observation. Table 1 likely presents these features along with the corresponding DNI values, allowing for a comprehensive overview of the dataset's structure and the solar intensity measurements.

To improve the study, the dawn-Sunset-API is used to gather dawn and sunset times for each day. Using this data, a new Boolean column named 'isDay' is added to the dataset. This column indicates whether a particular observation falls within the daytime or nighttime period based on the sunrise and sunset times. This additional feature provides valuable information for understanding solar intensity variations throughout the day and facilitates the analysis of solar energy generation during daylight hours.

By incorporating these data and features, the analysis aims to develop prediction models that utilize machine learning techniques. These models can then provide high-confidence forecasts of solar generation, enabling better regulation and integration of solar energy into the existing power grid infrastructure.

3.1.2 Exploratory Data Analysis

When analyzing a dataset, it is important to understand the distribution of each feature and the relationships between different features. To gain insights into these aspects, several visualizations and statistical measures can be employed.

Histograms are a common visualization tool used to examine the distribution of a single feature. They divide the range of values into bins and display the frequency or count of data points falling into each bin. Histograms provide an overview of the data's shape, central tendency, and spread. They are particularly useful for identifying patterns such as normal distribution,

skewness, or outliers. Pie charts, on the other hand, are used to represent categorical data. They display the proportion or percentage of each category as a slice of a circle. Pie charts help visualize the composition of categorical variables and can be useful for understanding the relative frequencies of different categories within a feature. Box plots, also known as box-and-whisker plots, provide a concise summary of the distribution of a feature. They display the minimum, first quartile, median, third quartile, and maximum values of the data. Box plots can reveal the presence of outliers, skewness, and overall spread of the data. They are particularly useful for comparing the distribution of multiple features or groups.

A correlation matrix can be created to investigate the correlations between characteristics. The correlation matrix is a table that displays the pairwise correlations between all feature pairings in a dataset. The degree and direction of a linear link between two variables is measured by correlation. A heatmap may be used to illustrate the matrix, with the color of each cell representing the correlation value. Correlation matrices aid in the identification of feature dependencies, connections, and possible multicollinearity. In addition to correlation, the skewness index can provide insights into the distribution of each feature. Skewness measures the asymmetry of a distribution. A positive skewness indicates a long tail on the right side, while a negative skewness indicates a long tail on the left side. Skewness values closer to zero suggest a more symmetric distribution. By examining the

skewness index for each feature, you can assess the departure from normality and identify any skewness patterns.

Figure 3-1 is the distribution plot for different parameter for temperature, solar zenith angle, wind direction and wind speed.

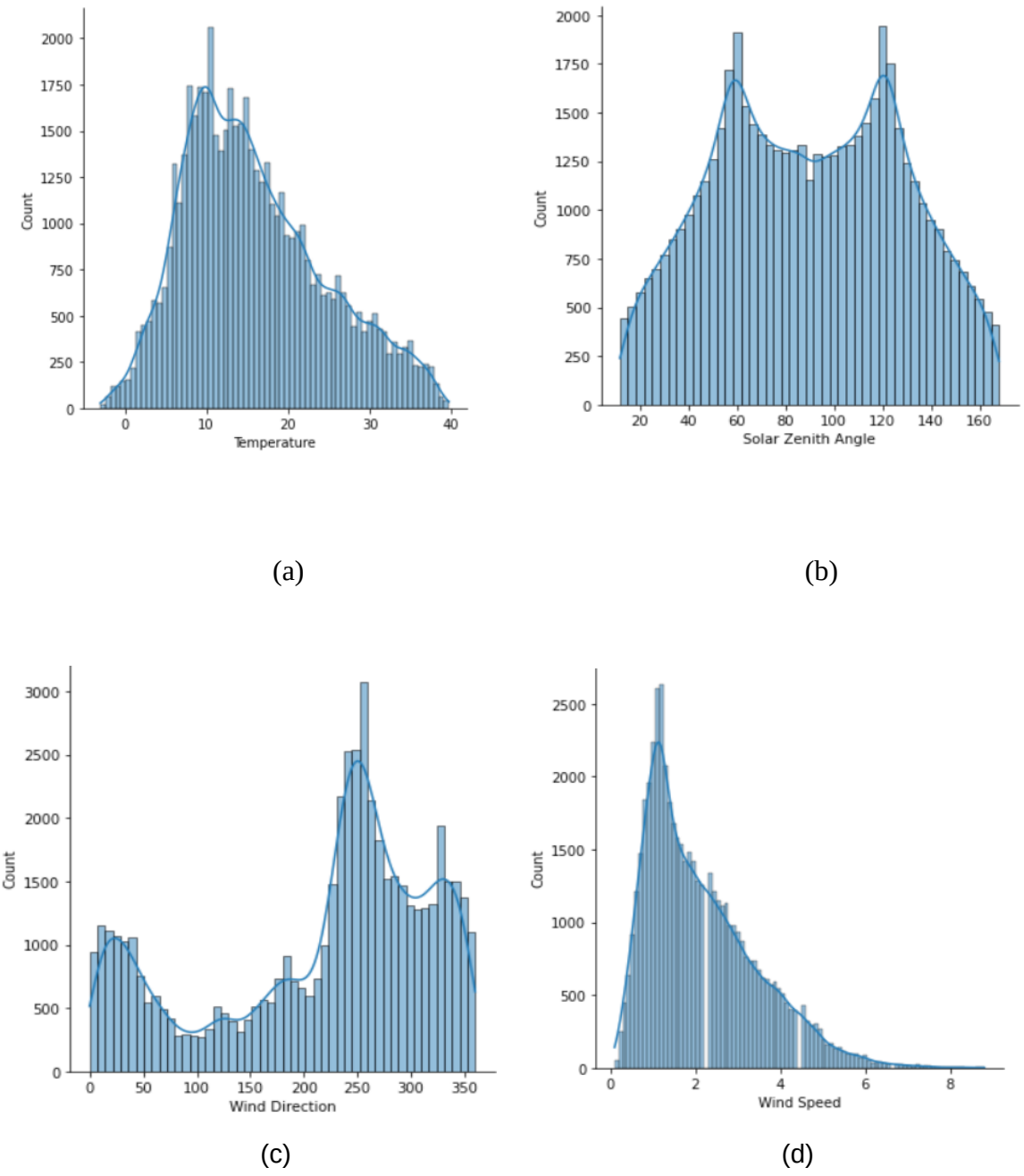

Figure 3-1 Distribution Plot for (a) Temperature and (b) Solar Zenith Angle (c) Wind Direction and (d) Wind Speed in the suitable location.

3.1.3 Skew Index

Skewness is a dimensionless quantity that indicates the extent to which a distribution deviates from symmetry. A positive skewness value indicates that the distribution has a longer or fatter tail on the right side, while a negative skewness value indicates a longer or fatter tail on the left side. A skewness value of zero suggests a symmetric distribution. **Table 3-1** describe the values of different features and their different skew index that is used in the models that have been used in the study.

Table 3-1: Skew Index table

Feature	Skew Index
Month	-0.01
Day	0.07
Hour	0
Minute Temperature	0 0.55
Cloud Type	1.30
Dew Point	-1.34
Fill Flag	3.96
Ozone	0.78
Relative Humidity	-0.091
Solar Zenith Angle	-0.00013
Surface Albedo	-0.71
Pressure	0.046
Precip. Water	0.62
Wind Direction	-0.73
Wind Speed	0.99
isDay	-0.038

3.2 Data Preprocessing

When analyzing the distribution curves, we detected outliers in the dataset. However, we made the decision to retain these outliers based on our assumption that they are a natural part of the weather observations we are studying. We believe that these extreme values hold significance within the context of our analysis. By opting not to remove the outliers, we acknowledge the potential impact of these values on the distribution and subsequent analysis. Outliers can have a notable influence on summary statistics, such as the mean and standard deviation, as well as the shape of the distribution. Their presence can introduce skewness and significantly affect calculated skewness indices, potentially indicating positive or negative skewness more prominently. Moreover, the outliers can also have implications for other statistical measures, including correlation coefficients. We recognize that outliers may have a disproportionate effect on the calculated correlations, potentially leading to misleading conclusions about the relationships between variables.

Regarding missing or NaN values, we are pleased to report that we did not find any in our dataset. This absence of missing data is advantageous for our analysis as it ensures a more balanced and comprehensive examination. We recognize that missing values can introduce challenges and biases, resulting in imbalanced observations. Without missing or NaN values, our dataset remains representative of the entire dataset, reducing potential biases and enabling more accurate assessments of the distribution, correlations, and other statistical measures.

In summary, **figure 3-2** shows the variable and feature relations between different parameter and their importance. our decision to retain outliers in the distribution curves is driven by our belief that they hold valuable information for the analysis of weather observations. This decision is made based on our domain-specific knowledge and

understanding of the data. Additionally, the absence of missing or NaN values in our dataset allows for a more reliable and balanced foundation for our data exploration and statistical analysis

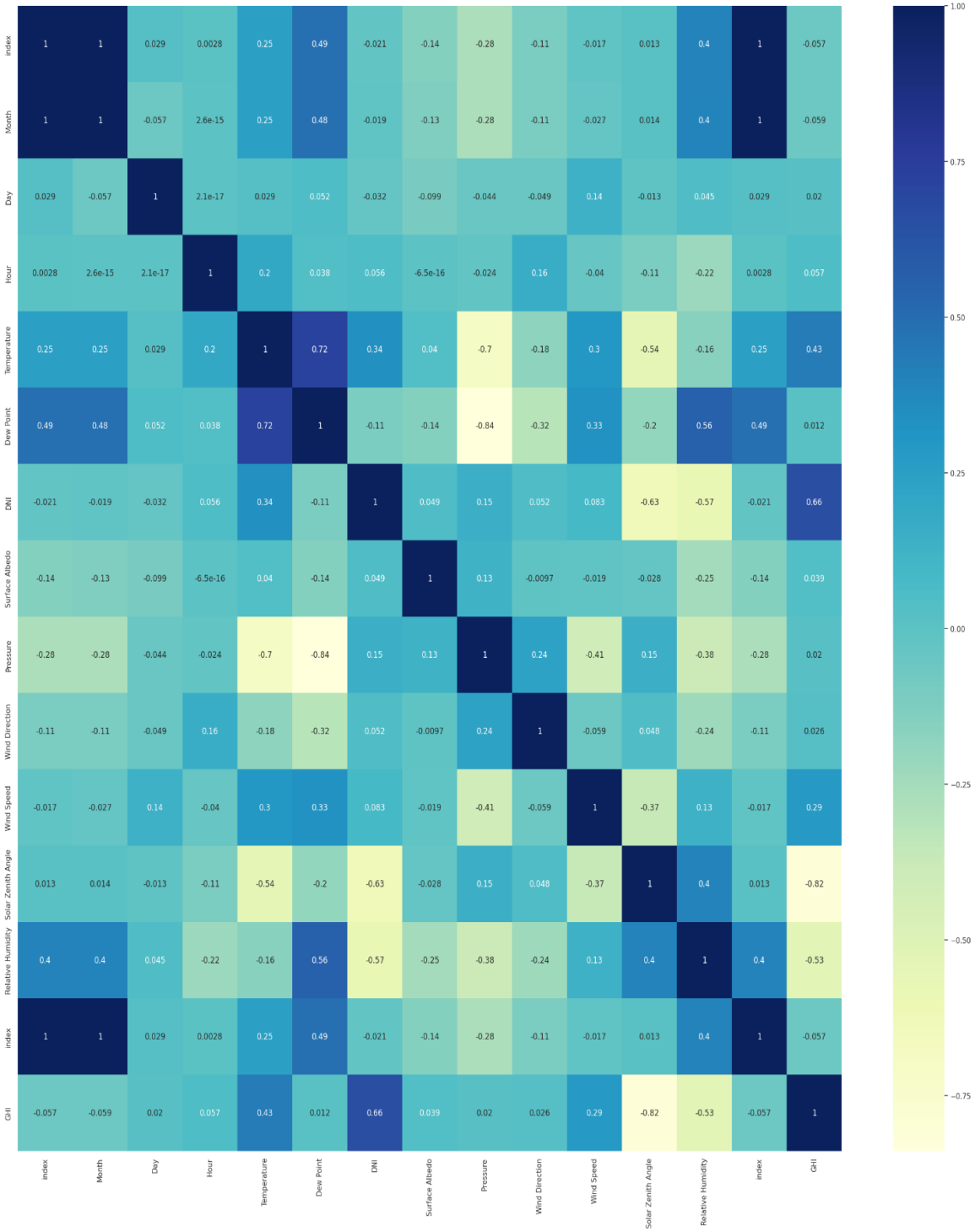

Figure 3-2 Heat Map for the Relationship Analysis Between Different Feature Parameter for Forecasting.

The Correlation Matrix has revealed a high correlation between the 'Dew Point' and 'Precipitable Water' features. When two features are highly correlated, it indicates that they exhibit a strong linear relationship. In this case, it suggests that changes in one variable are closely associated with corresponding changes in the other variable.

Since highly correlated features have almost the same effect on the dependent variable, keeping both features in the model may lead to multicollinearity issues. Multicollinearity occurs when there is a high correlation between predictor variables, which can make it challenging to accurately estimate the individual effects of these variables on the dependent variable.

To address this issue, the decision was made to drop one of the highly correlated features. By doing so, the model can avoid redundancy and potential multicollinearity problems. The next step was to test the performance of the baseline model by dropping each of the features, one at a time, and evaluating the impact on the model's performance. Based on the results obtained from these tests, the decision was made to drop the 'Dew Point' feature. The choice was likely based on various factors, such as the model's performance metrics (e.g., accuracy, precision, recall, etc.) or the feature's relative importance in contributing to the overall predictive power of the model. By dropping 'Dew Point', the model simplifies and reduces potential noise or redundant information while still maintaining a reasonable level of performance. It's important to note that the decision to drop a feature based on high correlation should be made in consideration of the specific context and goals of the analysis. Other factors, such as domain knowledge and the interpretability of the model, can also influence the choice of which feature to drop. Overall, the decision to drop the 'Dew Point' feature was made based on the evidence of high correlation with 'Precipitable Water' and the evaluation of the model's performance. This step helps optimize the model by reducing

multicollinearity and simplifying the feature set while preserving the model's predictive capabilities.

3.3 Dataset Preparation

Our job is to forecast sun intensity values for the next 48 hours. As a result, we create a one-to-one relationship between present weather measurements and DNI values 48 hours in the future.

3.4 Solar Energy Mapping

Python was used to create maps in order to discover a suitable location. These maps were created using a variety of data sources and algorithms. Over the map of Bangladesh, a rectangular grid was placed. This grid provided as a basis for dividing Bangladesh into smaller sections. In this scenario, the grid was made up of 27 columns and 23 rows, yielding 567 distinct points or cells inside the grid.

Data was collected for each of the individual points on the rectangular grid. This data collecting information about each point. Each point's data was processed and prepared after it was collected. This process entailed cleaning and categorizing the gathered data in order to ensure its uniformity and correctness. The data may have been prepared in a way that allows for additional analysis and visualization.

Heatmaps were developed based on the obtained information once the data was analyzed and compiled. Heatmaps are visual representations that employ color changes to indicate the intensity or density of a certain property over time and space.

The heatmaps created in the preceding phase were superimposed on a map of Bangladesh. This overlay enabled a visual comparison and study of the data against the country's

geographical characteristics. The heatmaps would emphasize areas with higher or lower intensity of the selected variables, revealing information about the applicability of certain locations.

"By submerging all three, we can find one of the suitable locations for our research."

The three heatmaps were merged to discover locations where the the value is in the higher range. **Figure 3-3** shows the flowchart for process mentioned.

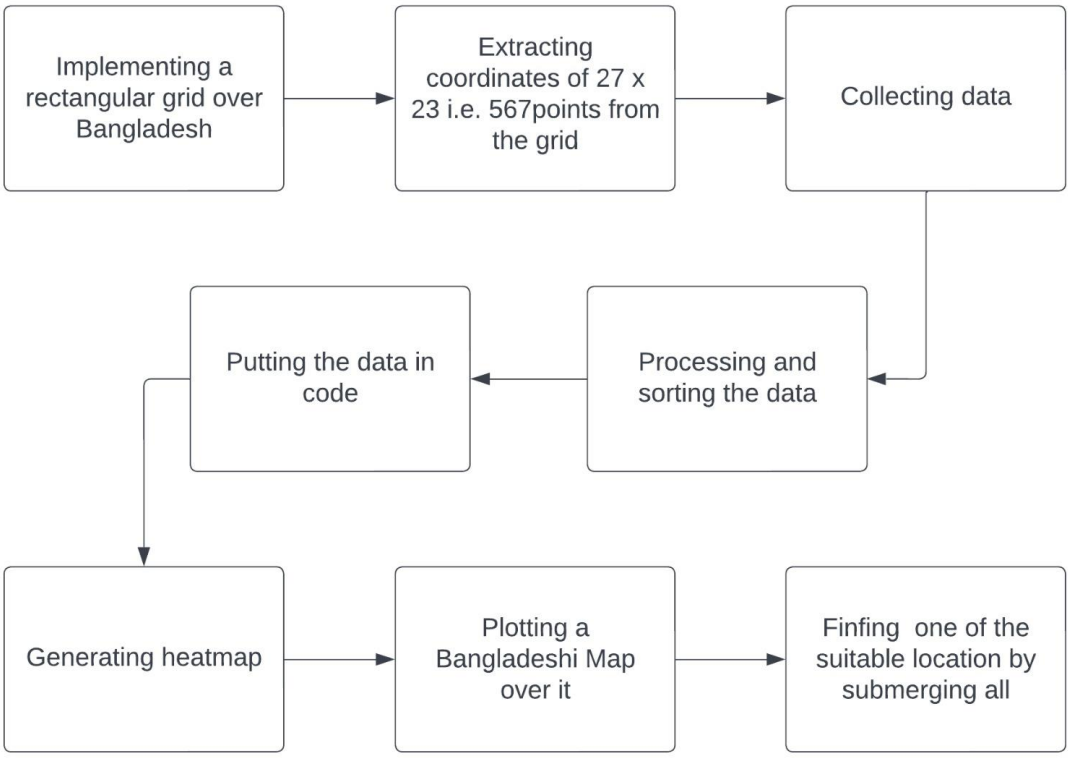

Figure 3-3 Flowchart for the solar mapping.

3.5 Statistical Models

Statistical methods for solar radiation forecasting entail the use of statistical models to forecast future solar radiation behavior based on historical data and pertinent meteorological variables without considering the physics of the system. These methods

seek to identify patterns and relationships in data in order to make precise predictions of solar radiation levels at certain time intervals.

3.5.1 Linear Regression

A linear regression model is a statistical approach for modeling the connection between one or more independent variables and a dependent variable. It presupposes that the variables have a linear connection, which means that the dependent variable may be written as a linear sum of the variables that are independent.

The formula for simple linear regression, where there is only one independent variable, can be represented as:

In this formula:

$$\boldsymbol{Y = \beta 0 + \beta 1 x X + \varepsilon} \quad \textbf{(1)}$$

- Y represents the dependent variable or the variable to be predicted.
- X represents the independent variable or the variable used to predict Y.
- β0 is the intercept term, which represents the value of Y when X is zero.
- β1 is the slope coefficient, which represents the change in Y for a unit change in X.
- ε represents the error term or the residual, which captures the deviation between the predicted value and the actual value of Y.

The goal of linear regression is to estimate the values of β0 and β1 that minimize the sum of squared residuals, which is a measure of the discrepancy between the predicted and actual values of Y. This estimation is typically done using a method called ordinary least squares (OLS), which finds the values of β0 and β1 that minimize the sum of squared residuals.

Once the values of β0 and β1 are estimated, they can be used to make predictions. Given a new value of X, the predicted value of Y can be calculated using the formula:

$$\boldsymbol{Y\_predicted = \beta 0 + \beta 1 X} \quad \textbf{(2)}$$

Multiple linear regression extends the concept to cases where there are multiple independent variables. The formula for multiple linear regression can be represented as:

$$\mathbf{Y = \beta 0 + \beta 1 X1 + \beta 2 X2 + \ldots + \beta n Xn + \varepsilon} \quad \textbf{(3)}$$

In this formula, X1, X2, ..., Xn represent the different independent variables, and β1, β2, ..., βn are the corresponding slope coefficients.

Linear regression can be further extended to include additional features such as interaction terms, polynomial terms, or logarithmic transformations to capture more complex relationships between the variables.

The coefficients (β0, β1, β2, ..., βn) in the linear regression model provide insights into the direction and magnitude of the relationship between the independent variables and the dependent variable. They can be interpreted as the change in the dependent variable for a unit change in the corresponding independent variable, assuming all other variables remain constant.

Lasso

Lasso (Least Absolute Shrinkage and Selection Operator) linear regression is a type of linear regression that uses regularization to improve prediction and feature selection. It introduces a penalty factor into the standard least squares objective function, urging the model to decrease the coefficients towards zero and essentially perform feature selection by pushing some coefficients to zero. The objective function in Lasso regression is modified by adding a penalty term based on the absolute values of the coefficients:

$$\boldsymbol{Minimize = Sum\ of\ Squared\ Residuals + \lambda \times Sum\ of\ Absolute\ Values\ of\ Coefficients} \quad \textbf{(4)}$$

The regularization parameter, also known as the tuning parameter, controls the penalty term. It defines how much regularization is given to the model. A higher value of causes the coefficients to shrink more, effectively forcing more of them to zero.

The Lasso regression approach promotes sparsity by reducing the coefficients of irrelevant or minor characteristics to zero. This attribute makes it beneficial for feature selection because it automatically finds and removes variables with little influence from the model.

Ridge

Ridge regression, also known as Tikhonov regularization, is a variant of linear regression that introduces a regularization term to the ordinary least squares objective function. Like Lasso regression, Ridge regression aims to improve the model's predictive performance and handle multicollinearity by shrinking the coefficients towards zero. However, Ridge regression uses a different type of penalty term.

The penalty term, like in Lasso regression, is controlled by the regularization parameter (lambda). However, in Ridge regression, is multiplied by the total of the coefficients' squared values, rather by the sum of their absolute values, as in Lasso regression. As a result, the coefficients have a varied effect.

Ridge regression's regularization term promotes the coefficients to shrink towards zero while keeping all predictors in the model. It lessens the impact of individual predictors without completely eliminating them. Ridge regression is therefore appropriate for scenarios with multicollinearity since it can assist stabilize coefficient estimates by lowering their susceptibility to correlated factors.

3.5.2 Polynomial Regression

Polynomial regression is a type of regression analysis that uses a polynomial function to represent the connection between the independent variable(s) and the dependent variable. By incorporating polynomial terms, it allows for a non-linear connection between the variables.

Polynomial regression may be expressed as follows:

$$\boldsymbol{Y = \beta 0 + \beta 1 X + \beta 2 X 2 + \beta 3 X 3 + \ldots + \beta n X n + \varepsilon} \quad \textbf{(5)}$$

In this formula:

- Y represents the dependent variable or the variable to be predicted.
- X represents the independent variable.
- β0, β1, β2, ..., βn are the coefficients to be estimated.
- X^2, X^3, ..., X^n represent the polynomial terms, where X^2 represents X squared, X^3 represents X cubed, and so on.
- ε represents the error term or the residual.

By introducing higher-order polynomial terms (e.g., X^2, X^3, etc.), polynomial regression can capture non-linear relationships between the variables. The coefficient estimates (β0, β1, β2, ..., βn) represent the effect of each term on the dependent variable.

The degree of the polynomial represents the highest power of X included in the model. For example, if the polynomial regression is of degree 2, the model would include the terms β0, β1*X, and β2* X^2. Increasing the degree of the polynomial allows for more flexibility in fitting the data but also increases the complexity of the model.

Polynomial regression is often performed using least squares estimation, similar to linear regression. The goal is to estimate the coefficients (β0, β1, β2, ..., βn) that minimize the sum of squared residuals, capturing the discrepancy between the predicted and actual values of the dependent variable.

It's important to note that while polynomial regression can capture non-linear relationships, using higher-degree polynomials can lead to overfitting the data, especially when the sample size is small. Regularization techniques such as Ridge regression or Lasso regression can be employed to mitigate overfitting and improve the model's generalization performance.

Polynomial regression may be an effective tool for modeling complicated interactions between variables, but it is critical to evaluate the trade-off between model complexity and interpretability, as well as to test the model's performance on unknown data.

3.5.3 Feature Expansion Regression

The methodology known as feature expansion entails the derivation of novel features through the utilization of transformational or combinatorial methods on extant features within a given dataset. This study endeavors to encapsulate non-linear connections or interactions between variables, thus facilitating the development of more intricate and eloquent models.

In the absence of Principal Component Analysis (PCA), the process of feature expansion generally entails the generation of novel features via the application of mathematical operations or transformations to the pre-existing features. The aforementioned computations may incorporate polynomial assets, interactional features, logarithmic modifications, exponential expressions, trigonometric functionalities, or alternative domain-specific conversions.

As an illustration, contemplate a dataset encompassing two distinct variables, namely X1 and X2. In the absence of Principal Component Analysis (PCA), the process of feature expansion may comprise the inclusion of polynomial expressions such as $X1^2$, $X2^{2,}$ X1X2 (representing interaction terms), or even more complex terms such as $X1^3$, $X1X2^2$, etc. This procedure endeavors to amplify the feature space through the generation of novel columns that encompass a diverse range of distinct combinations and transformations of the initial features.

The utilization of feature expansion methodology devoid of Principal Component Analysis (PCA) presents a versatile technique capable of capturing intricate interrelationships

between variables. Nonetheless, incorporating a larger number of features in a dataset may result in a concomitant increase in dimensionality. This, in turn, may foster an array of potential hurdles, such as the notorious curse of dimensionality, heightened computational complexity, and an elevated likelihood of overfitting when the quantity of features surpasses the quantity of observations.

On the contrary, the process of feature expansion utilizing PCA entails a dual-stage operation. Initially, the fundamental features are subjected to Principal Component Analysis (PCA) for the purpose of achieving a collection of linearly independent features, denominated as principal components. The present study demonstrates that the principal components derived in this investigation are formed through linear combinations of the initial features, and are subsequently ranked in order of the amount of variance that they account for. Subsequently, a subset of the primary components may be chosen to create an extended feature space.

Principal Component Analysis (PCA) enables the reduction of dimensionality through the selection of a subset of principal components that exhibit a significant proportion of the variance in the source data. By eliminating non-critical elements, the reduction of the dimensionality of the feature space results in the retention of significant data.

The principal components that have been selected may subsequently be utilized as extended features for subsequent modeling purposes. The strategy proposed herein serves to address the challenges that stem from having feature spaces with high-dimensionality. Specifically, it directs attention towards the salient components, effectively mitigating the impact of noise and duplicative information in the analysis.

The utilization of principal component analysis (PCA) for feature expansion can prove to be notably advantageous when managing datasets that possess an extensive array of features or when there exists a significant degree of intercorrelation amidst the initial

features. This method offers a means of diminishing the dimensionality of data while preserving its fundamental features for use in modeling.

It is imperative to acknowledge that employing Principal Component Analysis (PCA) can potentially diminish the comprehensibility of the augmented characteristics, given that they represent linear amalgamations of the primary features. Moreover, principal component analysis (PCA) postulates linear associations among variables and may not effectively capture intricate, nonlinear relationships.

In brief, the absence of principal component analysis (PCA) in feature expansion facilitates increased versatility in modeling through the generation of novel features rooted in mathematic operations and transformations. The incorporation of dimensionality reduction through the selection of a subset of principal components aiming to capture the most notable information from the original features is achieved through feature expansion employing Principal Component Analysis. The selection between these two methods is reliant upon the distinct features of the dataset, the intricacy of the associations, and the desired compromise between interpretability and the reduction of dimensional variables.

3.5.4 Regression Trees

The theoretical framework of regression trees is centered on the principle of recursive binary partitioning, whereby the feature space is systematically divided into increasingly smaller subsets in a hierarchical fashion, culminating in a tree-shaped configuration. The utilization of regression trees involves the projection of a tree-based structure onto the training dataset to facilitate predictions of continuous response variables.

The theoretical framework pertaining to regression trees is comprised of essential constituents, which include:

- The regression tree algorithm employs an approach to establish the most optimal splitting criterion at each node through partitioning the data into two subsets based on a selected feature and its corresponding threshold value. The prevalent criteria for splitting in regression trees involve the minimization of sum of squared errors through measures such as variance reduction or mean squared error reduction.
- The process of recursive splitting involves initiating the tree-building process with a root node that represents the entirety of the dataset. The algorithm ascertains the optimal feature and threshold value for partitioning the data into two child nodes. The aforementioned division procedure is repetitively implemented on every offspring node, leading to a hierarchical framework wherein each inner node characterizes a partitioning criterion and every terminal node indicates a prognosticated value.
- The process of constructing a tree perseveres until specific cessation criteria have been satisfied. Commonly employed stopping criteria involve attaining a specified maximum tree depth, ensuring a minimum number of samples assigned to each leaf, or terminating the splitting of nodes when there is no considerable enhancement in prediction accuracy.
- The prediction of leaf nodes: Upon the completion of the tree-building procedures, the terminal nodes store the anticipated values for the response variable. The anticipated output value assigned to each leaf node is commonly computed as the arithmetic or median average of the target variable encompassed by that particular region.
- The process of restricting the size and complexity of a decision tree model, commonly referred to as pruning, serves to minimize overfitting and simplify the structure of the model. After the initial decision tree is constructed, pruning techniques can be employed to achieve these objectives. The deployment of methodologies, such as cost complexity pruning, otherwise known as weakest link pruning, entails the utilization of a complexity

metric and an adjustment factor, in an effort to achieve the ultimate equilibrium between uncomplicated models and their corresponding predictive accuracy.

The theoretical underpinnings of regression trees facilitate their ability to effectively capture non-linear associations, interdependencies, as well as hierarchical structures within the data. The said representation furnishes interpretability and intuitiveness in regards to the associations that exist between distinct features and the target variable. Moreover, the utilization of regression trees offers the ability to adequately manage both numerical and categorical features, thereby obviating the necessity for profound data preprocessing.

Nonetheless, **figure 3-4** regression trees are susceptible to overfitting, which ultimately leads to insufficient generalization when applied to unfamiliar data. In order to address the issue of overfitting and enhance the efficacy of regression trees, ensemble approaches such as random forests or boosting techniques are frequently utilized. These methods involve the aggregation of multiple trees in order to generate predictions that are more robust and reliable.

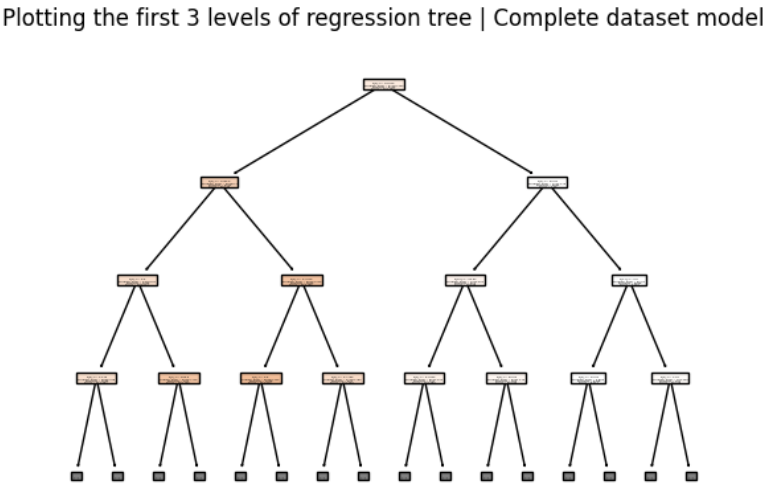

Figure 3-4 Regression Tree

3.5.5 SVM Regression

The utilization of Support Vector Machines (SVM) is not limited to classification alone, as it can also be employed for regression-based tasks. Support Vector Regression (SVR), which is also referred to as SVM regression, constitutes a machine learning approach that endeavors to ascertain a function that approximates the association between the input variables and the continual target variable.

The following section presents a succinct exposition on the operational mechanics of Support Vector Machine regression.

In regression analysis, it is standard practice to commence by procuring a collection of labeled data, comprising input features (X) and associated target values (Y), as the foundation for training.

The scaling of input features is of significant importance in achieving similarity in their ranges. Frequently utilized methods for scaling data comprise normalization (i. e, transforming to a predefined range) or standardization (i. e, centering on the mean and scaling to unit variance).

The model formulation for support vector machine (SVM) regression involves the identification of a hyperplane that optimally fits the training data while simultaneously minimizing the margin violations. The definition of a hyperplane is contingent upon a specific collection of support vectors which comprise a subset of the training data points. This subset of vectors is chosen due to their proximity to the hyperplane in question.

In the context of Support Vector Regression (SVR), the objective is to minimize the structural risk functional, comprising a loss function and a regularization term. This serves as an optimization approach aimed at minimizing the expected error between predicted and observed values. The loss function is responsible for quantifying the discrepancy between the predicted and factual target values, whereas the regularization term serves the function

of modulating the level of intricacy of the model, with the objective of staving off overfitting.

The kernel trick is a method utilized in SVM regression to address non-linear associations existing between input features and the target variable. Through the process of mapping the input features to a feature space of higher dimensions, the Support Vector Machine (SVM) regression model is equipped to perform non-linear transformations in an implicit manner, negating the requirement for explicit computation of such transformations.

The process of optimizing the performance of SVM regression involves tuning various parameters, including the regularization parameter (C),kernel-specific parameters (such as the degree of the polynomial kernel or the Gaussian kernel width) and the kernel type (such as linear, polynomial or radial basis function). The exploration of parameter space through cross-validation techniques is commonly employed for the purpose of achieving an optimal parameter combination.

Anticipated outcome: Following completion of training and optimization of the SVM regression model, it can be utilized to generate forecasts for unobserved data. The computational model derives the anticipated target values by relying on both the input features and the acquired hyperplane knowledge.

Support Vector Machine (SVM) regression can be a valuable approach for addressing non-linear associations between the input characteristics and the objective variable in situations where the data set is limited to small or medium sizes. The model is proficient in managing both linear and non-linear regression tasks through the implementation of suitable kernel functions. Support Vector Machine (SVM) regression is proficient in effectively managing outliers, owing to the margin-based formulation.

SVM regression encounters computational complexity issues when dealing with large-scale datasets. Furthermore, the interpretability of models may be restricted in comparison to that of linear regression models.

The SVM regression technique presents a potent methodology for performing regression tasks. It amalgamates the fundamental principles of support vector machines and regression analysis with the aim of identifying an optimal hyperplane that harmonizes well with the training data, and performs commendably on previously unseen data.

3.6 Neural Network Model

Neural networks are a type of machine learning algorithm based on a collection of connected units called neurons. These neurons are organized into layers and are connected to each other in a specific pattern. Neurons in one layer are connected to neurons in the next layer, forming a network of connected neurons. The neurons in each layer receive input signals from the previous layer, process the signals, and transmit the processed signals to the next layer. Once all the signals have been processed, the output of the network is the prediction of the data. **figure 3-5** Neural networks learn from the data they receive by adjusting the weights and biases of the neurons in response to the errors made in the prediction. Over time, the weights and biases of the neurons are adjusted until the error is minimized and the prediction is accurate.

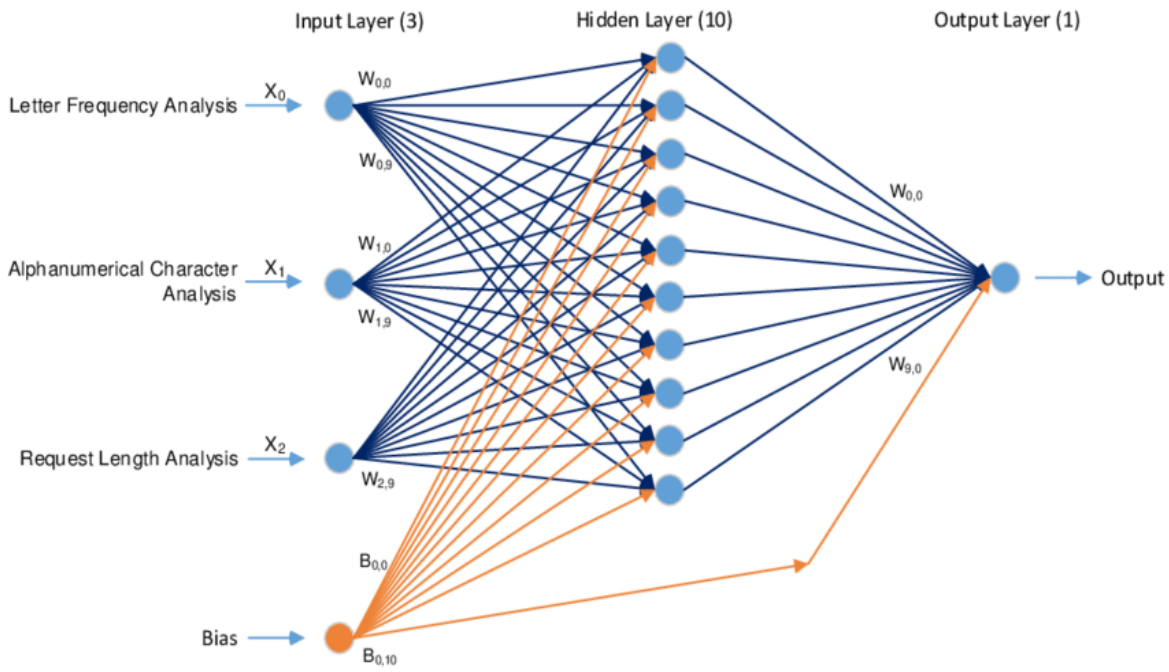

Figure 3-5 Neural Network for Training Data

3.6.1 Artificial Neural Networks (ANNs)

Artificial neural networks (ANNs) represent a specific category of machine learning models that draw their fundamental design inspiration from the structural and functional characteristics of the human brain. Every individual neuron within a neural network undergoes the reception of inputs from the preceding layer, proceeds with a computation, and ultimately generates an output that is subsequently disseminated to the successive layer. The synaptic connections established between neurons possess weights that depict the magnitude of connectivity.

An understanding of the operation of an artificial neural network can be achieved through the utilization of a diagram **figure 3-6** and a sequential description of the process.

1) The **input layer** is the foremost stratum of the neural network system. This refers to the attributes or variables that are offered as inputs to the network. Every input

is depicted as a solitary node, and no calculation is executed within this stratum. The input layer transmits the input values to the subsequent layer without any processing or manipulation.

2) The neural network structure often includes one or more **hidden layers** following the input layer. The concealed layers are endowed with the task of extracting and acquiring sophisticated patterns in the information. Every individual neuron within a concealed stratum is endowed with the capability to receive inputs from the preceding layer and thereafter, perform an executed manipulation by computing a weighted sum of the corresponding inputs, utilizing an activation function. The resultant of each neuron is utilized as the input for the subsequent layer.
3) The terminal layer of the neural network is known as the **output layer**. This function generates the ultimate forecast or outcome through the utilization of the knowledge acquired by the concealed layers. The quantity of nodes present in the output layer is reliant upon the type of problem that is being addressed. In the context of a binary classification task, it is possible to employ a solitary output node that signifies the probability of the affirmative class.
4) In neural networks, the interconnection between neurons is characterized by a weight, denoted as "w." The magnitudes of these weights establish the correlation intensity and are acquired through the training period of the network. Moreover, every individual neuron applies an activation function to the weighted accumulation of its inputs, thereby incorporating non-linear characteristics within the neural network. Activation functions, commonly utilized in neural networks, comprise of sigmoid, ReLU, or tanh.
5) The process of computing outputs within an artificial neural network (ANN) is commonly referred to as forward propagation. The neural network architecture

commences with the reception of inputs at the input layer, which subsequently transmit them to the initial hidden layer's neurons. In the hidden layer of a neural network, every individual neuron performs a calculation involving the summation of its inputs that are weighted accordingly, followed by the application of an activation function, which ultimately generates an output. This iterative process is executed for every successive layer until the final output layer is attained. The ultimate product of the neural network is generated by the output layer in the form of the predicted output.

6) Training and Backpropagation: An ANN is trained by altering the weights of the connections to minimize the discrepancy between expected and actual outputs. Backpropagation is a method that is commonly used in this procedure. It entails computing the error at the outcome layer and transmitting it back across the network to update the connection weights. This iterative approach is done until the network learns to anticipate accurately.

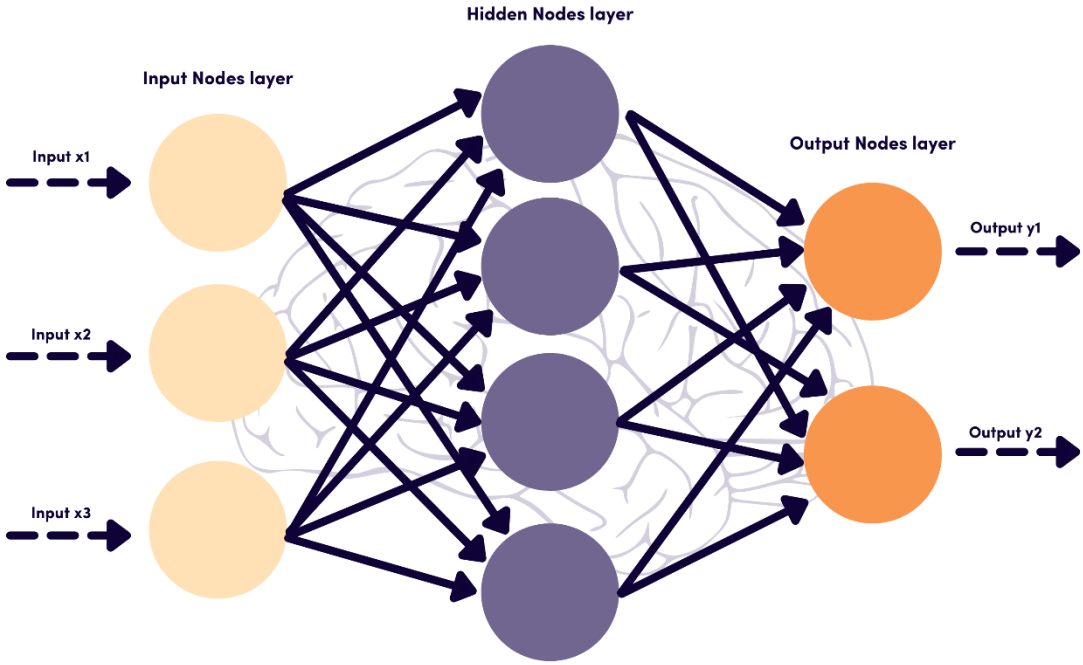

Figure 3-6 ANN

3.6.2 Neural Basis Expansion Analysis for Time Series

The N-BEATS algorithm employs fully connected neural networks to effectively capture both the historical and prospective patterns of a temporal sequence. Aiming to furnish precise and readily comprehensible projections for time series data, the present study endeavors to merge the retrospective (backcast) and prospective (forecast) estimations.

The retrospective approach, commonly known as backcasting, entails visualizing a future goal and working backwards to identify what steps need to be taken to achieve it. This method helps to create a path towards the desirable outcome by considering possible barriers and identifying strategies to overcome them. Backcasting is a widely used tool in several disciplines, including environmental planning, urban design, and social sciences. Its effectiveness lies in its ability to inspire creativity and generate innovative ideas for problem-solving.

The phase denoted as backcast assumes the task of capturing the historical behavior of the given time series. This methodology involves forecasting the antecedent historical data preceding a given target point. The process of executing the backcast involves the utilization of fully connected neural networks (FCNNs) to analyze and interface with the input time series data.

The given window effectively moves across the time series, systematically acquiring distinct portions of historical data. The Fully Convolutional Neural Network (FCNN) analyzes each segment and subsequently produces a forecast specific to that segment.

The architecture of the FCNN incorporates a multitude of fully connected layers that are augmented with nonlinear activation functions, characterizing its operational framework within an academic context. The determination of the number of layers and their respective dimensions is contingent upon the complexity inherent in the time series under consideration, as well as the desired capacity of the model.

The following prediction has been made regarding future occurrences:

The prognostication stage anticipates forthcoming values of the time series. The approach involves employing a secondary set of fully connected neural networks (FCNNs) to produce predictions by utilizing the outcomes derived from the backcasting phase.

The forecast phase employs a sliding window methodology akin to that used during the backcast phase. During the backcast phase, this particular approach moves in a sliding fashion across the anticipated values, effectively capturing diverse segments of these predictions. This takes place in a manner consistent with academic writing style. The Fully-Connected Neural Network (FCNN) employs a systematic approach to sequentially process individual segments, thereby producing a prognostication for each segmented unit.

The forecast architecture of FCNN may exhibit dissimilarities from the backcast architecture of FCNN. The architecture of a neural network may exhibit variability in the quantity of layers and dimensions, as well as in the choice of activation function. The pliability inherent in the model permits it to apprehend varied patterns within forthcoming projections.

The synthesis of forecasts or predictions, commonly referred to as combining predictions, is a widely applied technique in statistical analysis and decision-making processes. This method involves aggregating multiple predictions generated by various models or experts to improve the accuracy and reliability of the overall prediction. The combination of predictions can be executed using a variety of methods, including simple averaging, weighted averaging, or machine learning-based approaches. Overall, combining predictions has proven to be a valuable tool in enhancing the quality of predictions across a range of diverse applications.

The final forecast is derived by amalgamating the prognostications emanating from the backcasting and forecasting stages. In conventional practice, the ultimate prediction is acquired by computing a weighted aggregate or a sequential arrangement of the anticipated outcomes.

During the training process, the weights for amalgamating the predictions can be acquired through learning. The present model is designed to optimize the weights in order to minimize the discrepancy that exists between the predicted values and the actual values of the target time series.

One of the fundamental components of skill acquisition is training, which involves the systematic transfer of knowledge, skills, and behaviors from one person or group to another. In various fields, training serves as a crucial tool for improving performance, boosting efficiency, and enhancing the overall quality of work. It can be especially useful

when new technologies, methods, or processes are introduced. Additionally, training can also facilitate professional development and growth, leading to increased job satisfaction and opportunities for career advancement. Therefore, training is a vital aspect of organizational success, and it is essential for individuals to continually update their skills and knowledge through ongoing training initiatives.

The training of the N-BEATS model like **figure 3-7** is carried out through a supervised learning framework. The methodology aims to reduce a loss function which assesses the deviation between the forecasted and observed values of the target time series.

The selection of the loss function can be determined by the inherent characteristics of the prediction task at hand. An instance of a ubiquitous practice in the literature concerning continuous-valued time series analysis involves the frequent utilization of mean squared error (MSE) loss.

The aforementioned model is trained through the utilization of optimization techniques based on gradients, namely stochastic gradient descent (SGD) and Adam. The computation of gradients via back propagation facilitates the adjustment of the model's parameters, specifically its weights and biases, for the purpose of enhancing its predictive capabilities.

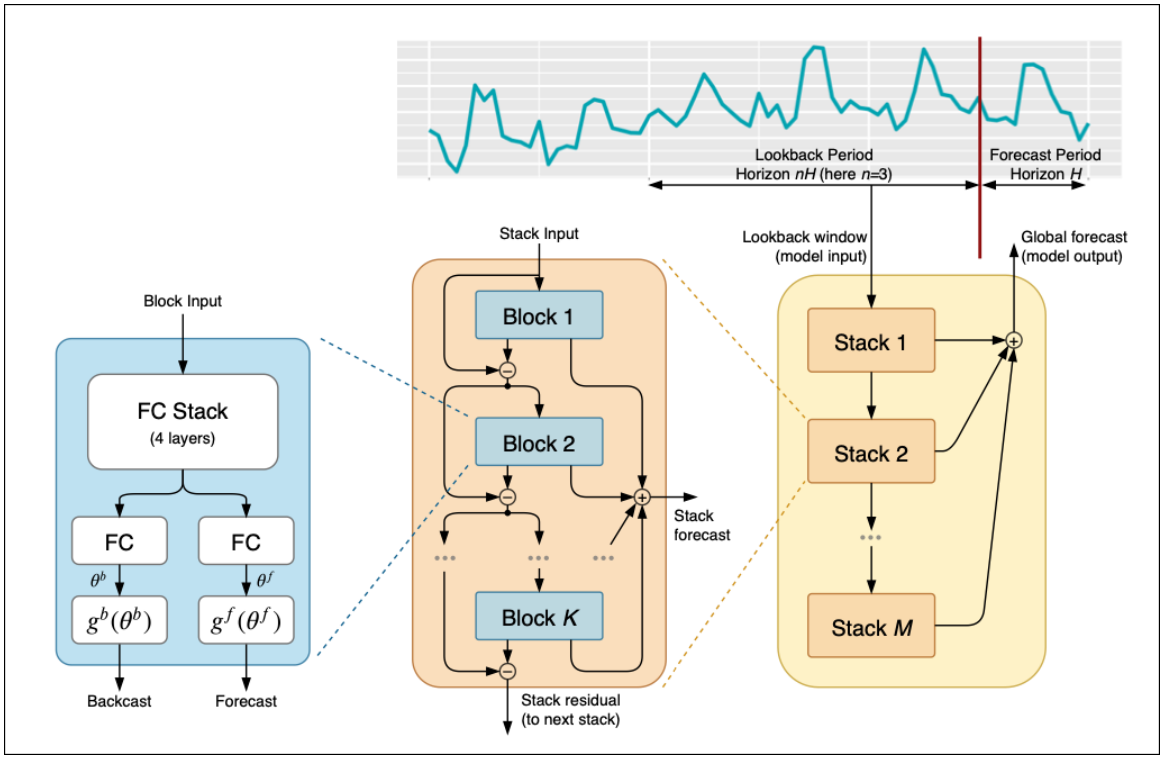

Figure 3-7 N-BEATS

3.6.3 Algorithm for Neural Networks

These following steps were taken for both the prediction algorithms

1. Data Collection: The first step for the Prediction analysis of solar radiation prediction is to collect data. The data should include historical solar radiation data from the past few years, depending on the geographical location, and other meteorological variables such as air temperature, wind speed, cloud cover, humidity, etc.

2. Data Pre-processing: The next step is to pre-process the data. This includes the removal of outliers and any other data points that might be corrupt. The data should also be normalized to ensure that all variables are on the same scale.

3. Model Selection: After the data is pre-processed, the next step is to select the appropriate model for the analysis. A neural network model is suitable for this task as it is capable of learning complex relationships between the input and output variables.

4. Model Training: Once the model is selected, it needs to be trained on the pre-processed data. This involves adjusting the model parameters to find the optimal configuration for the model. This is done by running a number of trials and testing the model's performance on the training data.

5. Model Testing: After the model is trained, it needs to be tested on unseen data to check its performance. This is done to check if the model is able to generalize to new data.

3.7 Forecasting

These approaches were designed to explore different strategies and evaluate their effectiveness in predicting the target variable. The two methodologies are described as follows:

1. In the first technique, we created a single model and trained it using 80% of the available data. This model was then used for testing as well. The training set comprised a representative portion of the data, allowing the model to learn patterns and relationships within the features. By training and testing the model on the same dataset, we aimed to evaluate its performance in terms of metrics such as accuracy, precision, recall, or the root mean squared error (RMSE).
2. Day and Night Model Approach: The second methodology involved adopting an alternative approach where we developed two separate models: one for the day data and another for the night data. To implement this approach, we divided the training set into two distinct subsets based on the "isDay" column. The day subset contained instances corresponding to

daytime observations, while the night the subset consisted of instances representing nighttime observations. We then trained the day model using the day training data and the night model using the night training data.

During the testing phase, we again divided the test set into separate day and night subsets using the "isDay" column. We used the day model to predict the Direct Normal Irradiance (DNI) values for the day subset and the night model to predict the DNI values for the night subset. Finally, we combined the two prediction sets to obtain the complete set of predicted DNI values. Subsequently, we computed the root mean squared error (RMSE) of the test set by comparing the predicted DNI values with the actual values.

By implementing these two methodologies, we aimed to explore different modeling strategies and assess their effectiveness in predicting the DNI values. This allowed us to compare the performance of the single model approach with the day and night model approach, providing insights into which approach yielded better results in terms of accuracy and predictive capability.

The issue of zero values in the dataset was addressed in the second way we used. We discovered that the majority of the zero values correlate to the time periods before sunrise and after dusk when there is no direct sunlight accessible. We took extra effort in constructing the second technique to accommodate for this.

In this approach, we divided the training set into two subsets: one for daytime data and another for nighttime data. This division was based on the "isDay" column, which indicated whether a particular observation occurred during the day or night. By separating the data into these subsets,

we ensured that the models were trained and tested specifically for the corresponding time periods.

During the training phase, the day model was trained using the daytime training data, which mainly consisted of non-zero values. Similarly, the night model was trained using the nighttime training data. This separation allowed the models to capture the specific patterns and relationships relevant to each time period.

When it came to testing, we divided the test set into two subsets, day and night, based on the "isDay" column. We then used the day model to predict the DNI values for the day subset and the night model to predict the DNI values for the night subset. By doing so, we accounted for the presence of zero values during the corresponding time periods, as the models were specifically trained to handle these situations.

To evaluate the performance of our models, we utilized the root mean squared error (RMSE) score as the evaluation metric. The RMSE score measures the average difference between the predicted DNI values and the actual DNI values. Lower RMSE scores indicate better model performance, as it indicates that the model's predictions are closer to the actual values.

In our analysis, we considered linear regression, along with lasso and ridge regression, as our baseline models. These models provided a starting point for our analysis and helped establish a benchmark for comparison. Additionally, we explored linear regression with feature expansions, both with and without principal component analysis (PCA), to improve the performance of our models. Feature expansion techniques, such as polynomial features or interaction terms, allow for capturing more complex relationships between variables, potentially enhancing the model's predictive power.

By considering these different models and techniques, we aimed to assess the performance of various approaches and identify the best-performing model that minimizes the RMSE score. The use of different methodologies and model variations allowed us to thoroughly evaluate and compare their performance in predicting GHI values, leading to insights on the effectiveness of each approach.

$$\mathbf{RMSE} = \sqrt{\sum_{\mathbf{i=1}}^{\mathbf{n}} \frac{(\hat{\mathbf{y}}_\mathbf{i} - \mathbf{y}_\mathbf{i})^\mathbf{2}}{\mathbf{n}}} \tag{6}$$

3.8 Feature Expansion

We incorporated weather observations from neighboring historical time periods to broaden the feature set for forecasting DNI values. We began with 15 features and expanded the number of features to 15*(n+1) after the nth expansion. We incorporated weather observations from neighboring historical time periods to broaden the feature set for forecasting DNI values. We began with 15 features and expanded the number of features to 15*(n+1) after the nth expansion.

3.9 Principal Component Analysis

As the feature set expanded with the inclusion of weather observations from adjacent past time points, it became evident that the size of the feature set increased significantly for larger values of 'n'. This expansion posed a challenge in terms of model complexity. Having a large number of features can lead to computational burdens, longer training times, and potential overfitting. To address this issue, we employed Principal Component Analysis

(PCA) to reduce the dimensionality of the feature space while retaining the most relevant information.

PCA allowed us to transform the expanded feature set into a set of linearly uncorrelated variables, known as principal components. These principal components were obtained by projecting the original features onto a new orthogonal basis that captured the maximum amount of variance in the data. By selecting a subset of the principal components with sufficiently high explained variance, we effectively reduced the dimensionality of the feature set while preserving the most informative aspects.

In addition to linear regression, we explored various other regression models to compare their performance in predicting DNI values. These included polynomial regression, regression trees, support vector machine (SVM) regression, and artificial neural networks (ANN). Each of these models offered distinct advantages and capabilities in capturing non-linear relationships, handling complex decision boundaries, and learning from intricate patterns in the data. By applying these alternative regression techniques to both methodologies, we aimed to evaluate their effectiveness and identify the best-performing model for DNI prediction in our specific context. This comparative analysis provided valuable insights into the strengths and limitations of different modeling approaches and helped inform our final choice of models for predicting DNI values.

In **figure 3-8** Data training, is an important phase in the development and training of machine learning models. It is the act of giving a huge quantity of data to an algorithm or model to enable it to understand patterns, correlations, and make predictions or judgments based on that data.

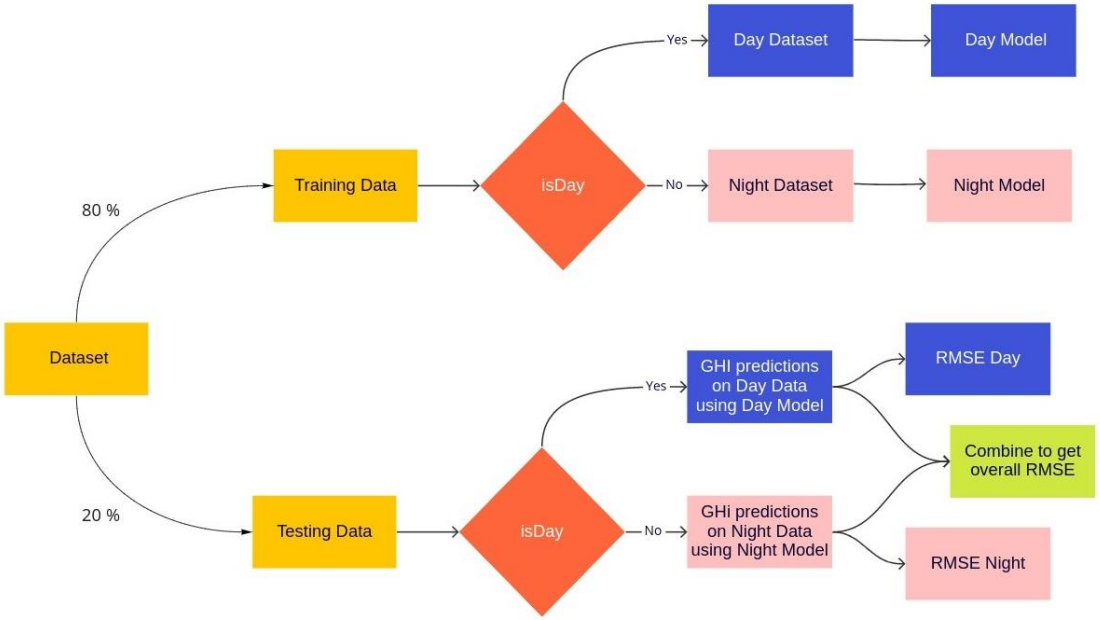

Figure 3-8 Schematic Diagram of Dataset Training

3.10 Overall System Flow Chart

After finding out the best model, it is used to forecast the prediction data that will be used in the cold storage model. The green part is the machine learning part and the blue color part is for the Integration of cold storage with the double effect VAR system. **Figure 3-9** shows the flowchart of our study. The orange steps are for the data processing, training other filtration. The green steps are for the implementation of the forecasted data. Finally, the blue part is for the cold storage application.

Figure 3-9 Flowchart for Our Overall System Model.

3.11 Schematic of an Integrated Cold Storage and Double-Effect VAR System

The **figure 3-10** shows the schematic diagram of an overall system that is under consideration. Here, the PTC array is attached with a storage tank to hold the thermal energy. As there is variable energy input from the solar system it is necessary. The storage system will send hot fluid to the VAR system. The Fuel generator will send the remaining necessary to meet the VAR generation input.

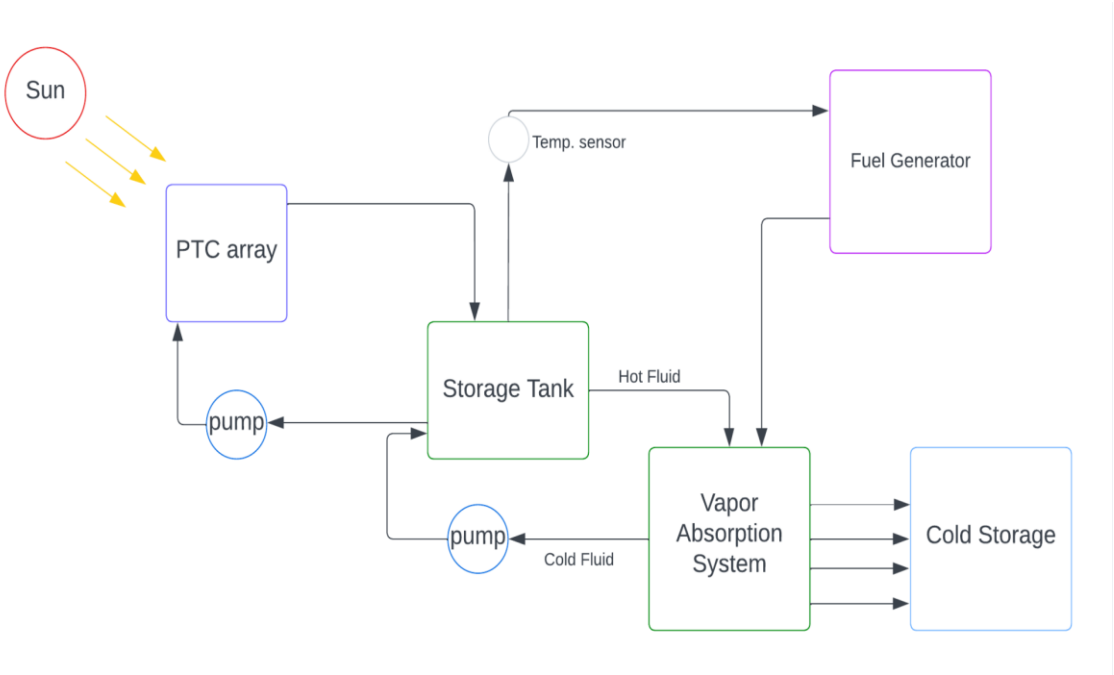

Figure 3-10 Schematic Diagram of the Overall System.

Figure 3-11 is the cold storage considered. The commodities in (Onion, Potato and Tomato) considered can rot easily. They also grow in the different months of the year. **Table 3-2** is the list of commodities and when will they be stored is mentioned.

Table 3-2 commodities list along with month of storage

Commodities considered	Month of storage
Onion	March to May
Potato	May-September
Tomato	November- January

In February not many crops grow. It is considered to be the month for annual maintenance. The dimension of the cold storage is length 20m, breadth 10m and height 5m.

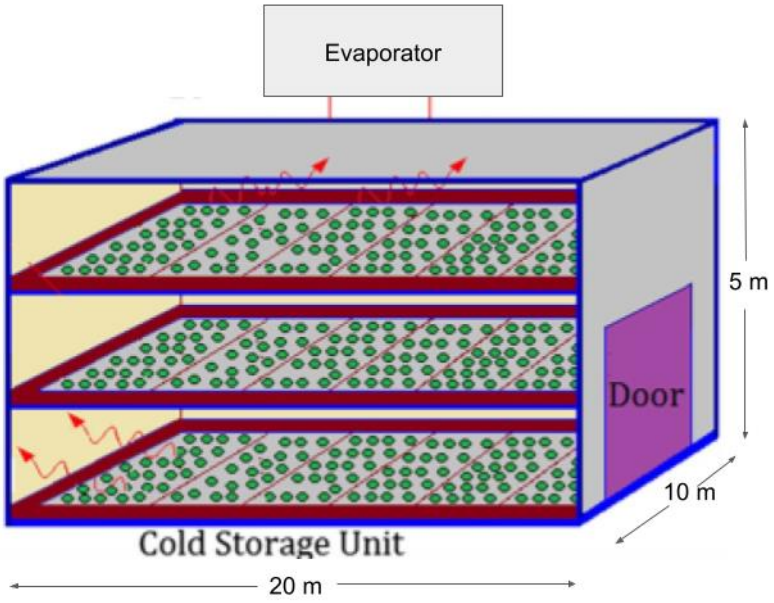

Figure 3-11 Schematic Diagram of a Cold Storage System.

Figure 3-12 is the schematic diagram of the single effect vapor absorption cycle. In this cycle, a liquid within the absorber known as the absorbent absorbs the refrigerant vapor. The heat is then delivered to the generator, usually from an external heat source like natural gas or leftover heat, using the mixture of absorbent and refrigerant vapor. The high-pressure vapor is created when the refrigerant vapor separates from the absorbent due to heat. The single-effect vapor absorption cycle's major advantage is that it has the potential for greater energy efficiency than vapor compression systems, especially when renewable heat is employed. But it frequently works at lower performance levels, has a bigger footprint, and uses more complicated parts. The input parameter for single-effect vapor absorption cycle Main generator temp for single effect = 90°C, absorber and condenser temp.= 10°C above ambient temperature and evaporator temp. = 6 °C

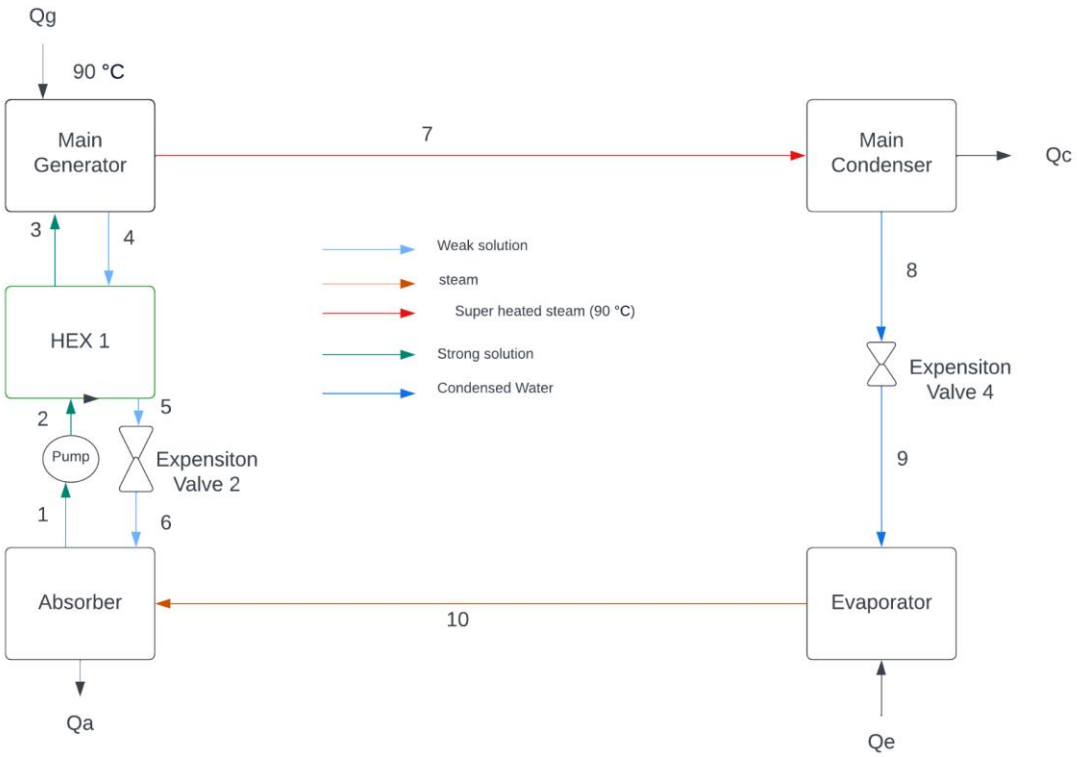

Figure 3-12 Schematic Diagram of a Single Effect Vapor Absorption Refrigeration Cycle

The double effect vapor absorption refrigeration cycle is shown in the **figure 3-13**. The double effect cycle, like the single effect cycle, has four major components: the generator, condenser, evaporator and absorber. It does, however, include an extra generator and absorber, thus the moniker "double effect." The main advantage of the twofold effect cycle over the single effect cycle is its enhanced efficiency. The cycle can generate increased cooling or refrigeration capacity without requiring additional external heat sources by using the heat from the first generator to drive a second generator. The double effect cycle, on the other hand, is more complicated and involves more components than the single effect cycle. It has greater capital expenses and maybe more demanding design and operating specifications. So a comparison is necessary. The input parameter for double-effect vapor absorption cycle. Main generator temperature for double effect = 140°C, Secondary

generator =90 °C, Absorber and condenser temperature= 10°C above ambient temperature and Evaporator temperature= 6 °C

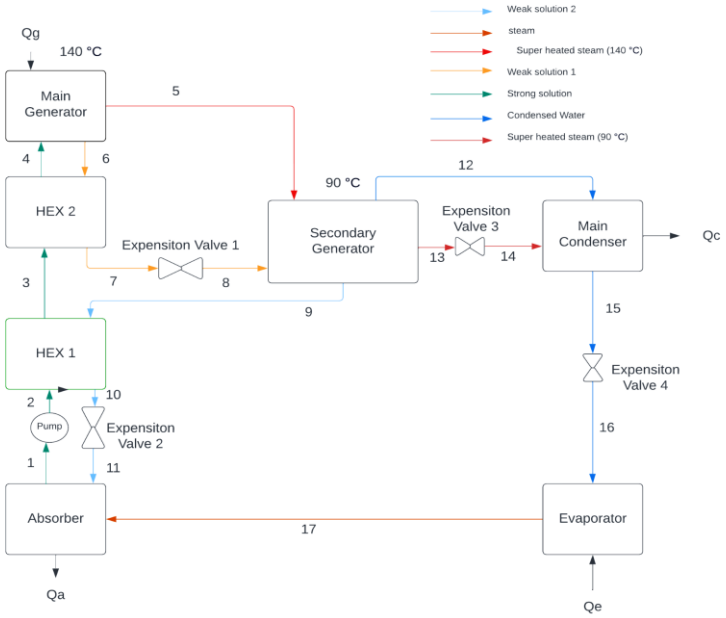

Figure 3-13 Schematic Diagram of a Double Effect Vapor Absorption Refrigeration Cycle

3.12 Thermal Model Development of Cold Storage, Single and Double Effect System

A single stage of refrigeration is utilized in a single effect cold storage system to provide the necessary chilling effect. An evaporator, a compressor, a condenser, and an expansion valve are the most common components of this system.

Thermal Model Elements:

The evaporator collects heat from the cold storage area and evaporates the refrigerant. The evaporator's thermal model takes into account the heat transfer coefficient, evaporator surface area, and refrigerant characteristics.

The compressor boosts the pressure and temperature of the refrigerant vapor. The compressor's thermal model focuses on the power input and energy losses related with compression.

Condenser: The condenser is responsible for transferring heat from the refrigerant to the surrounding environment, causing it to condense into a liquid. The condenser's thermal model takes into account the heat transfer coefficient, condenser surface area, and refrigerant characteristics.

Expansion Valve: The expansion valve lowers the refrigerant's pressure and temperature, preparing it for the next cycle of evaporation in the evaporator.

When compared to a single effect system, a double effect cold storage system uses two stages of refrigeration to provide improved efficiency and reduced energy use. It drives the second stage of refrigeration with waste heat or low-grade thermal energy.

Thermal Model Elements:

High-Temperature Generator (HTG): The HTG provides energy for the second stage of refrigeration by using a heat source (e.g., waste heat). The HTG thermal model incorporates heat transfer mechanisms such as absorption and desorption, as well as the temperature of the heat source and the parameters of the absorbent and refrigerant fluids.

Low-Temperature Generator (LTG): The LTG, like the single effect system, offers the initial step of refrigeration. The LTG's thermal model is comparable to that of a single effect system.

Other Components: The other components in a double effect system, such as condensers, evaporators, compressors, and expansion valves, are comparable to those in a single effect system and would have matching thermal models.

3.12.1. Energy Model of the Cold System

The total cooling load (Q_{Total})was calculated from the following equation, [32]

$$\boldsymbol{Q_{Total} = Q_{Str} + Q_{inf} + Q_{prod} + Q_{man} + Q_{equip}} \quad (7)$$

Here, (Q_{Str}) is the load of the structure. Infiltration load (Q_{inf}) that is the load due to entering and leaving the col\d storage. Product load (Q_{prod}) the load from the commodities equipment loads and occupancy load.

The equipment load (Q_{equip}) and occupancy load (Q_{man}) can be calculated from the detailed expression shown in Ganguly and DE [33].

Unpredicted leakage and inaccuracy can happen, if it happens 5% additional load is considered. So, the evaporator load can be calculated from the equation: [34]

$$\boldsymbol{Q_E = 1.05 \times Q_{Total}} \quad (8)$$

3.12.2 Energy Model of a Single Effect VAR System

The heat input in the main generator of the single- effect VAR system can be determined by: [35]

$$\boldsymbol{Q_G = m_4h_4 + m_7h_7 - m_3h_3} \quad (9)$$

$$\boldsymbol{Q_C = m_7 (h_7 - h_8)} \quad (10)$$

And the heat released from the absorber can be estimated by [35]

$$\boldsymbol{Q_A = m_{10}h_{10} + m_6h_6 - m_1h_1} \quad (11)$$

3.12.3 Energy Model of a Double-Effect VAR System

The heat input in the main generator of the double - effect VAR system can be determined by: [36]

$$\boldsymbol{Q_G = m_5h_5 + m_6h_6 - m_4h_4} \quad (12)$$

The Condenser Load calculated by [36]

$$\boldsymbol{Q_C = \ m_{14}h_{14} + m_{12}h_{12} - \ m_{15}h_{15}} \quad (13)$$

And the heat released from the absorber can be estimated by [36]

$$\boldsymbol{Q_A = \ m_{17}h_{17} + m_{11}h_{11} - \ m_1h_1} \quad (14)$$

The second generator will satisfy the energy balance equation. The energy balance equation can be given by: [36]

$$\boldsymbol{m_5h_5 + m_8h_8 = \ m_9h_9 + \ m_{12}h_{12} + m_{13}h_{13}} \quad (15)$$

The work input in the pump for both the system can be determine from [36]

$$\boldsymbol{W_P = \frac{m_1}{\eta_P}\int_{P1}^{P2} vdp \ = m_1\,(h_1\text{-}h_2)} \quad (16)$$

The efficiency for the pump is taken as η_P as 90% [36]

The coefficient of performance of the cold storage in application can be determined from the equation for both systems. [37]

$$\textbf{COP} = \frac{Q_E}{Q_G + QW_P} \quad (17)$$

Li-Br-water solution was taken as working fluid for both cases where Li-Br is the absorbent and Water is the refrigerant.

3.13 Power System Model

A parabolic trough collector is a form of solar thermal power system that uses curved mirrors to focus sunlight onto a receiver tube situated at the parabolic trough's focal line. The focused sunlight warms a fluid that flows through the receiver tube and is subsequently utilized to produce steam. The steam powers a turbine, which in turn powers a generator, which generates electricity.

Parabolic Trough Collectors: The power system is made up of many rows of parabolic trough collectors. Each collector includes a parabolic-shaped reflector that directs sunlight onto a receiver tube that runs parallel to the trough's focal line.

The receiver tube is located at the focal point of the parabolic trough. It contains a heat transfer fluid, such as synthetic oil or molten salt, that absorbs concentrated sunlight and heats to extreme temperatures.

The heat transfer fluid travels through the receiver tube, absorbing thermal energy from the focused sunlight. The temperature of the fluid rises as it absorbs heat.

Thermal storage devices are used in some parabolic trough power systems to store surplus heat created during periods of strong solar radiation. This enables for continuous power generation even when there is no sunlight available, for as when it is overcast or at night.

The heated heat transfer fluid from the receiver tube transmits its thermal energy to water, resulting in high-pressure steam. Steam can be generated directly in a heat exchanger or indirectly via a heat transfer fluid loop.

Steam Turbine: A turbine is powered by high-pressure steam, which converts thermal energy into mechanical energy. The steam turbine is linked to a generator, which transforms mechanical energy into electrical energy.

Power generation occurs while the generator rotates owing to the mechanical energy given by the steam turbine. The produced electricity may be utilized to power various electrical loads or it can be supplied into the grid.

A control system monitors and adjusts several aspects of the parabolic trough collector power system, such as reflector position, fluid flow rate, and temperature management, in order to maximize the system's efficiency and performance.

Table 3-3 Shows the design parameters of the PTC (Parabolic Trough Collector) that were taken as input:

Table 3-3: Design Parameters for the PTC solar system

Parameter	Values
Concentrator length, L	6 m
Inner dia. of absorber tube,D_O	8.1 cm
Inner dia. of absorber tube,D_i	7.5 cm
Overall loss of coefficient, U_l	6.2 W/m^2K
Convective heat transfer coefficient of the inside surface of the absorber tube, h_f	205 W/m^2K
Specific heat of thermal fluid, C_{Pf}	2.3 KJ/KgK
Intercept factor, ɤ	.94
Beam radiation tilt factor, r_b	1.2
$(\tau \propto)_b$	.81
Reflectivity, ρ	.86

The generation of power coming from the PTC in an hour can be calculated from [36]

$$\mathbf{Q_{u,PTC}=F_R[SA_a - A_r U_l(T_{fl} - T_a)} \quad (18)$$

The incident flux can be estimated by [36]

$$\mathbf{S = I_b r_b \rho ɤ(\tau \propto)_b + I_b r_b (\tau \propto)_b (\frac{D_0}{W-D_0})} \quad (19)$$

3.14 **Emission Analysis**

The practice of measuring and quantifying the emissions of numerous contaminants from a certain source or activity is known as emission analysis. Emission analysis in the context of a parabolic trough collector power system would entail examining the system's environmental effect by quantifying the emissions connected with its operation.

Greenhouse Gas Emissions: The burning of fossil fuels needed for auxiliary functions, such as startup, backup, or operation during periods of low solar radiation, produces the most substantial greenhouse gas emissions connected with a parabolic trough collector power system. Carbon dioxide (CO_2) is one of the principal greenhouse gasses responsible for climate change.

Air Pollutants: During the burning of fossil fuels, parabolic trough collector power systems may release air pollutants such as nitrogen oxides (NO_x)), sulfur oxides (SO_X), particulate matter (PM), and volatile organic compounds (VOCs) in addition to greenhouse gasses. These contaminants can have a negative impact on both air quality and human health.

The **table 3-4** is used to calculate the emission analysis. Here the table have the values of mass in kilogram that is produced when one kilowatt-hour is generated.

Table 2-4: Emission analysis chart

Emission factors (kg/kWh)				
Source	$\boldsymbol{CO_2}$	$\boldsymbol{SO_2}$	$\boldsymbol{NO_X}$	**CO**
Coal	1.18	0.0139	0.0052	0.0002
Petroleum	0.85	0.0164	0.0025	0.0002
Natural Gas	0.53	0.0005	0.0009	0.0005
Hydro	0	0	0	0
Others	**0**	**0**	**0**	**0**

3.15 Conclusion

Finally, statistical approaches like regression, support vector machine (SVM) regression, neural network models, and, in particular, N-BEATS, provide strong tools for data analysis and predictive modeling. These strategies give useful insights and solutions in a variety of fields.

We may use regression analysis to understand the connection between a dependent variable and one or more independent variables, allowing us to make predictions and reveal important patterns in the data. It provides a framework for evaluating and analyzing the effects of various factors on the desired outcome.

SVM regression is a machine learning approach that can handle non-linear correlations and complicated data patterns. SVM regression seeks the best-fitting hyperplane that maximizes the margin between the data points and the regression line by mapping the data into a high-dimensional feature space.

Neural network models, on the other hand, provide a dynamic and adaptable technique to representing complicated data interactions. Neural networks excel at image identification, natural language processing, and time series forecasting due to their ability to capture non-linearities and hierarchical representations. N-BEATS stands out among neural network models as a particularly good solution for time series forecasting. N-BEATS use a stack of fully connected neural networks to detect both local and global patterns in time series data. It has outperformed standard approaches in terms of accuracy and computing efficiency in a variety of forecasting jobs.

A thermally driven refrigeration technique that uses waste heat or low-grade heat sources for cooling is the double-effect vapor absorption refrigeration system. This system is more efficient than traditional vapor compression refrigeration systems because it uses a double-

effect design. It is a more ecologically responsible option since it reduces power use and reliance on synthetic refrigerants, both of which contribute to greenhouse gas emissions. The double-effect vapor absorption refrigeration system is used in industrial cooling, commercial refrigeration, and air conditioning, allowing for excellent waste heat use and energy reduction.

The parabolic trough collector, on the other hand, is a solar thermal technique that focuses sunlight onto a receiver tube. It's commonly employed in solar power generation and process heating. By capturing the sun's energy, parabolic trough collectors may generate high-temperature heat that can be used for a variety of applications such as steam generation, industrial operations, or driving a power turbine. This technology delivers a sustainable and renewable energy alternative that reduces reliance on fossil fuels while also minimizing environmental concerns. The parabolic trough collector has shown to be an efficient and cost-effective solar thermal technology, especially in areas with plentiful solar resources.

In conclusion, statistical approaches such as regression, SVM regression, and neural network models, such as N-BEATS, are effective tools for data analysis and predictive modeling. Their use allows us to get useful insights, create accurate forecasts, and solve complicated issues across several disciplines. Continued research and development in these fields hold promise for further advancements, improved performance, and wider adoption, leading to a more sustainable and energy-efficient future.

Chapter 4 Result and Discussions

4.1 Map to Find a Suitable Location

The generated heat map and geographical map for DNI, GHI and $\boldsymbol{PV_{OUT}}$ have been shown in this section. After that a suitable location has been picked from all the figures.

4.1.1 DNI Variation along Longitude and Latitude

A rectangular grid was set up over Bangladesh in 20°34' to 26°38’ latitude and 88°01' to 92°41' longitude. The grid has 27 x 23 i.e., 567 points over Bangladesh. For each point the average DNI per day was collected from the solar atlas database. The collected data was then processed and sorted before using it in python code. From the python code the heat map in the **figure 4-1** was generated.

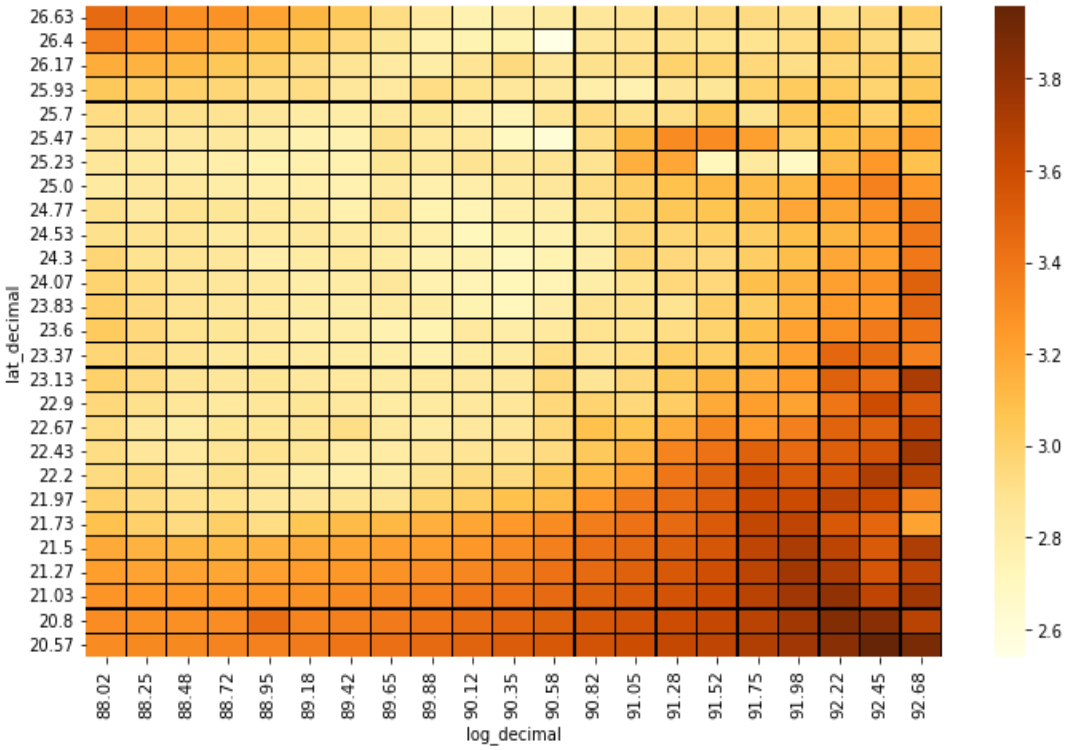

Figure 4-1 Generated Heat Map from using DNI

4.1.2 Data on a Geographical Map for DNI Mapping

In the heat map, according to the latitude and longitude a Bangladeshi map was set over it. As a result, the figure was generated. In the **figure 4-2** the range of DNI was found to be from 2.5 to 3.9 kW per day. The darker the orange color the more the DNI value. It can be found that most of the areas in Bangladesh have below 3.2 kW value. So, most of the area is not suitable for this study. The color in the south part of the country is dark orange but most of the area is in the sea. The darkest color for the land area is found in the south-east region of Bangladesh. Especially around Coxs' Bazar and Chittagong district.

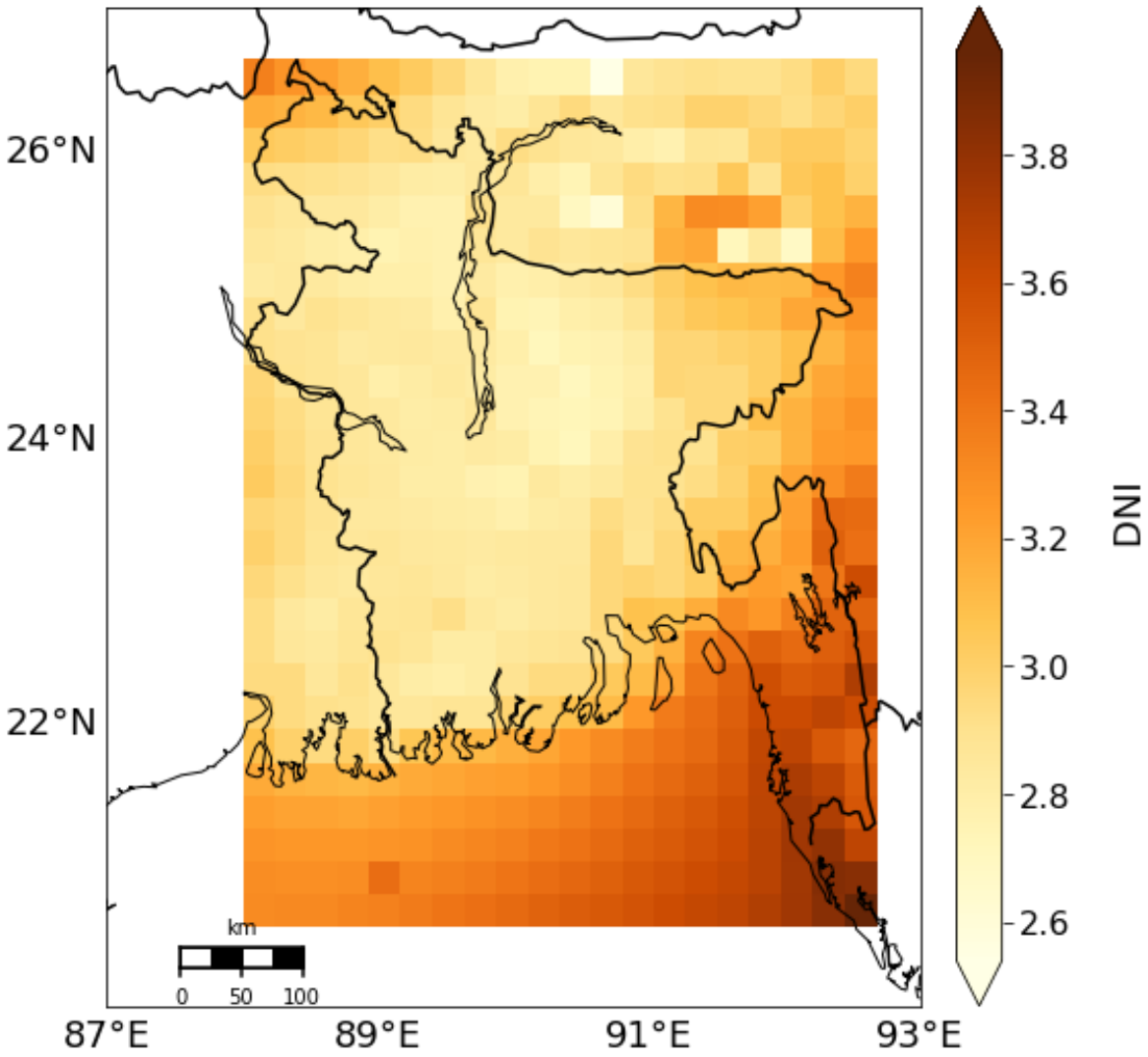

Figure 4-2 DNI Distributed Map in Bangladesh.

4.1.3 GHI Variation along Longitude and Latitude

Similarly, a rectangular grid was built up over Bangladesh in the latitude range of 20°34 to 26°38' and the longitude range of 88°01' to 92°41'. The grid is 27 x 23, resulting in 567 points over Bangladesh. The average GHI per day for each location was obtained from the solar atlas database. After collecting the data, it was processed and sorted before being used in Python code. The heat map in the **figure 4-3** was created using Python programming.

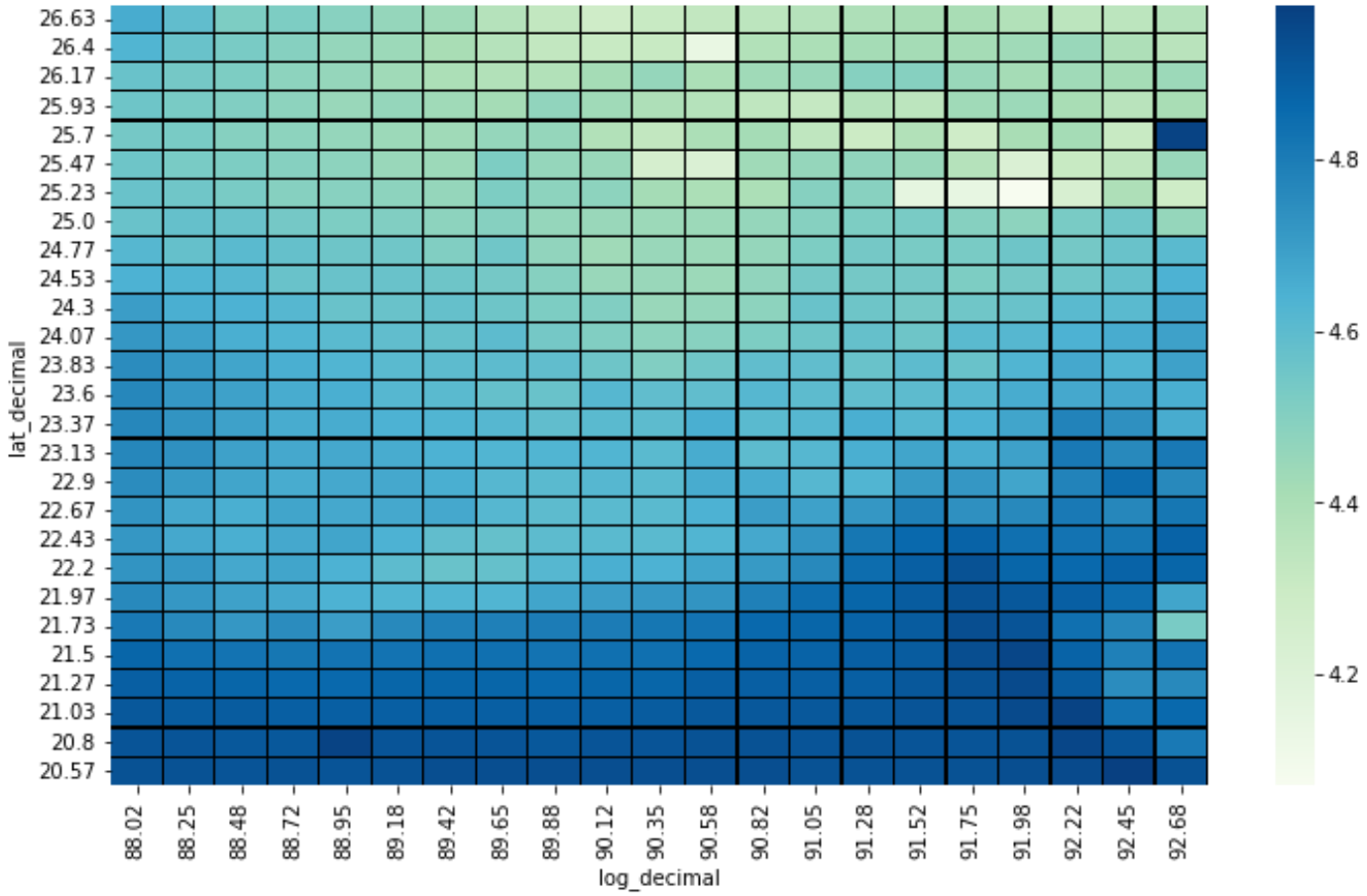

Figure 4-3 Generated Heat Map from using GHI

4.1.4 Data on a Geographical Map for GHI Mapping

A Bangladeshi map was superimposed over the heat map based on the latitude and longitude. As a consequence, the graph was created. The GHI range was discovered to be between 4kW and 5 kW per day in the **figure 4-4**. The greater the GHI value, the deeper the orange color. The majority of places in Bangladesh have a value of less than 4.6 kW. As a result, the majority of the region is unsuitable for this research. The hue in the south of the nation is dark blue, however the majority of the land is under water. The darkest hue for land area is seen in Bangladesh's south-east region. Particularly in the Cox's Bazar and Chittagong districts.

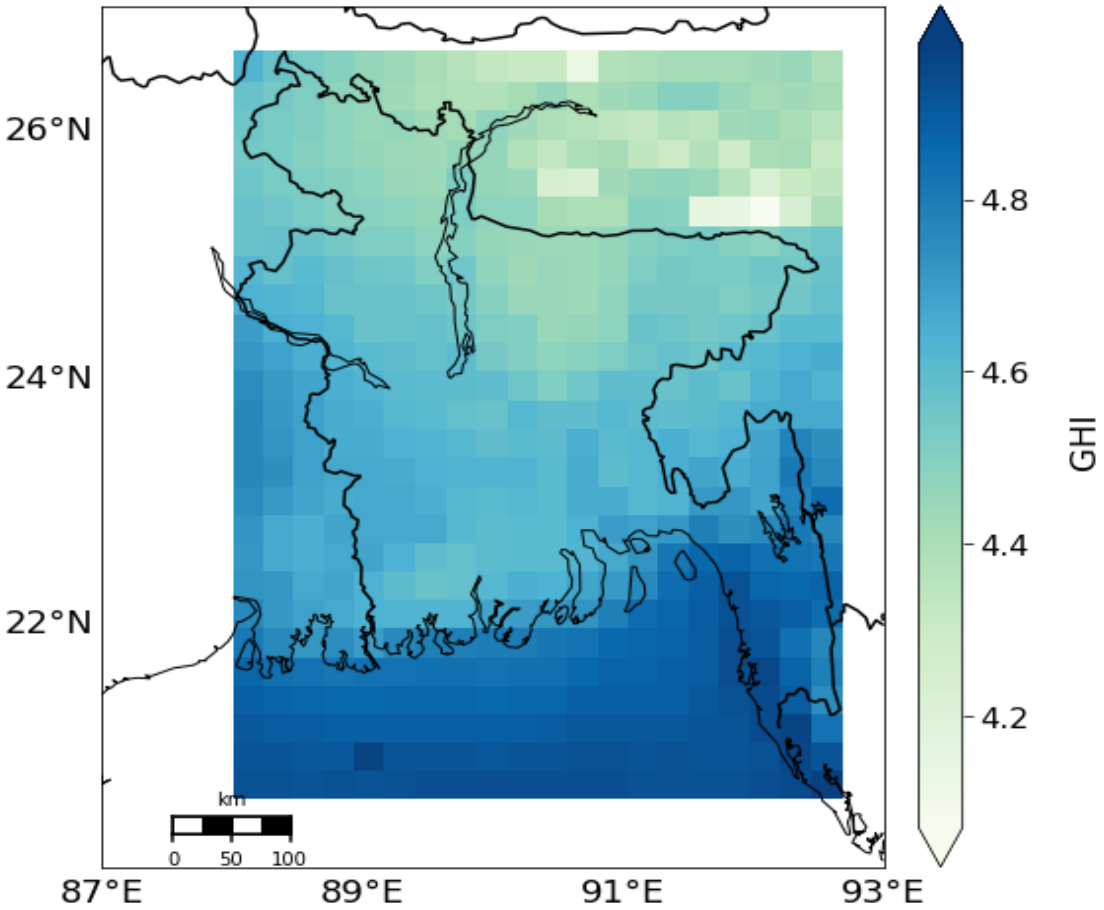

Figure 4-4 GHI Distributed Map in Bangladesh.

4.1.5 PV_{OUT} Variation along Longitude and Latitude

Like before a rectangular grid was constructed across Bangladesh in the latitude range of 20°34 to 26°38' and the longitude range of 88°01' to 92°41', as was done before. The grid measures 27 x 23, yielding 567 locations over Bangladesh. The solar atlas database was used to calculate the average $\boldsymbol{PV_{OUT}}$ per day for each location. Data was collected, analyzed, and sorted before being used in Python code. Python programming was used to construct the heat map in the **figure 4-5**.

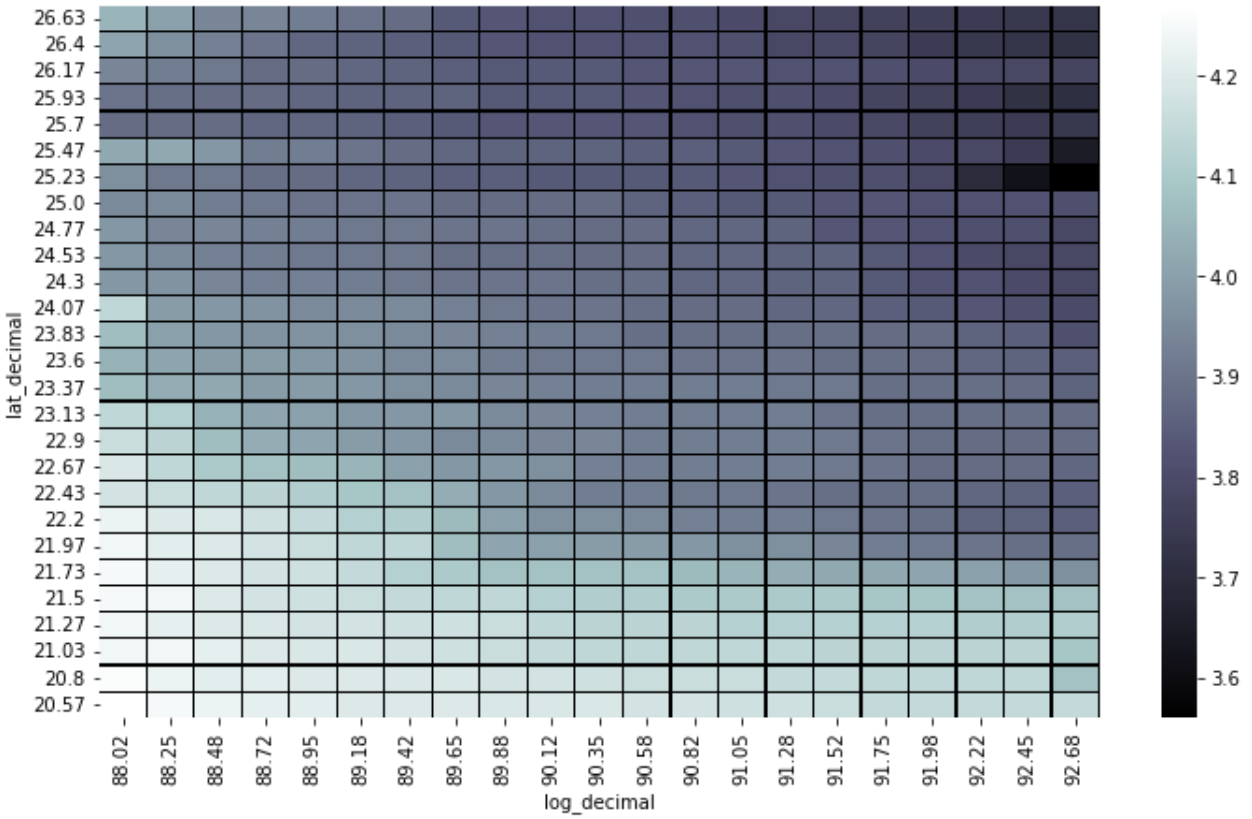

Figure 4-5 Generated Heat Map from using PV_{OUT}

4.1.6 Data on a Geographical Map for PV_{OUT} Mapping

Based on the latitude and longitude, a Bangladeshi map was placed on the heat map. As a result, the graph was formed. In the **figure 4-6**, the DNI range was revealed to be between 3.6 and 4.3 kW per day. The darker the black tint, the higher the $\boldsymbol{PV_{OUT}}$value. The bulk of Bangladeshi locations have a rating of less than 3.9 kW. As a result, the vast majority of the region is ineligible for this study. The color of the nation's south is dark orange, yet the majority of the land lies beneath water. This occurred because there is less disturbance from the solar panel to sun in the sea. Bangladesh's south-east region has the darkest color for land area. Particularly in the districts of Cox's Bazar and Chittagong.

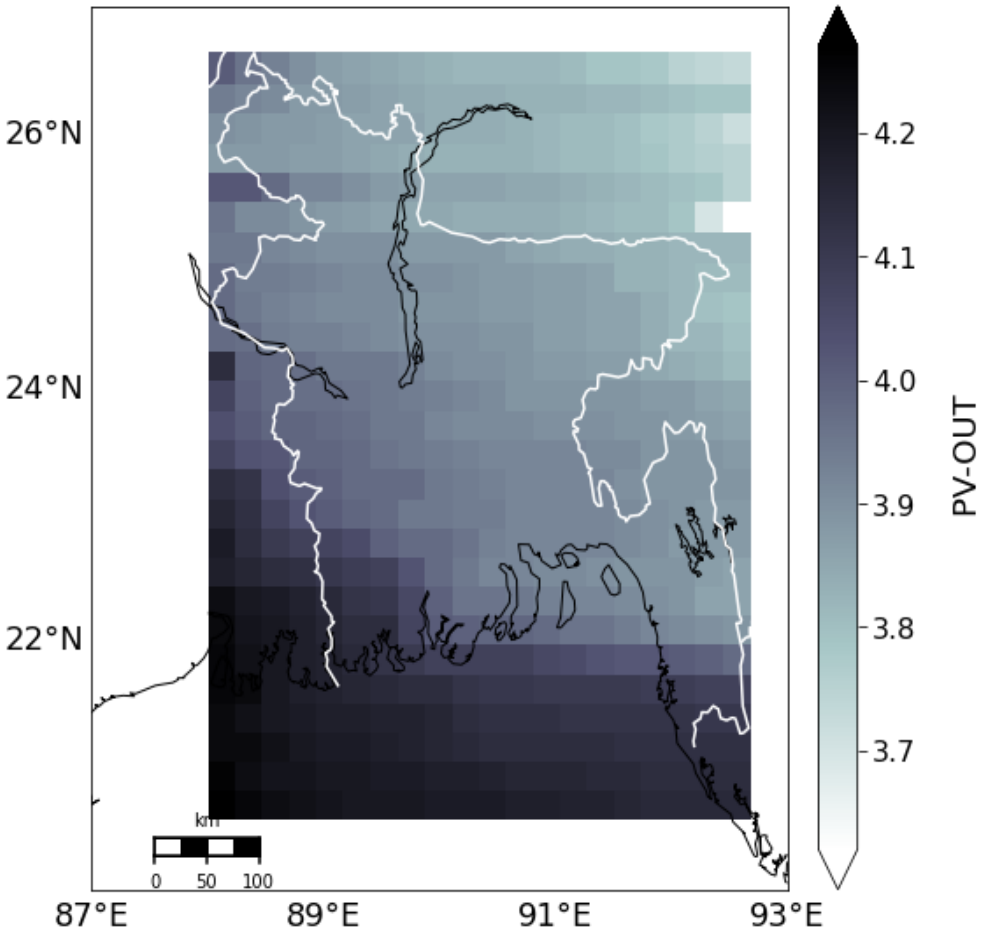

Figure 4-6 PV_{OUT} Distributed Map in Bangladesh.

4.1.7 Finding the One of the Most Suitable Location

After generating all the maps, the suitable locations are in the south-east region. One of the suitable locations is pin point by the red mark in the **figure 4-7**.

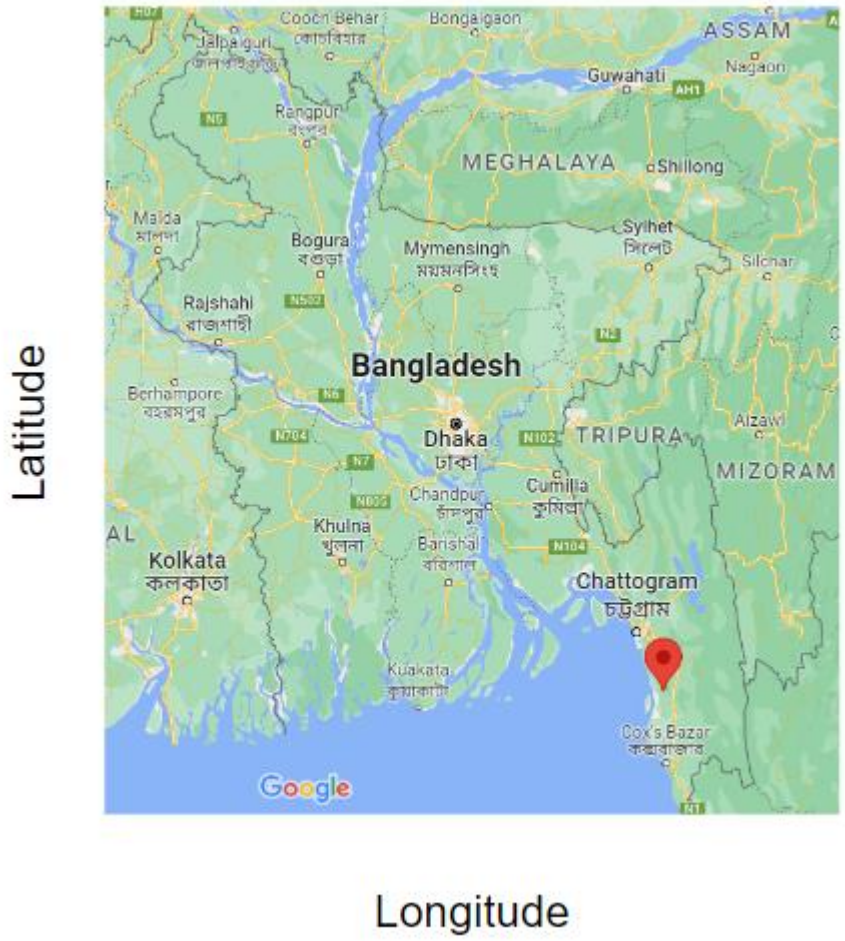

Figure 4-7 Finding a Suitable Location

Here, the right side of the figures in general have value in the higher range. The darker the color the higher the value. As it can be seen around the south east zone in Bangladesh the color is the darkest. So, this is our optimum zone for our study. So, optimum result is around Latitude 21° 57' 36" N, Longitude 91° 59' 24" E.

4.2 Linear Regression: Baseline Model

During our analysis, we noticed that the baseline linear regression (LR) models, both the single model in **table 4-1** and the day-night model in **table 4-2**, exhibited low variance. This indicates that the models were not overly sensitive to changes in the training data and were able to provide consistent predictions. However, despite the low variance, we observed that the day-night model outperformed the single model. This superior performance can be attributed to the sparsity in the dataset. The sparsity in the data set refers to the presence of a large number of zero values, particularly during the nighttime periods. The day-night model, designed specifically to handle this sparsity by separating the data into daytime and nighttime subsets, was able to capture the distinct patterns and relationships for each time period more effectively. Consequently, it achieved better prediction accuracy compared to the single model, which treated all observations as a single entity.

Table 4-1: Single Model (Baseline)

Model	Train RMSE	Test RMSE
Linear	151.554	152.019
Lasso	151.554	152.018
RIdge	151.554	152.017

Table 4-2: Day-Night Model (Baseline)

Model	Train RMSE	Test RMSE
Linear	81.135	82.182
Lasso	81.135	82.182
RIdge	81.135	82.182

In our attempt to further enhance the models, we applied regularization techniques such as lasso and ridge regression. Regularization helps in reducing the impact of irrelevant features and preventing overfitting, which occurs when the model becomes too complex and performs well on the training data but poorly on unseen data. However, in our case, we did not observe a significant improvement in performance after applying lasso and ridge regression. This suggests that the baseline models were already well-optimized and not prone to overfitting. The lack of improvement from regularization techniques indicates that the baseline LR models were able to capture the essential patterns and relationships in the data without introducing excessive complexity. The absence of overfitting suggests that the models were generalizing well to unseen data, further supporting their effectiveness. Hence, in this particular scenario, the application of lasso and ridge regression did not provide additional benefits in terms of improving the model's predictive performance.

4.3 Linear Regression: Feature Expansion

To expand on the baseline linear regression model for predicting solar intensity, we sought to incorporate additional weather observations into our feature set. This was achieved by including weather data from adjacent past time points like in **table 4-3**. By including these past observations, we aimed to capture the temporal dynamics and dependencies in weather conditions that could impact solar intensity. This approach allowed us to consider the influence of historical weather patterns on the current solar intensity levels, enabling the model to make more accurate predictions. By expanding the feature set with this adjacent past time point observations, we enhanced the model's ability to capture the nuanced relationships between weather variables and solar intensity, leading to improved predictive performance.

Table 4-3: Expansion v/s Features for Linear Regression

Expansion	1	2	5	30	60
# Features	30	45	90	465	915

During our analysis in **figure 4-8**, we found that as we increased the number of feature expansions, both the training and testing RMSE values initially decreased up to 25 expansions. This indicated that incorporating weather observations from adjacent past time points improved the accuracy of our models in predicting solar intensity. However, beyond 25 expansions, we observed a different trend. The RMSE values began to increase, signaling a rise in the variance of the model predictions. This increase in variance can be attributed to the high dimensionality of the data resulting from a large number of features. The higher dimensionality introduced more complexity and noise into the models, leading

to less stable and less reliable predictions. Therefore, it became evident that there was a trade-off between incorporating more past observations to capture temporal patterns and the risk of over fitting and increased variance associated with a higher dimensional feature space.

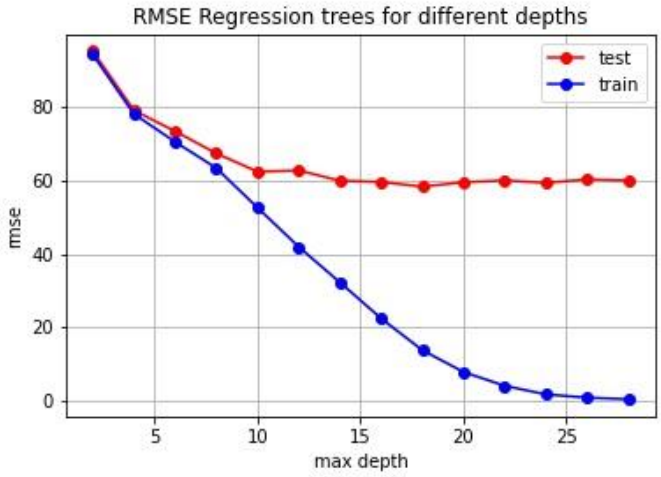

Figure 4-8 Feature Expansion without PCA

In order to reduce the dimensions and the complexity of our model, we applied PCA to get the features with high explained variance.

Table 4-4: Single model with PCA

Degree	PCA components	Train Rmse	Test Rmse
1	7	162.11	162.19
5	15	161.53	161.55
25	50	114.45	115.91
40	80	107.04	107.84
100	250	97.94	99.39

Table 4-5: Day night model with PCA

Degree	PCA components	Train Rmse	Test Rmse
1	7	82.90	83.83
5	15	83.44	84.39
25	50	82.41	83.74
40	80	80.32	81.86
100	250	78.03	79.84

When we applied feature expansion with Principal Component Analysis (PCA), the complexity of the model decreased due to the dimensionality reduction achieved by PCA. As we increased the number of feature expansions, the expanded feature set became more informative and captured additional patterns in the data. By applying PCA, we selected the principal components that explained the highest variance, effectively condensing the expanded features into a smaller set of meaningful components. From **table 4-4** and **table 4-5** this reduction in complexity allowed the models to better capture the underlying patterns and relationships in the data, resulting in improved predictive performance. Consequently, as the number of feature expansions increased, both the train and test RMSE decreased, indicating that the models became more accurate in predicting the solar intensity.

4.4 Polynomial Regression

To further expand our feature set, we employed a mathematical feature expansion technique. This involved adding new features to our dataset by considering the square of

each existing feature, as well as the pairwise interactions between each pair of features. By including these additional polynomial features, we aimed to capture non-linear relationships and interactions between the variables, which could potentially enhance the predictive power of our models.

However, due to the exponential increase in the number of features resulting from this expansion, it was not feasible to include all possible combinations. Instead, we limited the expansion to polynomial degrees 2, 3, and 4. This allowed us to incorporate the squared values and higher-order interactions while still managing the computational complexity associated with a large number of features.

By incorporating these polynomial features like **table 4-6**, we aimed to capture more complex relationships and non-linear dependencies within the data, potentially improving the models' ability to capture the intricacies of the solar intensity prediction problem.

Table 4-6: Degree v/s Features Polynomial Regression

Degree	2	3	4
# Features	136	816	3876

Table 4-7: Single model for Polynomial Regression

Polynomial degree	Train RMSE	Test RMSE
2	78.95	79.96
3	69.49	70.53
4	51.98	55.99

Table 4-8: Day Night Model for **Polynomial Regression**

Polynomial degree	Train RMSE	Test RMSE
2	75.66	76.81
3	63.36	65.58
4	45.11	55.63

As we increased the degree of the polynomial regression, we observed from **table 4-7** and **table 4-8** reduction in both the train and test RMSE values. This indicated that the higher-order polynomial features allowed the models to capture more complex relationships and better fit the training data. By incorporating these higher-degree polynomial terms, the models became more flexible and able to capture non-linear patterns in the data, resulting in improved predictive performance.

However, at degree 4, we started to notice an increase in the variance of the model predictions. This increase in variance suggests that the models might be overfitting the

training data, as they were becoming too complex and sensitive to small variations in the input features. It is worth noting that due to limited computational resources, we were unable to further increase the degree of the polynomial beyond 4. This limitation prevented us from exploring whether higher-degree polynomials would continue to reduce the RMSE or exacerbate the overfitting issue. Nonetheless, our results up to degree 4 demonstrated the potential benefits of incorporating polynomial features in capturing non-linear relationships in the data.

4.5 Regression Trees

In our analysis, we employed regression trees as an alternative approach to predict solar intensity. Unlike linear regression techniques, regression trees have the ability to capture non-linear relationships and accommodate arbitrarily shaped decision boundaries. This flexibility allows regression trees to potentially outperform linear regression models in situations where the relationships between variables are complex and cannot be adequately represented by linear functions. By using regression trees, we aimed to leverage their ability to partition the feature space into distinct regions and make predictions based on the average or median value of the target variable within each region. This approach allows regression trees to capture intricate patterns and interactions among the predictors, which may not be captured by linear regression.

From the **figure 4-9** given the non-linear and complex nature of the relationship between weather variables and solar intensity, we expected that regression trees would yield improved performance compared to the linear regression techniques discussed earlier. By utilizing the inherent flexibility of regression trees, we sought to uncover and exploit the underlying non-linear patterns in the data to enhance the accuracy and predictive power of our models.

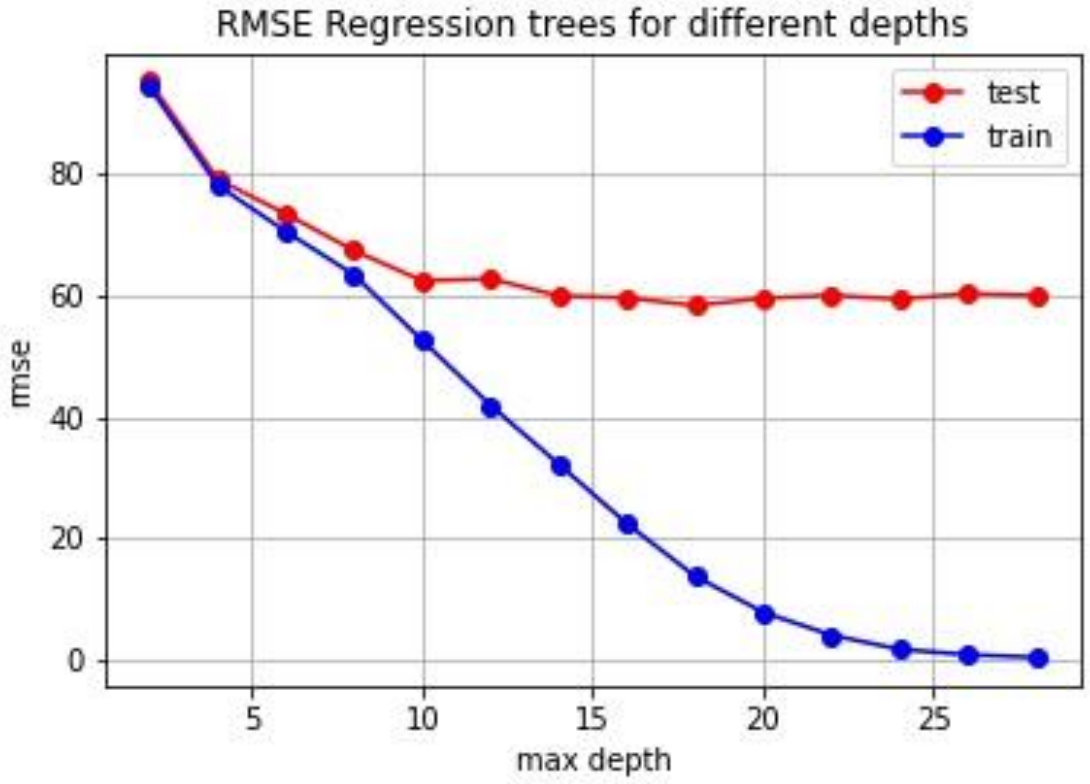

Figure 4-9 Regression Tree RMSE vs depth

Table 4-9: Regression Tree

Regression Tree	Train RMSE	Test RMSE
Without Pruning	0	59.9
Pre-Pruning	52.6	62.4

From **table 4-9** When we initially applied regression trees without any pruning, we observed high variance and low bias in our models. This means that the trees were able to capture the complexities and nuances in the data, resulting in a lower bias, but they were also prone to overfitting the training data, leading to higher variance. This overfitting could result in models that are not generalizable and may perform poorly on unseen data.

To address this issue and strike a balance between bias and variance, we employed pruning techniques. Pruning involves restricting the maximum depth of the decision tree, effectively limiting the number of splits and nodes in the tree structure. By constraining the maximum depth, we aimed to simplify the models and reduce their complexity, mitigating the risk of overfitting.

To determine the optimal maximum depth, we evaluated the bias-variance tradeoff. We plotted the bias and variance values against different maximum depths and observed how they changed. From the graph, we noticed that the bias-variance tradeoff improved significantly when the maximum depth was set to 10.

This choice struck a balance between capturing complex patterns in the data and avoiding excessive model complexity, leading to a more favorable tradeoff between bias and variance.

By choosing a maximum depth of 10, we aimed to achieve a more robust and well-performing regression tree model that effectively balanced between capturing important relationships and minimizing the risk of overfitting. This decision helped improve the bias-variance tradeoff and ensured a more reliable and generalizable model for predicting solar intensity.

4.6 SVM Regression

In order to address the non-linearity present in the data, we applied Support Vector Machines (SVM). SVM is a powerful machine learning algorithm that can handle non-linear relationships and complex decision boundaries. The performance of SVM depends on the selection of an appropriate kernel function and the tuning of its parameters.

In our analysis in **table 4-10** and **table 4-11**, we utilized four distinct SVM kernel functions: Linear Kernel, Polynomial Kernel, Sigmoid Kernel, and Radial Basis Function (RBF). The choice of kernel function determines how the data is transformed from the original input space to a high-dimensional feature space. Each kernel function has its own characteristics and is suitable for capturing different types of non-linear relationships.

The Linear Kernel is commonly used for linearly separable data, where the decision boundary is a hyperplane. The Polynomial Kernel can capture polynomial relationships by mapping the data to a higher-dimensional space.

The Sigmoid Kernel is suitable for non-linear relationships that exhibit sigmoidal behavior. Finally, the RBF Kernel is a versatile kernel that can capture complex non-linear relationships by mapping the data to an infinite-dimensional feature space.

By employing these different kernel functions, we aimed to capture various types of non-linearities present in the data. The choice of the most appropriate kernel and its parameters depended on the specific characteristics of the data and the performance of the models. Through careful selection and tuning, we sought to leverage the power of SVM to accurately predict solar intensity by capturing the underlying non-linear patterns in the data.

Table 4-10: Single Model for SVM Regression

Kernel	Train RMSE	Test RMSE
Rbf	118.57	119.5
Sigmoid	220.51	221.05
Linear	152.72	153.97
Polynomial	171.53	169.9

Table 4-11: Day Night Model for SVM Regression

Kernel	Train RMSE	Test RMSE
Rbf	90.52	90.64
Sigmoid	113.21	13.81
Linear	85.63	87.71
Polynomial	11.65	110.97

4.7 Artificial Neural Networks

Recognizing that the previously discussed models may not capture the full complexity of the data, we explored the use of Artificial Neural Networks (ANN) as an additional approach. Implementing ANN models allowed us to leverage the flexibility and capability of deep learning to capture intricate patterns and relationships in the data. To construct our ANN models, we utilized the Keras library, which provides a user-friendly interface for building and training neural networks.

During the experimentation process, we tested various combinations of activation functions number of layers, and layer sizes to find the best-performing ANN model. Our objective was to minimize the root mean squared error (RMSE) on both the training and test sets while considering the computational time required for training the model. We compared the obtained train and test RMSE values for each combination, aiming to strike a balance between model complexity, computational efficiency, and predictive performance.

To facilitate the selection of the most suitable ANN model, we compiled a table showcasing the three best RMSE values achieved from the different combinations we explored. This table allowed us to compare and identify the combinations that yielded the lowest errors, indicating better model performance. By considering the trade-off between complexity,

training time, and RMSE values, we were able to identify the top-performing ANN configurations for predicting solar intensity in our analysis in **figure 4-10**.

Table 4-12: Single Model (LeakyR means LeakyRelu)

# layers	Layer sizes	Activation Functions	Train RMSE	Test RMSE
4	14-64-32-1	LeakyR, LeakyR LeakyR, LeakyR	41.42	46.93
4	14-64-32-1	Relu, LeakyR LeakyR, LeakyR	54.21	56.69
4	14-64-32-1	Relu, Relu LeakyR, LeakyR	73.79	74.43

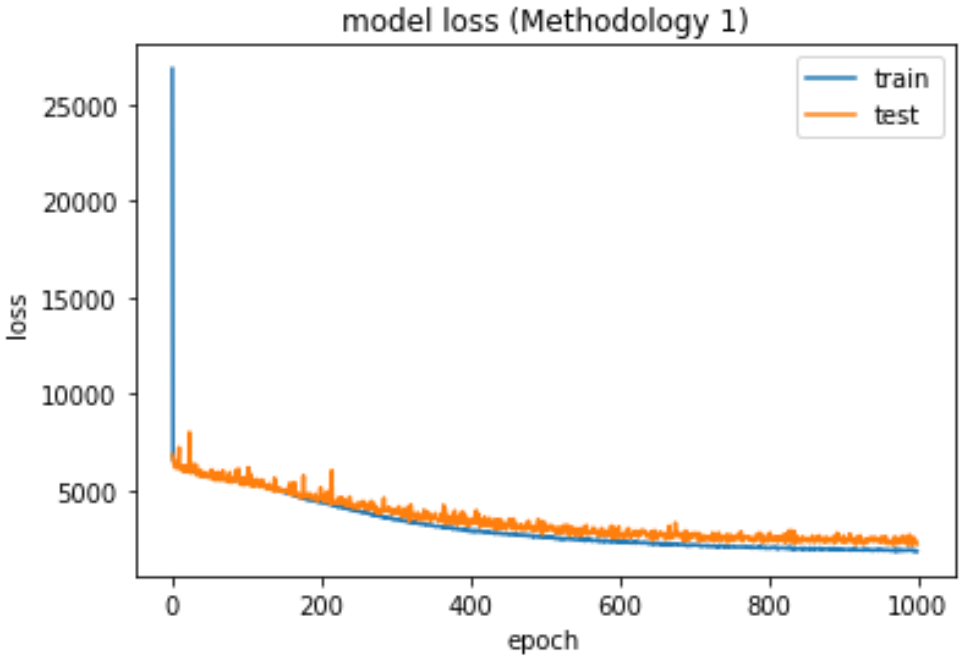

Figure 4-10 Loss Plot: Single Model

Table 4-13: Day Night Model (LeakyR means LeakyRelu)

# layers	Layer sizes	Activation Functions	Train RMSE	Test RMSE
4	14-64-32-1	LeakyR, LeakyR LeakyR, LeakyR	50.36	45.58
4	14-64-32-1	Relu, LeakyR LeakyR, LeakyR	59.95	53.33
4	14-64-32-1	Relu, Relu LeakyR, LeakyR	64.88	60.91

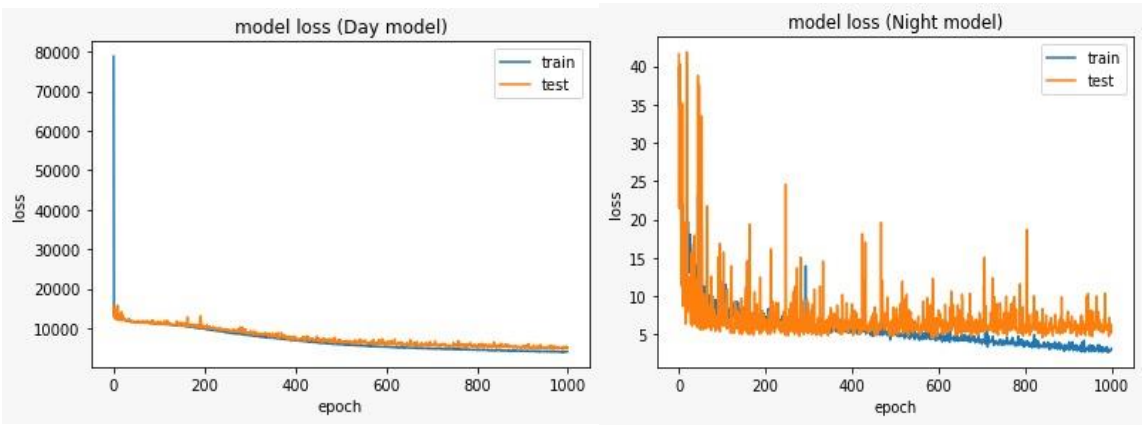

(a) **(b)**

Figure 4-11 Loss Model (a) Day Model and (b) Night Model

Upon analyzing the two tables like in **table 4-12** and **table 4-13**, showcasing the performance of various combinations, it becomes evident that the best results were achieved when employing a specific configuration. In both types of methodologies, the most favorable outcomes were obtained when utilizing a neural network architecture

consisting of four layers with sizes 14, 64, 32, and 1, respectively. Furthermore, the activation functions used in the respective layers were LeakyReLU, LeakyReLU, LeakyReLU, and LeakyReLU.

In **figure 4-11** The choice of architecture and activation functions greatly influenced the performance of the neural network models. The use of multiple layers allowed for the extraction of increasingly complex features and patterns from the input data. By progressively increasing the layer sizes, the models were able to capture more intricate relationships and representations within the data.

LeakyReLU activation functions were employed throughout the network layers. LeakyReLU is a variant of the popular Rectified Linear Unit (ReLU) activation function that addresses the problem of dead neurons, which can occur when ReLU outputs zero for negative input values. The LeakyReLU function introduces a small non-zero slope for negative inputs, allowing for the propagation of gradients and avoiding the issue of dead neurons.

The selection of the 4-layer architecture with specific layer sizes and activation functions proved to be successful in achieving the best results for both types of methodologies. This configuration likely provided a good balance between model complexity and generalization capabilities, enabling the neural network to effectively learn the underlying patterns in the data and make accurate predictions of solar intensity.

4.8 Neural Basis Expansion Analysis for Time Series:

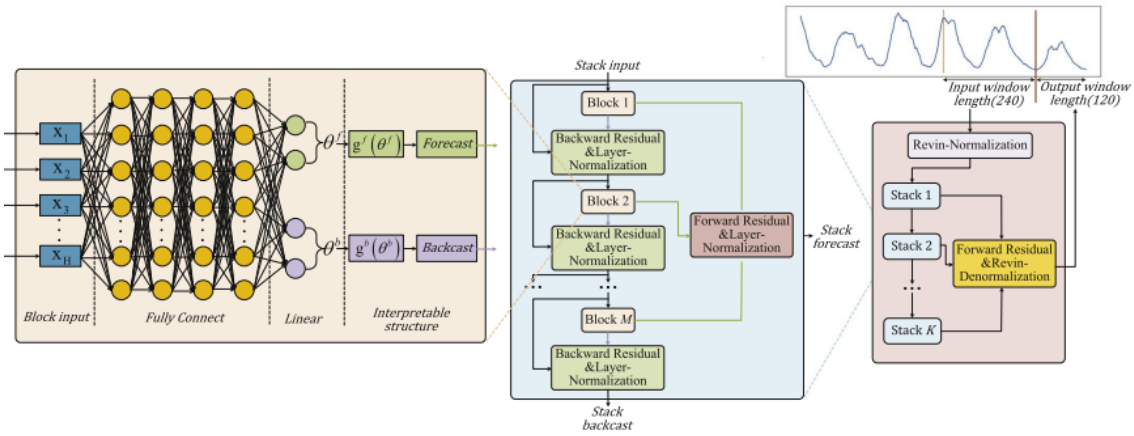

Figure 4-12 Structure of N-BEATS model

In the present study, a proficient N-beats model like the structure in **figure 4-12** is employed within our methodology to serve as a proximate mapping mechanism for linking the input and output data. The dataset has an input comprising of observed values spanning over a period of 240-time steps and an output consisting of predicted values for a duration of 120-time steps.

To assess the effectiveness of the model, an examination is conducted to compare the discrepancy between the actual values and the forecasted values. This evaluation permits the assessment of the precision of the model's prognostications, as well as ascertaining its efficacy in apprehending the implicit patterns and trends within the data.

One salient feature of our methodology is that it incorporates the prognostications of two consecutive cycles. The aforementioned forecasts incorporate inputs separated by a minimum of one cycle time step, leading to a considerable variance in the input dataset. Subsequently, the anticipation of every solar cycle is acknowledged as a comparatively autonomous procedure within scholarly discourse. This approach recognizes that each iteration may possess distinctive attributes and is subject to multifarious factors that may fluctuate over time.

Furthermore, it is crucial to acknowledge that the parameters fed into the model are exclusively derived from empirically obtained data. This implies that there is an absence of error accumulation or propagation across successive operational cycles. Every forecast is formulated exclusively on the basis of the observed data available at that specific point in time, ensuring that any errors or inaccuracies from preceding cycles do not prejudice subsequent predictions.

By adopting an approach of treating each prediction of solar cycles in isolation and relying solely on observational data as inputs, the possibility of error accumulation and potential biases that may arise from propagating errors across cycles is effectively mitigated. This methodology permits the concentration on the detection and delineation of distinctive attributes and trends associated with every unique cycle, thereby enhancing the precision of prognostication and diminishing the likelihood of accumulative inaccuracies.

The present study introduces a methodology that capitalizes on the independent prediction process like in **figure 4-13** and integrates observed values as inputs to augment the precision and dependability of the N-beats model when forecasting solar energy generation.

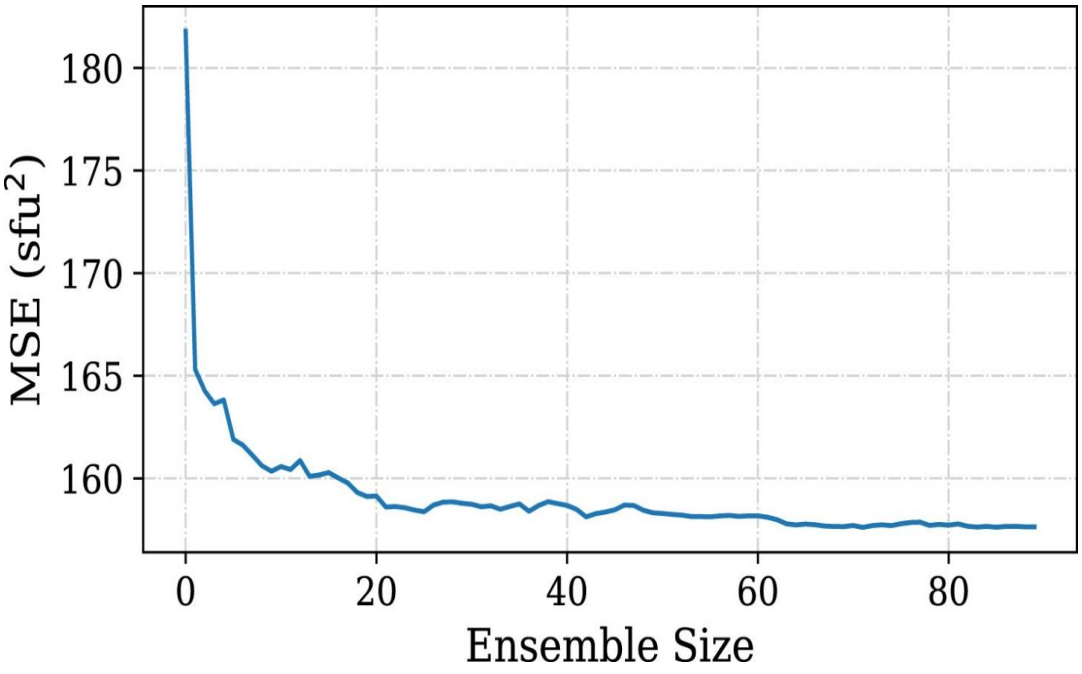

Figure 4-13 Forecasting using N-Beats

4.8 Single Effect Vapor Absorption Refrigeration Cycle

The single effect vapor absorption refrigeration cycle is a thermally powered cooling system that uses the absorption principle to create cooling. It is made up of four major parts: a generator, an absorber, a condenser, and an evaporator. The following is a step-by-step explanation of how a single effect vapor absorption refrigeration cycle works: The cycle starts in the generator, where a high-pressure liquid refrigerant-absorbent combination is introduced. A volatile refrigerant (e.g., ammonia) and an absorbent (e.g., water) are often present in the combination. Heat is often provided to the generator by a heat source such as a natural gas burner or waste heat. As a result of the heat, the refrigerant vaporizes and separates from the absorbent, resulting in a refrigerant vapor-rich mixture and an absorbent-rich solution.The absorber receives the refrigerant vapor-rich mixture from the generator. The refrigerant vapor is absorbed in the absorber into a weak absorbent solution with a reduced refrigerant concentration. The absorption process is exothermic, meaning it generates heat. As a result, the mixture's temperature drops.

Condenser: The absorber's refrigerant-rich solution flows into the condenser. The refrigerant vapor is condensed in the condenser by rejecting heat to a cooling medium (such as air or water). The vaporized refrigerant condenses into a high-pressure liquid, which is then fed via an expansion valve.

Expansion Valve: A pressure decrease occurs when high-pressure liquid refrigerant goes through the expansion valve. As a result, the refrigerant is throttled, resulting in a drop in temperature and pressure.

The evaporator receives the low-pressure, low-temperature refrigerant. It absorbs heat from the space to be cooled (e.g., air or water) in the evaporator, causing the refrigerant to vaporize and evaporate. The absorption of heat causes the surrounding environment to cool. The vaporized refrigerant then returns to the generator to restart the cycle.

To complete the cycle, the absorbent-rich solution from the absorber is often fed back to the generator. The process continues as long as the generator's heat input and the evaporator's cooling load remain constant.

Table 4-14 shows the output of the cycle for single effect vapor refrigeration cycle in each of the state points.

Table 4-14: States value for the single effect VAR system

State Point	Enthalpy (KJ)	Mass Flow rate (Kg/s)
1	83.31	6.3
2	83.37	6.3
3	128.81	6.3
4	235.28	5.3
5	181.2	5.3
6	181.2	5.3
7	2668.4	.97
8	146.645	.97
9	146.645	.97
10	2511.91	.97

Plugging the values in the equation 9, 10 and 11 we can determine the generator input, the rate of heat released in the condenser and the input. The deviation from the reference paper in very small. The **table 4-15** showed the resulted output values.

Table 4-15: Output for the single effect VAR system

Results	De[38]	Present study	Deviation (%)
Generator input (kW)	3036.9	3023.87	.43
The rate of heat released by the condenser (kW)	2473.4	2446.14	.5
The rate of heat rejected by the absorber (kW)	2858.4	2872.6	1.1

4.9 Double Effect Vapor Absorption Refrigeration Cycle

The double effect vapor absorption refrigeration cycle is a more sophisticated form of the vapor absorption refrigeration cycle that employs two phases of absorption to increase efficiency and cooling capacity. Two generators, two absorbers, two condensers, and one evaporator make up the system. The following is a step-by-step explanation of the operation of a twofold effect vapor absorption refrigeration cycle: the generator and the cooling load in the evaporator are kept constant.

High-Temperature Generator (HTG): The cycle begins with a high-pressure refrigerant-absorbent combination entering the HTG. A volatile refrigerant (e.g., ammonia) and an absorbent (e.g., water or lithium bromide solution) are commonly present in the combination. Heat is often delivered to the HTG via a heat source such as steam or hot water. As a result of the heat, the refrigerant vaporizes and separates from the absorbent, resulting in a refrigerant vapor-rich mixture and an absorbent-rich solution.

Low-Temperature Generator (LTG): The LTG receives the refrigerant vapor-rich mixture from the HTG. The refrigerant vapor is then absorbed in the LTG into a second absorbent

solution with a lower refrigerant concentration than the first. Heat is often provided to the LTG via waste heat or a lower-grade heat source. The method of absorption process is exothermic, meaning it generates heat and cools the mixture.

Absorbers: Each generator's refrigerant-rich solution flows into its own absorber. The refrigerant vapor is absorbed into the absorbent solutions in the absorbers. Because of the cooling impact of the LTG, the absorption process occurs at lower temperatures. Depending of the absorbent employed, heat may be emitted in the absorbers.

Condensers: The absorbers' refrigerant-rich solutions flow into the condensers. The refrigerant vapor is condensed in condensers by rejecting heat to a cooling medium such as air or water. In each condenser, the refrigerant condenses into a high-pressure liquid.

Expansion Valve: Each condenser's high-pressure liquid refrigerant travels through independent expansion valves, creating pressure and temperature decreases. The refrigerant is throttled, resulting in a drop in temperature and pressure in both branches.

Evaporator: A common evaporator receives the low-pressure, low-temperature refrigerant from both expansion valves. The refrigerant absorbs heat from the area to be cooled (e.g., air or water) in the evaporator, causing it to vaporize and evaporate. The absorption of heat causes the surrounding environment to cool.

To complete the cycle, the absorbent-rich solutions from the absorbers are normally pumped back to their respective generators. The continuous functioning of the double effect vapor absorption refrigeration cycle is driven by the heat input to both generators and the cooling load in the evaporator.

The double effect cycle outperforms the single effect cycle in terms of efficiency by using waste heat or lower-grade thermal energy in the LTG to increase cooling capacity. It is frequently used in large-scale applications requiring larger cooling loads, such as industrial operations, district cooling, or commercial air conditioning systems.

Table 4-16 shows the output of the cycle for double effect vapor refrigeration cycle in each of the state points.

Table 4-16: States value for the double effect VAR system

State Point	Enthalpy (KJ)	Mass Flow rate (Kg/s)
1	83.31	6.5
2	83.8	6.5
3	128.81	6.5
4	197.63	6.5
5	2759.11	.45
6	306.69	6.06
7	232.87	6.06
8	232.87	6.06
9	235.22	5.51
10	181.63	5.51
11	181.63	5.51
12	376.97	.55
13	2659.54	.45
14	2668.99	.45
15	146.645	1
16	145.645	1
17	2511.91	1

Plugging the values in the equation 12, 13, 14 and 15 we can determine the generator input, the rate of heat released in the condenser and the input. The deviation from the reference paper in very small. The **table 4-17** showed the resulted output values.

Table 4-17: Output for the single effect VAR system

Results	De [38]	Present study	Deviation (%)
Generator input (kW)	1803.8	1815.55	.65
The rate at which the condenser emits heat (in kW).	1265	1261.734	.26
The rate at which the absorber emits heat (in kW).	2895	2971.18	2.56

4.10 Comparison Study between Single-Effect and Double Effect Vapor Refrigeration Cycle

The **figure 4-14** show the visualization and the difference in heat input in different component in both single and double effect vapor absorption refrigeration cycle. There is not much different between the two-evaporator load and the rate of heat rejected in the absorber. Generator input and in condenser heat released is much less for double effect vapor absorption refrigeration.

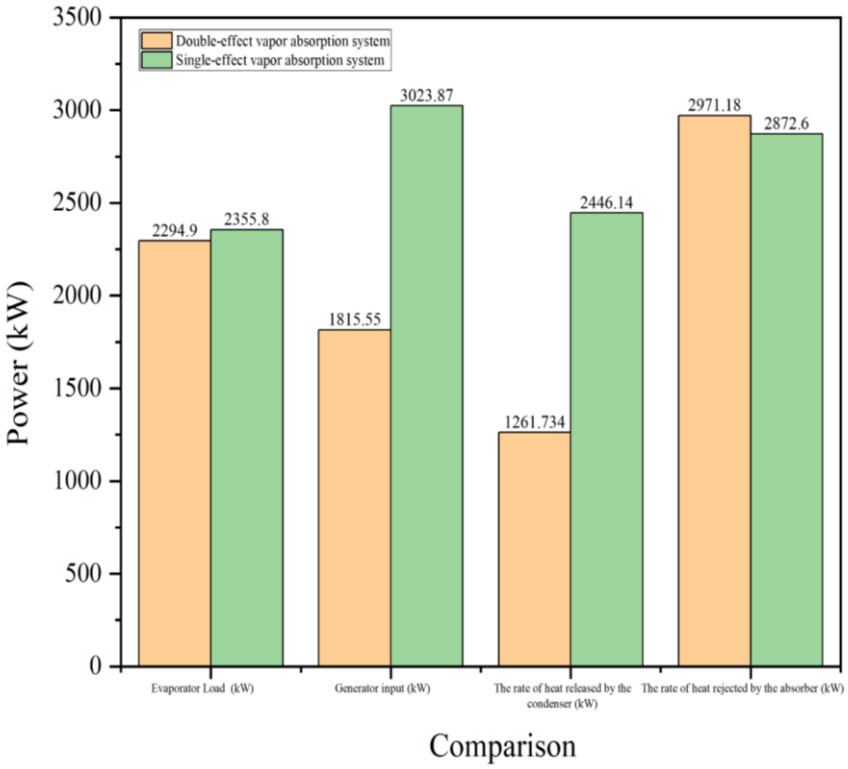

Figure 4-14 Comparison bar chart for the Single-effect and double effect vapor refrigeration cycle

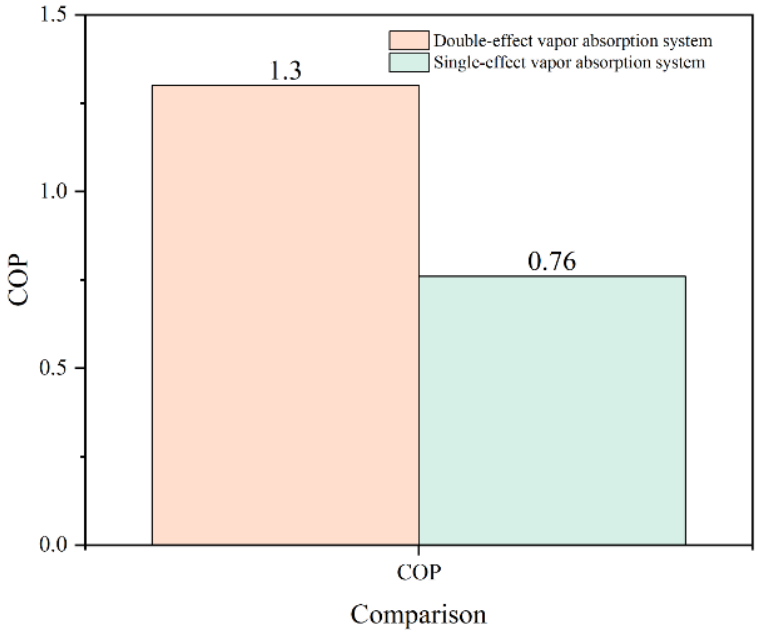

Figure 4-15 COP comparison between Single effect and double effect refrigeration cycle

The **figure 4-15** show difference in COP in both single and double effect vapor absorption refrigeration cycle.

The COP is determined to be .76 for single effect vapor absorption refrigeration cycle. And 1.3 for double effect vapor absorption refrigeration cycle.

4.11 Annual Energy Consumption Analysis

Figure 4-16 show the different requirement in different month of the year. The most requirement is in the June, July and august month. This is because of the disturbance between the solar panel and the sun. These months are mostly rainy season months.

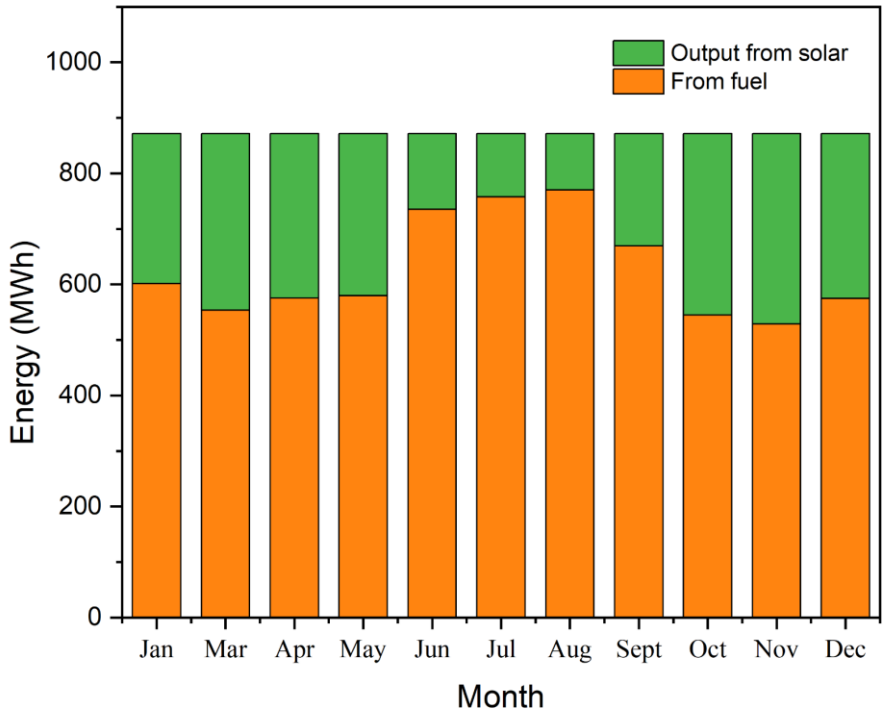

Figure 4-16 Month Wise energy requirement from solar and fuel

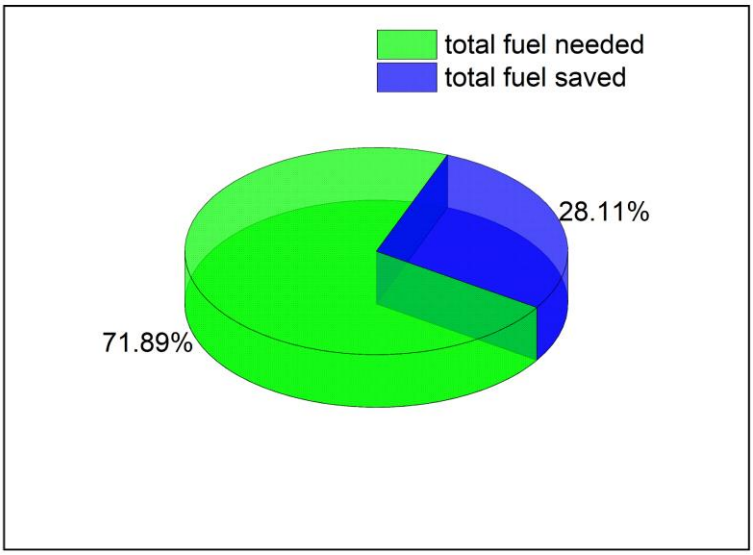

Figure 4-17 Amount of Fuel Saved from Using Solar Energy

There is more solar energy accessible during the summer and winter seasons than during the other seasons. This is mostly due to greater daylight hours in the summer, as the days are longer. The clear sky during the winter allows more direct sunlight to reach the Earth's surface, resulting in higher solar energy output. In contrast, gloomy skies diminish solar energy available during the rainy season. Cloud cover reduces solar energy output by obstructing sunlight. As a result, additional fuel is often necessary to satisfy energy demands as an alternate source of power during the rainy season. Solar panels, as an energy producing technology, may considerably reduce dependency on fossil-fuel-based energy sources. According to the statement, capturing solar energy through the use of solar panels may save roughly 28.11% of fuel use. This demonstrates solar energy's promise as a renewable and sustainable alternative to existing fuel-based energy sources. **Figure 4-17** show the overall amount of fuel that can be saved after using the solar system .

4.12 Solar Output and Fuel Requirement in Various Days

A single day in various days of all the months in the year was done to see the requirement of fuels throughout the day. There is a lot of fluctuation in many of the days. This is because of the clouds that will cover the solar panel. Also, as the hours goes by the requirement becomes less and less. As in the noon the most amount of DNI is found. In night and before sun set the whole system will run on fuel.

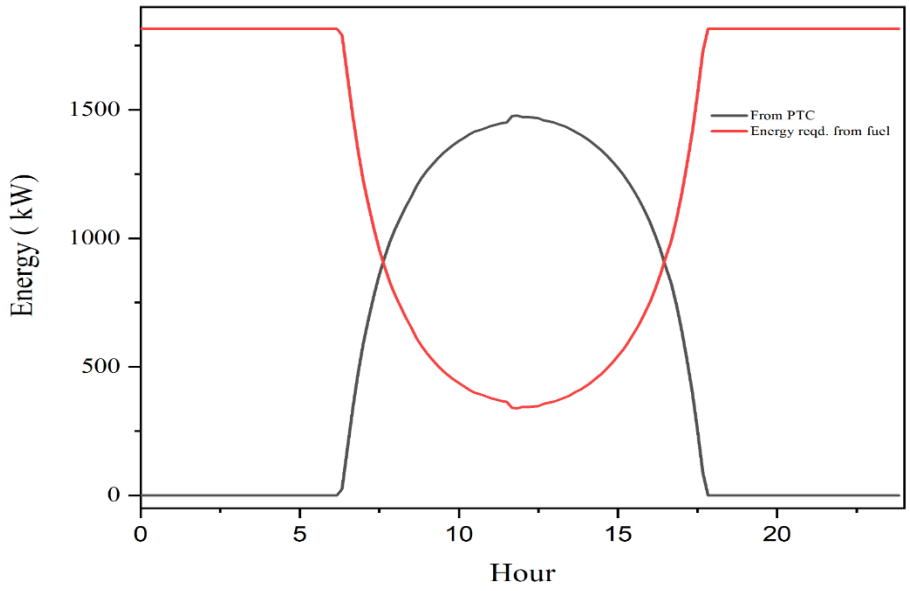

(a) 17 Jan ,2020

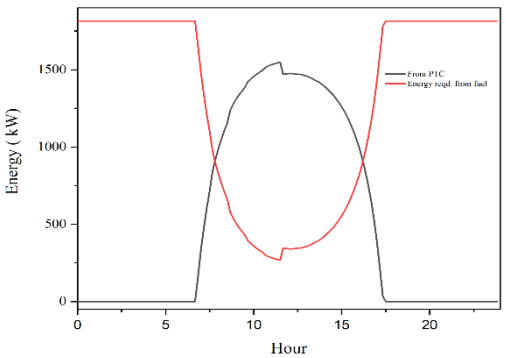

(b) 10 Mar,2020

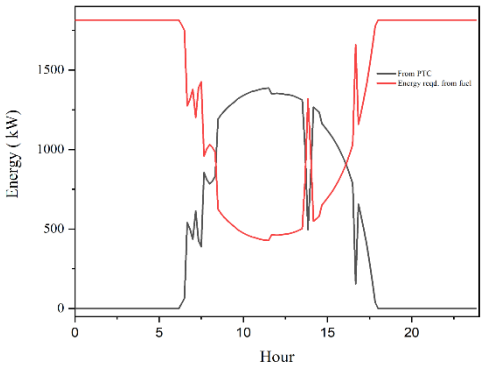

(c) 30 Apr ,2020

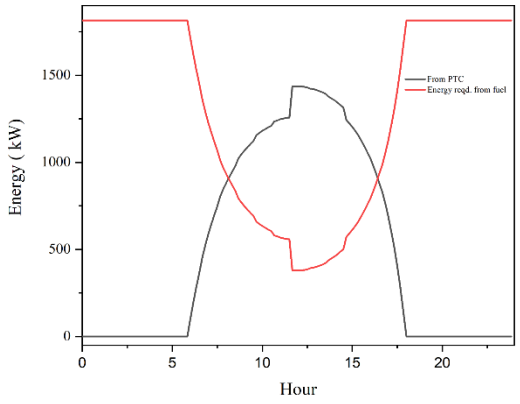

(d)7 May ,2020

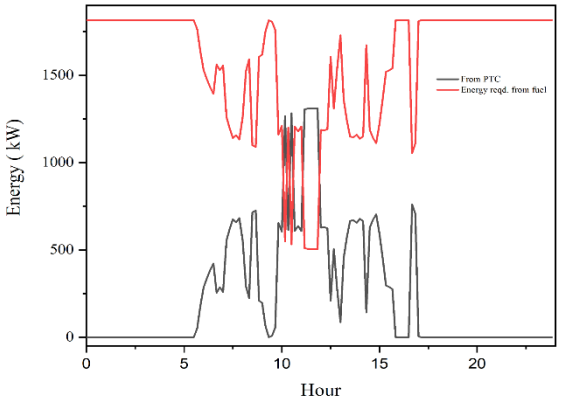

(e) 24 Jun ,2020

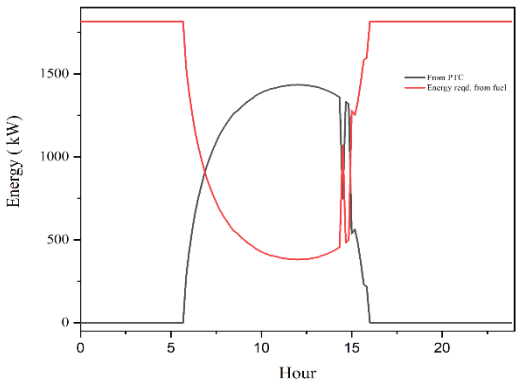

(f) 25 Jul ,2020

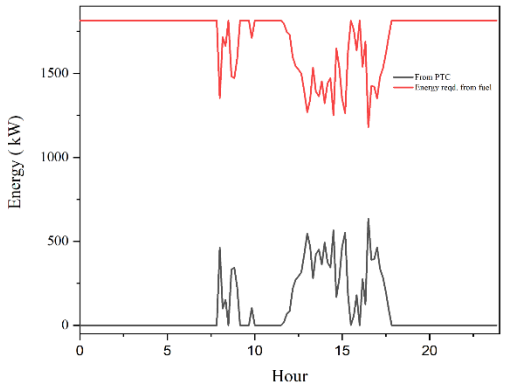

(g) 26 Aug ,2020

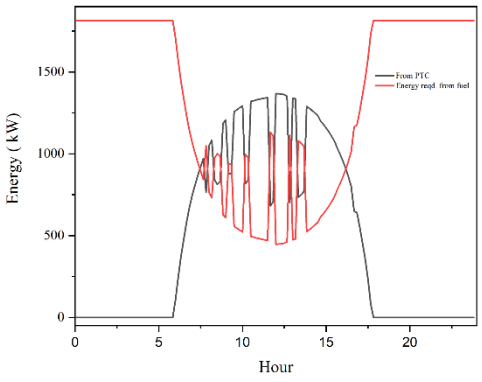

(h) 3 Sep ,2020

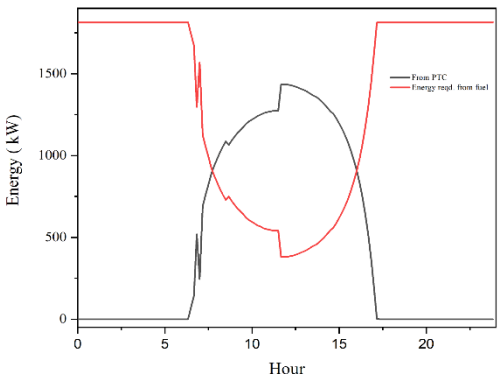

(i) 26 Oct ,2020

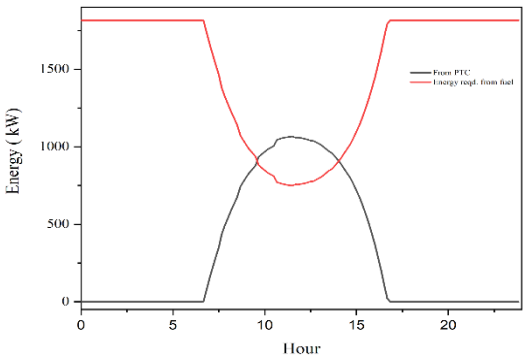

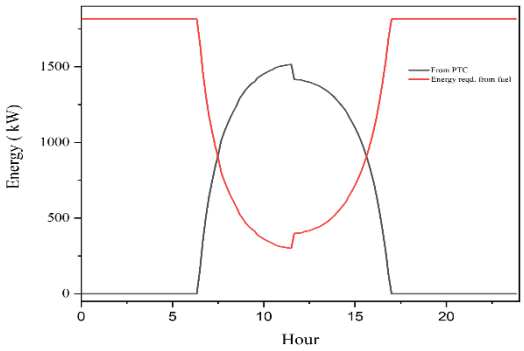

(j) 20 Nov,2020 **(k) 1 Dec,2020**

Figure 4-18 Solar Output and fuel requirement for different days across the year 2020.

From the above **figure 4-18** it can be said that solar energy never fulfills the requirement to run the system. The fluctuation is because of the obstacle between the sun and the PTC panels.

4.13 Economic Analysis

The Capital cost and the cost after the installment were calculated in the following tables. In the **table 4-18** the capital cost or initial investment is provided. From the table it can be viewed that we need about 18.55 lakh just to set up the system that include the energy storage and the VARS system. The items are mentioned in the first column. The cost for each item in second column and amount needed un the third column. Overall, cost to buy all the items in the last column.

Table 4-18: Capital Cost and Initial Investment

Items	Rate	Quantity	Cost
Balance of system			105000
Bricks	15.225 / piece	35000	532875
RCC slab	4567.5 / m^3	80	365400
EPS layer	137.55 / m^2	700	96285
Door			42000
Sand			63000
Cement	578.55 / packet	120	69426
TMT Rebar	51765 / ton	2	103530
Labor cost	210 / sq. Ft	2153	452130
Miscellaneous			26250
Total			18,55,896

Solar panel installment breakdown in the **table 4-19**. From it can be found that to install the solar system alongside the fuel system an extra 4.91 lakh taka is necessary. To increase the amount of solar panels, the amount of cost will increase. Here the quantity is about 200 PTCs.

Table 4-19: Solar panel installment breakdown in the table

Items	Rate	Quantity	Cost
Parabolic Trough Collector	24570/units	200	491400
Storage Tank	$8.4/m^2$	9000	75600

The revenue was also estimated in the **table 4-20.**

Table 4-20: Solar panel installment breakdown in the table

Items	Rate	Quantity	Cost
Revenue	$500/m^3$	1000	500000

Revenue will be generated by renting the space per meter cube. The space will be used though out the month. The initial cost of the installment and also to install the solar system the amount to pay was taken from the current situation and price rate of the country. The highest amount of the range was taken in the table. The payback period for the capital and installment cost for the PTC is 4.85 years. **Figure 4-19** shows amount of cost for each investment and revenue.

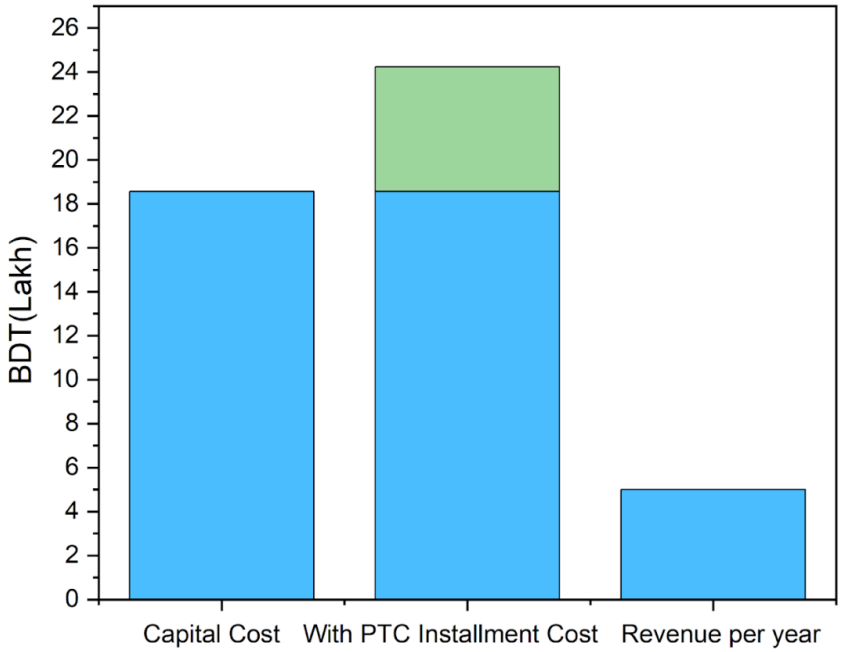

Figure 4-19 Economic Analysis Chart

4.14 Emission Analysis

If the system fully run-on fuel the amount of greenhouse gas emission is given in the **table 4-21 and in the table 4-22** emission from only from fuel generator

Table 4-21: Emission if the system is fully run-on fuel

	Coal	**Petroleum**	**Natural Gas**	**Hydro**
CO_2 (×100 kg)	113091	81464	50795	0
SO_2	133217	157177	4792	0
NO_X	49837	23960	8626	0
CO	1917	1917	4792	0

After integrating with the solar panel, the emission is reduced by in table

Table 4-22: Emission saved from using Solar energy

	Coal	Petroleum	Natural Gas	Hydro
CO_2 (×100 kg)	31793	22902	14280	0
SO_2	37451	44187	1347	0
NO_X	14010	6736	2425	0
CO	539	539	1347	0

The **figure 4-20** and **figure 4-21** show the amount of greenhouse gas emission for both the system. That is for both with solar power and without the use of solar power. About 30% of greenhouse gas can be reduced.

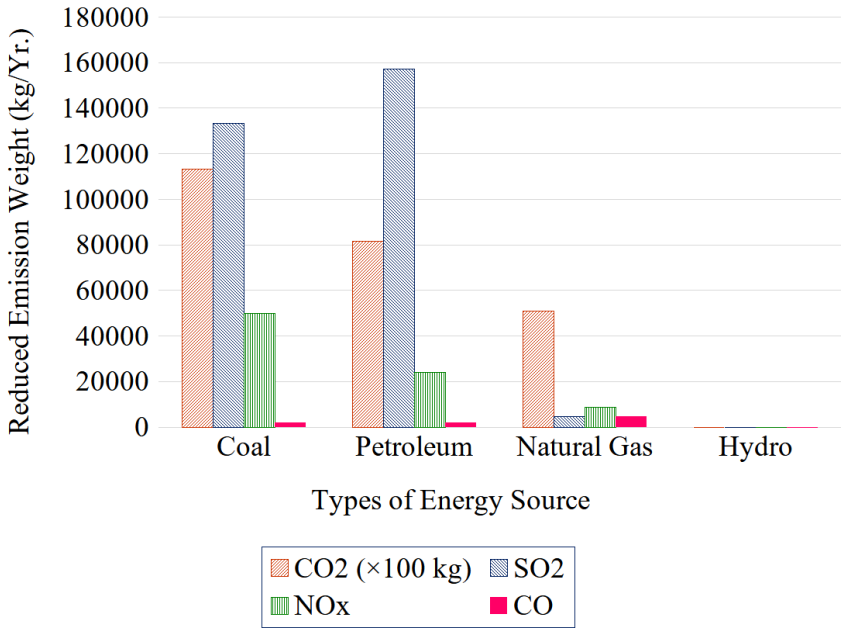

Figure 4-20 Greenhouse Gas Emission in Only Fuel Run System

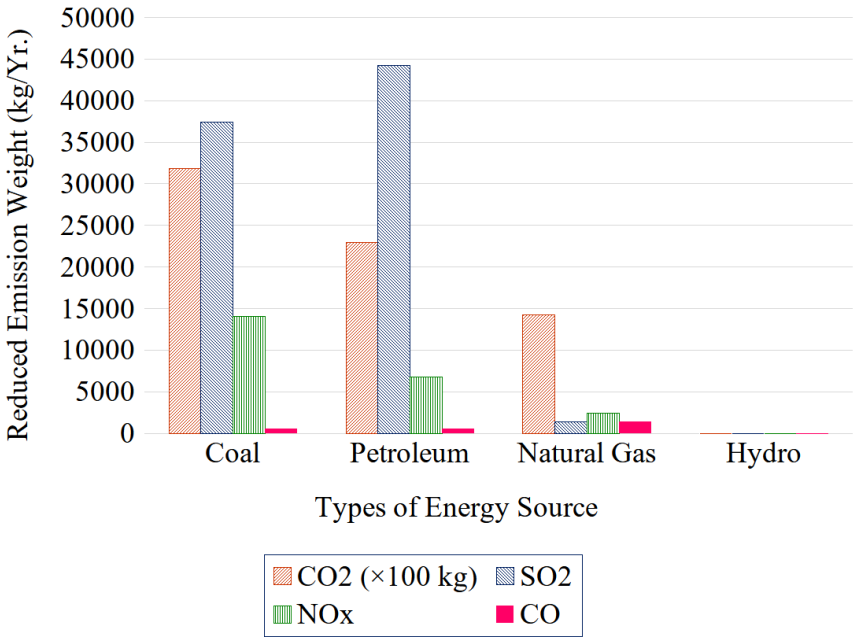

Figure 4-21 Saved Greenhouse Gas After Using Solar

4.15 Conclusion

Important findings from the study

- The south-east side have the most solar radiation.it is our suitable location. One of the suitable locations for our study is Latitude 21° 57' 36" N, Longitude 91° 59' 24" E.
- In linear regression when we applied feature expansion with Principal Component Analysis (PCA), the complexity of the model decreased due to the dimensionality reduction achieved by PCA. Consequently, as the number of feature expansions increased, both the train and test RMSE decreased, indicating that the models became more accurate in predicting the solar intensity.
- In polynomial regression our results up to degree 4 demonstrated the potential benefits of incorporating polynomial features in capturing non-linear relationships in the data.

- Regression tree, by choosing a maximum depth of 10, we aimed to achieve a more robust and well-performing regression tree model that effectively balanced between capturing important relationships and minimizing the risk of overfitting
- SVM regression through careful selection and tuning, we sought to leverage the power of SVM to accurately predict solar intensity by capturing the underlying non-linear patterns in the data.
- For ANN the selection of the 4-layer architecture with specific layer sizes and activation functions proved to be successful in achieving the best results
- N-BEATS stands out among neural network models as a particularly good solution for time series forecasting.
- Double effect vapor absorption refrigeration is comparatively better than single effect vapor absorption refrigeration.
- By implementing the solar system, about 28.11% of fuel can be saved.
- From solar output and fuel requirement in various days the solar energy never comes close to the requirement to run the cold storage.
- From economic analysis, the payback period for the installment for the system is about 4.85 years.
- From emission analysis, about 30% of greenhouse gas can be reduced.

Chapter 5 Conclusion and Future Scope

5.1 Conclusion

Predicting future renewable energy generation is critical to ensuring the power grid's efficient and stable operation. Renewable energy generation, unlike conventional power sources such as fossil fuels, is susceptible to variability and intermittency due to factors such as weather and time of day. As a result, it is critical to precisely estimate renewable energy generation in order to successfully balance the grid and optimize the use of fossil fuel-based energy sources. In this context, the NSRDB (National Solar Radiation Database) database is a valuable resource that provides comprehensive solar radiation data across various locations. By leveraging this database, researchers and practitioners can develop prediction models for solar power generation using machine learning techniques. Machine learning techniques offer a data-driven approach to develop predictive models based on historical solar radiation data. Multiple regression techniques are commonly employed to generate accurate prediction models for solar power generation. Regression models aim to establish relationships between input variables (such as solar radiation, temperature, cloud cover, etc.) and the output variable (solar power generation). The choice of regression technique depends on the specific requirements of the prediction task and the nature of the available data. Each technique has its strengths and limitations, and their performance is evaluated based on metrics like root mean square error (RMSE). Training and testing different models using historical solar radiation and solar power generation data from the NSRDB database is required for the comparison of numerous regression algorithms. To evaluate the models' performance on unknown data, the data is frequently separated into training and testing sets. The models are trained to capture the links between input variables

(such as solar radiation and temperature) and output variables (such as solar power generation), allowing them to generate reliable forecasts for future time periods.

From the study Conducted it reveals the following:

1. The generator input for the double effect is less than the single effect vapor absorption cycle.
2. The COP is also higher for the double effect VAR system.
3. By introducing the solar system we can reduce the fuel consumption by 28.11%.
4. The payback period to cover the initial installment is about 4.85 years.
5. The emission that can be reduced from using solar energy is about 30% less than only using the fuel generator.

5.2 Future Scope

In future, we want to introduce the transformer prediction model and other latest models that are used in forecasting.

Also, we used the existing PTC model. An optimized design of PTC can also be used. Other systems to produce solar energy can also be an option to produce solar energy.

For the cold storage power requirement, the demand can be met by solar energy only. This will save a huge amount of fuel as well as greenhouse gas emissions.

- Transformer prediction models can be compared alongside others.
- The use of other methods to gain solar energy like CSP, SPV, solar tower etc. can make the system fully run-on solar power.
- Also, the PTC can be designed without the use of design parameters.

Chapter 6 References

[1]Li DHW, Cheung KL, Lam TNT, Chan W. A study of grid-connected photovoltaic (PV) system in Hong Kong. Appl Energy 2012;90:122–7

[2] Budyko, M. I. (1969). The effect of solar radiation variations on the climate of the Earth. Tellus 21, 611–619. doi: 10.3402/tellusa. v21i5.10109

[3] Islam, M. D., Kubo, I., Ohadi, M., and Alili, A. A. (2009). Measurement of solar energy radiation in Abu Dhabi, UAE. Appl. Energy 86, 511–515. doi: 10.1016/j. apenergy.2008.07.012

[4] Beer, C., Reichstein, M., Tomelleri, E., Ciais, P., Jung, M., Carvalhais, N., et al. (2010). Terrestrial gross carbon dioxide uptake: Global distribution and covariation with climate. Science 329, 834–838. doi: 10.1126/science.11 84984

[5] Siingh, D., Singh, R. P., Singh, A. K., Kulkarni, M. N., Gautam, A. S., and Singh, A. K. (2011). Solar activity, lightning and climate. Surv. Geophys. 32, 659–703. doi: 10.1007/s10712-011-9127-1

[6] Ohunakin, O. S., Adaramola, M. S., Oyewola, O. M., Matthew, O. J., and Fagbenle, R. O. (2015). The effect of climate change on solar radiation in Nigeria. Sol. Energy 116, 272–286. doi: 10.1016/j.solener.2015.03.027

[7] Iziomon, M. G., and Mayer, H. (2002). Assessment of some global solar radiation parameterizations. J. Atmos. Solar Terrestrial Phys. 64, 1631–1643. doi: 10.1016/ S1364-6826(02)00131-1

[8] Mellit, A. (2008). Artificial Intelligence technique for modelling and forecasting of solar radiation data: a review. Int.J. Artif.Intell. Soft Comput. 1:52.

doi: 10.1504/ijaisc.2008.021264

[9] Li, M., Tian, J., and Chen, F. (2008). Improving multiclass pattern recognition with a co-evolutionary RBFNN. Pattern Recognit. Lett. 29, 392–406. doi: 10.1016/j. patrec.2007.10.019

[10] Li, M. F., Fan, L., Liu, H. B., Wu, W., and Chen, J. L. (2012). Impact of time interval on the ångström-Prescott coefficients and their interchangeability in estimating radiation. Renew. Energy 44, 431–438. doi: 10.1016/j.renene.2012.01.107

[11] Li, X., Wang, L., and Sung, E. (2008). AdaBoost with SVM-based component classifiers. Eng. Appl. Artif. Intell. 21, 785–795. doi: 10.1016/j.engappai.2007.07. 001

[12] Halabi, L. M., Mekhilef, S., and Hossain, M. (2018). Performance evaluation of hybrid adaptive neuro-fuzzy inference system models for predicting monthly global solar radiation. Appl. Energy 213, 247–261. doi: 10.1016/j.apenergy.2018. 01.035

[13] Makade, R. G., Chakrabarti, S., and Jamil, B. (2019). Prediction of global solar radiation using a single empirical model for diversified locations across India. Urban Clim. 29:100492. doi: 10.1016/j.uclim.2019.100492

[14] Lee, H.-J., Kim, S.-Y., & Yun, C.-Y. (2017). Comparison of Solar Radiation Models to Estimate Direct Normal Irradiance for Korea. Energies, 10(5), 594. doi:10.3390/en10050594

https://www.researchgate.net/publication/316639367_Comparison_of_Solar_Radiation_Models_to_Estimate_Direct_Normal_Irradiance_for_Korea

[15] Lou, S., Li, D. H. W., Lam, J. C., & Chan, W. W. H. (2016). Prediction of diffuse solar irradiance using learning and multivariable regression. Applied Energy, 181, 367–374.

doi:10.1016/j.apenergy.2016.08.093

https://www.sciencedirect.com/science/article/abs/pii/S0306261916311916

[16] R. Lizarte, M. Izquierdo, J.D. Marcos, E. Palacios, An innovative solar-driven directly air-cooled LiBr–H2O absorption chiller prototype for residential use, Energy Build. 47 (2012) 1–11, https://doi.org/10.1016/j.enbuild.2011.11.011.

[17] D.N. Basu, A. Ganguly, Conceptual design and Performance Analysis of a Solar Thermal-Photovoltaic-Powered Absorption Refrigeration System, J. Sol. Energy Eng. 137 (2015) 31020–31029, https://doi.org/10.1115/1.4029910.

[18] E. Bellos, C. Tzivanids, C. Symeou, K.A. Antonopoulos, Energetic, exergetic and financial evaluation of a solar driven absorption chiller – a dynamic approach, Energy Convers. Manage. 137 (2017) 34–48 0.1016/j.enconman.2017.01.041.

[19] G.A. Florides, S.A. Kalogirou, S.A. Tassou, L.C. Wrobel, Design and construction of a LiBr–water absorption machine, Energy Convers. Manage. 44 (15) (2003)2483–2508, https://doi.org/10.1016/S0196-8904(03)00006-2.

[20] D.N. Basu, A. Ganguly, Solar thermal–photovoltaic powered potato cold storage conceptual design and performance analyses, Appl. Energy 165 (1) (2016) 308–317, https://doi.org/10.1016/j.apenergy.2015.12.070.

[21] A. Ganguly, R.K. De, Conceptual design and performance analysis of a parabolic trough collector supported multi-commodity cold storage, IOP Conference Series, Mater. Sci. Eng. 402 (0120497) (2018) 1–10, https://doi.org/10.1088/1757-899X/402/1/012049.

[22] A. Hmida, N. Chekir, A. Laafer, M.E.A. Slimani, A.B. Brahim, Modeling of cold room driven by an absorption refrigerator in the south of Tunisia: a detailed energy and thermodynamic analysis, J.Cleaner Prod. 211 (2019) 1239–1249 https://doi.org/1016/j.jclepro.2018.11.219.

[23] F. Agyenim, I. Knight, M. Rhodes, Design and experimental testing of the performance of an outdoor LiBr/H2O solar thermal absorption cooling system with a cold store, Sol. Energy 84 (5) (2010) 735–744, https://doi.org/10.1016/j.solener.2010.01.013.

[24] R.K. De, A. Ganguly, Energy and economic analysis of a solar supported multicommodity cold storage, J. Brazil. Soc. Mechan. Sci. Eng. 41 (393) (2019) 1–17,

https://doi.org/10.1007/s40430-019-1893-6.

[25] A. Arora, S.C. Kaushik, Theoretical analysis of LiBr/H2O absorption refrigeration systems, Int. J. Energy Res. 33 (2009) 1321–1340, https://doi.org/10.1002/er.1542

[26] N. C. Srivastava, Solar operated system for a 100 tons potato cold store, Proc.e Int. Solar Energy Society Congress (New Delhi, India, 1978)

[27] F. Agyenim, I. Knight and M. Rhodes, Design and experimental testing of the performance of an outdoor LiBr/H2O solar thermal absorption cooling system with a cold store, Solar Energy 84 (2010) 735–744.

[28] D. N. Basu and A. Ganguly, Solar thermal–photovoltaic powered potato cold storage–conceptual design and performance analyses, Appl. Energy 165 (2016) 308–317.

[29] A. Hmida, N. Chekir, A. Laafer, M. E. A. Slimani and A. B. Brahim, Modeling of cold room driven by an absorption refrigerator in the south of Tunisia: A detailed energy and thermodynamic analysis, J. Cleaner Production 211 (2019) 1239–1249.

[30] A. Ganguly and R. K. De, Conceptual design and performance analysis of a parabolic trough collector supported multi-commodity cold storage, IOP Conf. Series: Materials Science and Engineering 402 (2018) 1–10.

[31]. A. Arora and S. C. Kaushik, Theoretical analysis of LiBr/H2O absorption refrigeration systems, Int. J. Energy Res. 33 (2009) 1321–1340

[32] R.K. De, A. Ganguly, Energy and economic analysis of a solar supported multicommodity cold storage, J. Brazil. Soc. Mechan. Sci. Eng. 41 (393) (2019) 1–17,

https://doi.org/10.1007/s40430-019-1893-6.

[33] A. Ganguly, R.K. De, Conceptual design and performance analysis of a parabolic trough collector supported multi-commodity cold storage, IOP Conference Series, Mater. Sci. Eng. 402 (0120497) (2018) 1–10, https://doi.org/10.1088/1757-899X/402/1/012049

[34] D.N. Basu, A. Ganguly, Solar thermal–photovoltaic powered potato cold storage–conceptual design and performance analyses, Appl. Energy 165 (1) (2016) 308–317, https://doi.org/10.1016/j.apenergy.2015.12.070

[35] G.A. Florides, S.A. Kalogirou, S.A. Tassou, L.C. Wrobel, Design and construction of a LiBr–water absorption machine, Energy Convers. Manage. 44 (15) (2003) 2483–2508, https://doi.org/10.1016/S0196-8904(03)00006-2

[36] R.K. De, A. Ganguly, Energy, exergy and economic analysis of a solar hybrid power

system integrated double-effect vapor absorption system based cold storage, Int. J.

Air-Condition. Refriger. 27 (2) (2019) 1–13, https://doi.org/10.1142/S2010132519500184

[37] A. Arora, S.C. Kaushik, Theoretical analysis of LiBr/H2O absorption refrigeration systems, Int. J. Energy Res. 33 (2009) 1321–1340, https://doi.org/10.1002/er. 1542

[38] De RK, Ganguly A. Performance comparison of solar-driven single and double-effect LiBr-water vapor absorption system based cold storage. Therm Sci Eng Prog [Internet]. 2020;17(August 2019):100488. Available from:

https://doi.org/10.1016/j.tsep.2020.100488

[39] Hasanuzzaman, M., Rahim, N. A., Saidur, R., & Rahim, N. A. (2020). Performance evaluation of a solar-driven vapor absorption refrigeration system in Bangladesh. Journal of Cleaner Production, 253, 119954.

[40] "BP.Statistical review of world energy 2012," BP, 2012. [Online]. Available: http://www.bp.com/assets/bp_internet/globalbp/globalbp_uk_english/reports_and_publications/statistical_energy_review_2011/STAGING/local_assets/pdf/statistical_review_of_world_energy_full_report_2012.pdf. [Accessed 2018]

[41] M. T. Islam, "Current energy scenario and future prospect of renewable energy," Renewable and Sustainable Energy Reviews, p. 1074–1088, 2014.

[42]"AkbarMS.EnergyandnuclearpowerplanninginBangladesh.Nuclearenergy," 2012. [Online]. Available:

http://www.iaea.org/INPRO/activities/Joint_SE/2._Bangladesh_Shawkat_Akbar.pdf. [Accessed 2018].

[43] A. F, "Alternative energy resources in Bangladesh and future prospect.," Renew Sustain Energy Rev, p. 698–707., 2013.